ROLE OF PROTEIN ACETYLATION, FORMATION AND DISPERSAL OF

BIOFILMS, AND THEIR IMPACT ON INSECTS

A Dissertation

by

QUN MA

May 2011

Major Subject: Chemical Engineering

ROLE OF PROTEIN ACETYLATION, FORMATION AND DISPERSAL OF

BIOFILMS, AND THEIR IMPACT ON INSECTS

A Dissertation

by

QUN MA

Submitted to the Office of Graduate Studies of
Texas A&M University
in partial fulfillment of the requirements for the degree of

DOCTOR OF PHILOSOPHY

Approved by:

Chair of Committee,	Thomas K. Wood
Committee Members,	Arul Jayaraman
	Mariah Hahn
	Kung-Hui Chu
Head of Department,	Michael Pishko

May 2011

Major Subject: Chemical Engineering

ABSTRACT

Role of Protein Acetylation, Formation and Dispersal of Biofilms, and Their Impact on Insects.

(May 2011)

Qun Ma, B.S., Zhejiang University

Chair of Advisory Committee: Dr. Thomas K. Wood

Bacterial biofilms form on liquid/air and liquid/solid surfaces and consist of cells combined with an extracellular matrix such as exopolysaccharides, extracellular DNA, and glycoproteins. Bacteria have up to a 1000-fold increase of antibiotic resistance in biofilms compared to planktonic cells. Furthermore, biofilm cells show better tolerance to adverse environmental conditions such as nutrition limitations, temperature changes, pH changes, and non-optimal osmotic conditions.

In *Escherichia coli*, the outer membrane protein OmpA increased biofilm formation on polystyrene, polypropylene, and polyvinyl chloride surfaces while it decreased biofilm formation on glass surfaces. This surface-dependent phenotype was because OmpA inhibits cellulose production by inducing the CpxRA two-component signal transduction pathway, and cellulose inhibits biofilm formation on plastic due to its hydrophilic nature.

We discovered, and then engineered, BdcA (formerly YjgI), for biofilm dispersal. We found that in *E. coli*, BdcA increases motility and extracellular DNA production while it decreases exopolysaccharide production, cell length, and aggregation. We reasoned that the 3, 5-cyclic diguanylic acid (c-di-GMP) levels increase upon deleting *bdcA,* and showed that BdcA binds c-di-GMP in vitro. In addition, we used protein engineering to evolve BdcA for greater c-di-GMP binding and found that the single amino acid change E50Q causes nearly complete biofilm dispersal.

We isolated *Proteus mirabilis* from the blowfly *Lucilia sericata*, which swarmed significantly. By motility screening and complementation with putative interkingdom signal molecules that have been shown to attract flies, we found lactic acid, phenol, NaOH, KOH, putrescine, and ammonia restore the swarming motility of seven different swarming deficient mutants. These mutants and putative signal molecules will be further tested for fly attraction and oviposition.

Acetylation of lysine residues is conserved in all three kingdoms although its role in bacteria is not clear. We demonstrated that acetylation enables *E. coli* to withstand environmental stresses. Specifically, the bacteria became more resistant to heat and oxidative stress. Furthermore, we showed that the increase in oxidative stress resistance is due to the induction of catalase gene *katG*. Hence we demonstrate for the first time a specific physiological role for acetylation in prokaryotes.

ACKNOWLEDGEMENTS

TABLE OF CONTENTS

4.5.2   Static biofilms for screening biofilm dispersal 72
4.5.3   Flow cell biofilms and image analysis........................ 74
4.5.4   EPS, swimming motility, aggregation, and eDNA
        assays 74
4.5.5   RNA isolation from biofilms 75
4.5.6   Whole-transcriptome analysis.................................. 75
4.5.7   Quantification of c-di-GMP 76
4.5.8   PDE assay 76
4.5.9 ^{31}P NMR 77
4.5.10 c-di-GMP binding assays.. 77
4.5.11 Random mutagenesis and saturation mutagenesis 77
4.5.12 Electron microscopy 78
4.5.13 qRT-PCR 79
4.5.14 Protein modeling.. 79
4.5.15 Phylogenetic tree construction................................. 79

V   QUORUM-SENSING   SWARMING   SIGNALS   FOR   *PROTEUS
        MIRABILIS* AND THEIR RELATION TO BLOWFLIES 80

        5.1   Overview 80
        5.2   Introduction 81
        5.3   Results 85
              5.3.1   *P. mirabilis* isolated from fly salivary glands............ 85
              5.3.2   Swarming deficient mutants 85
              5.3.3   Complementation of swarming mutations via known
                      fly attractants 88
              5.3.4   RfaL is required for fly attraction and oviposition 92
        5.4   Discussion.. 92
        5.5   Future work.. 95
        5.6   Experimental procedures 96
              5.6.1   Maggot salivary gland extraction................. 96
              5.6.2   *P. mirabilis* identification 96
              5.6.3   Transposon mutagenesis and swarming-based
                      screening.. 97
              5.6.4   DNA sequencing to identify transposon insertion
                      positions.. 97
              5.6.5   Swarming complementation 98
              5.6.6   Fly attraction and oviposition assay............. 99

VI   PROTEIN   ACETYLATION   IN   *ESCHERICHIA   COLI*   INCREASES
        STRESS RESISTANCE 101

        6.1   Overview 101
        6.2   Introduction 101
        6.3   Results 103

LIST OF FIGURES

LIST OF TABLES

CHAPTER I

INTRODUCTION

1.1 Background

Escherichia coli is the best-studied bacterium in the world with around 4000 genes in its genome. Although there are still many genes that have not been characterized, the availability of gene chips for DNA microarrays and libraries with 3985 single gene knockout mutants (KEIO collection (Baba et al., 2006)) and 4267 complementation plasmids (ASKA collection (Kitagawa et al., 2005)) makes it the most-suitable research model for understanding biological processes in living organisms.

Biofilm are aggregated cells attached to an interface in the presence of water. The cells in biofilms are embedded in an extracellular matrix comprised of exopolysaccharide (Karatan and Watnick, 2009), extracellular DNA (Barken et al., 2008), and glycoproteins (Nakao et al., 2008). Compared to free-swimming cells (planktonic cells), biofilm cells are more resistance to antimicrobial agents (bacteria in biofilms are as much as 1000-fold more resistant to antibiotics) (Mah et al., 2003) and are tolerant to adverse environmental conditions such as limited nutrients (Steinberger et al., 2002) and temperature fluctuations (Kubota et al., 2008). Thus, biofilms are very difficult to be remove and cause problems in regard to surgery (Bendouah et al., 2006) and industrial biofouling (Flemming et al., 1992).

There are six stages for biofilm development, movement to the surface (Wood et al., 2006), initial reversible attachment, irreversible attachment, formation of small aggregates, maturation of the biofilm, and biofilm dispersal (Van Houdt and Michiels, 2005). This process is dynamic (Wood et al., 2011). Cells can detach from a mature biofilm matrix and re-colonize in a new location in order to get more nutrition and expand.

_____

This dissertation follows the style of Environmental Microbiology.

Cell appendages play an important role in biofilm development and dispersal. These appendages include flagella, fimbriae, autotransporter proteins, curli, exopolysaccharide, and conjugative pili (Van Houdt and Michiels, 2005). For example, in the first stage of biofilm development, bacteria need flagella to move to solid surfaces (via motility). In the last stage of biofilm development, bacteria also need flagella to move away from biofilm matrix and change back to planktonic cells. Hence motility is considered to be a virulence factor since it is responsible for initial cell-to-surface contact.

Bacterial behavior is influenced by the environment. There are some signal transduction systems that can sense specific environmental cues and regulate gene expression as well as lead to cell physiology changes (Kjelleberg and Givskov, 2007). One important intracellular signal molecule that conveys these changes in the environment is 3, 5-cyclic diguanylic acid (c-di-GMP). c-di-GMP is synthesized by diguanylate cyclases, characterized by the GGDEF motif, from two guanosine-5'-triphosphate molecules and is degraded by phosphodiesterases (PDEs) which are characterized by the EAL domain and HD-GYP domain (Kulshina et al., 2009).

Signal transduction not only occurs intracellularly to regulate cell physiology, but also occurs intercellularly to make cell-cell communication (termed quorum sensing (QS)). Signal transduction also occurs between kingdoms (interkingdom signaling); for example, between bacteria and their hosts and involves small molecules that are produced by both eukaryotes and bacteria (e.g., hormone-like chemicals) (Hughes and Sperandio, 2008). For millions of years, prokaryotes and eukaryotes have maintained a close relationship. This relationship can be either beneficial or detrimental. The possibility of beneficial association indicates that bacteria can communicate with eukaryotes such as insects and mammals through some specific chemicals and these chemicals should be able to control both organisms' physiology.

Protein acetylation is a post-translational modification conserved in both mammals and

microbes (Wang et al., 2010). In bacteria, previous work has focused primarily on histones and transcription-associated proteins (Hu et al., 2010). Recent reports showed that acetylation involves proteins in almost every aspect of cellular physiology (Yu et al., 2008).

1.2 Motivation

Biofilm formation causes serious problems to industry and human health due to its resistance to extreme environments as well as to high concentrations of antimicrobial reagents. Biofilms can grow in extremely hot waters, frozen glaciers, very acidic conditions, and very alkaline conditions. Biofilm formation increases heat transfer resistance and leads to significant energy losses in heat exchange equipment (Characklis et al., 1981). Biofilms also cause substantial corrosion problems (20% of industry corrosion) in marine engineering systems, such as in pipelines of the offshore oil and gas industry (Duan et al., 2008). Biofouling organisms increase fuel consumption by over 20% and cost the Navy each year $75-100M for drag-related fuel increases (Dürr and Thomason, 2009). Biofilms also exist in humans and are intimately related to diseases. For example, infections of the Shiga toxin-producing *E. coli* O157:H7 have been estimated to be responsible for 73,000 illnesses annually in the United States, with more than 2,000 hospitalizations and 60 deaths (Frenzen et al., 2005). Hence understanding the mechanisms of biofilm development should lead to novel methods to remove biofilms is a powerful strategy with significant importance to the economy and health. In addition, the characterizations of beneficial biofilms encourage people to think about the idea about using biofilms in a positive way. For example, *Bacillus subtilis* biofilm formation helps to control infection from plant pathogens (Morikawa, 2006) as well as to reduce mild steel corrosion (Jayaraman et al., 1999c; Jayaraman et al., 1999a). The potential of utilizing beneficial biofilms also requires a better understanding of the genetic basis of biofilm formation and dispersal.

1.3 Research objectives, importance, and novelty

This study seeks to improve the current understanding of biofilm formation and dispersal using *E. coli* as the reference organism. Engineering applications for controlling biofilms, the interaction between pathogen and host, and the effect of post-translational modifications on bacterial stress response are also discussed.

The specific aims are:

- Determine how OmpA influences *E. coli* biofilm formation

- Determine how BdcA controls *E. coli* biofilm dispersal

- Construct a powerful biofilm dispersal protein via protein engineering of BdcA

- Identify the interkingdom signal molecules between *Proteus mirabilis* and blowflies

- Determine how acetylation changes cell stress resistance

The Wood group discovered previously that OmpA is an outer membrane protein which influences biofilm formation (González Barrios et al., 2006a), and here we show OmpA influences biofilm formation in a surface-dependent manner. The *ompA* mutant has completely abolished biofilm formation on hydrophobic surfaces, and this phenotype can be complemented with OmpA production from a plasmid. Our goal was to explore the genetic basis of how OmpA influences biofilm formation in this manner. Our novel finding was that OmpA inhibits cellulose production by inducing the CpxRA two-component signal transduction pathway, and cellulose inhibits biofilm formation on plastic due to its hydrophilic nature.

BdcA (previously YjgI) was an uncharacterized protein involved in the transport of QS signal autoinducer 2 (AI-2) (Herzberg et al., 2006). Here we discovered that BdcA is a positive factor for biofilm dispersal. The novelty of our work is that we connected BdcA with the important intracellular signal c-di-GMP since BdcA was found to be a c-di-GMP-binding protein.

Protein engineering of BdcA was also performed by random mutagenesis and saturation mutagenesis of *bdcA* to obtain a more powerful protein for biofilm dispersal. The importance of this research is that we obtained a more effective biofilm dispersal protein (enhanced dispersal by an order of magnitude) with only one amino acid replacement that may be a general method for dispersing all bacterial biofilms.

The interkingdom signaling between pathogen *P. mirabilis* and blowfly *Lucilia sericata* was also investigated. Our goal was to discover QS signals and then use them to control insect behavior. Our novel finding was that lactic acid, phenol, NaOH, KOH, putrescine, and ammonia restore the swarming motility of seven different swarming deficient mutants. These chemicals may be interkingdom signal molecules that work for the communication between *P. mirabilis* and *L. sericata*.

The role of protein acetylation at lysine residue was also investigated. We discovered that protein acetylation is related to bacterial stress resistance, especially oxidative stress and heat stress, and related this acetylation to the regulation of catalase genes by stress-activated two-component systems.

CHAPTER II

LITERATURE REVIEW

2.1 *Escherichia coli*

      Escherichia coli is a typical Gram-negative bacterium which is commonly found in the lower intestine of warm-blooded organisms (Savageau, 1983). Some *E. coli* strains are harmful to humans by causing serious food poisoning, such as the O157:H7 (Johnsen et al., 2001). *E. coli* is also one of the most widely-used research models. The MG1655 was chosen as the first sequenced strain of *E. coli* K-12 by the Blattner lab (Blattner et al., 1997) since it has been maintained as a lab strain with minimal genetic manipulation. The *E. coli* K-12 BW25113 was used to make the Keio collection of single-gene knockouts (Baba et al., 2006), which further improves the speed of *E. coli* research by supplying thousands of ready-to-use single-gene knockouts.

2.2 Genetic basis of biofilm development

2.2.1 Biofilm development

      There are six stages for biofilm development (Fig. 2.1) and different cell adhesins are required for each stage (Table 2.1). In the first stage, bacteria need flagella to move to the solid surface (Wood et al., 2006; Wood, 2009); in the second stage, flagella help bacteria to attach to the solid surface reversibly (Van Houdt and Michiels, 2005); in the third stage, the initial attachment changes into irreversible attachment (Van Houdt and Michiels, 2005), and in this step, type 1 fimbriae is required while curli and polysaccharide also have a positive effect (Van Houdt and Michiels, 2005); in the fourth stage, small biofilm matrix forms with the help of extracellular matrix such as poly-β-1,6-GlcNAc polysaccharide (PGA) and autotransporter protein antigen 43 (Ag43) protein (Van Houdt and Michiels, 2005); in the fifth stage, a mature biofilm is formed with architecture that is dependent on colanic acid, curli, and conjugative pili (Van Houdt and

Michiels, 2005); and in the sixth stage, bacteria leave biofilm matrix with the help of flagella and change back to free-swimming cells again (Van Houdt and Michiels, 2005). Among these cell adhesins, the conjugative plasmid is notable since it enhances biofilm formation while overriding the importance of flagella, type 1 fimbriae, Ag43, and curli (Reisner et al., 2003).

To understand the genetic pathway of biofilm formation, several sets of DNA microarrays were conducted to compare the gene transcription profile between biofilm cells and planktonic cells. Beloin et al. studied biofilm cells grown on removable glass slides with *E. coli* TG1 strains (Beloin et al., 2004). Schembri et al. used biofilm cells from glass surfaces in a flow chamber system to perform DNA microarray for *E. coli* MG1655 strain (Schembri et al., 2003). Ren et al. studied gene expression profile with *E.* coli JM109 and ATCC 25404 by comparing glass wool biofilm cells with planktonic cells (Ren et al., 2004a). Hancock et al. collected biofilm cells from Petri dish to check the gene expression profile with two uropathogenic *E. coli* isolates, CFT073 and 536 (Hancock and Klemm, 2007). Moreover, a temporal study showed a more detailed gene expression profile for biofilm cells at different time points (Domka et al., 2007). The application of DNA microarrays for biofilm research rapidly unveiled many important genes that regulate various cell processes during biofilm development. The most important genes are selected and studied for their role in cell physiology and their mechanism for controlling biofilm development.
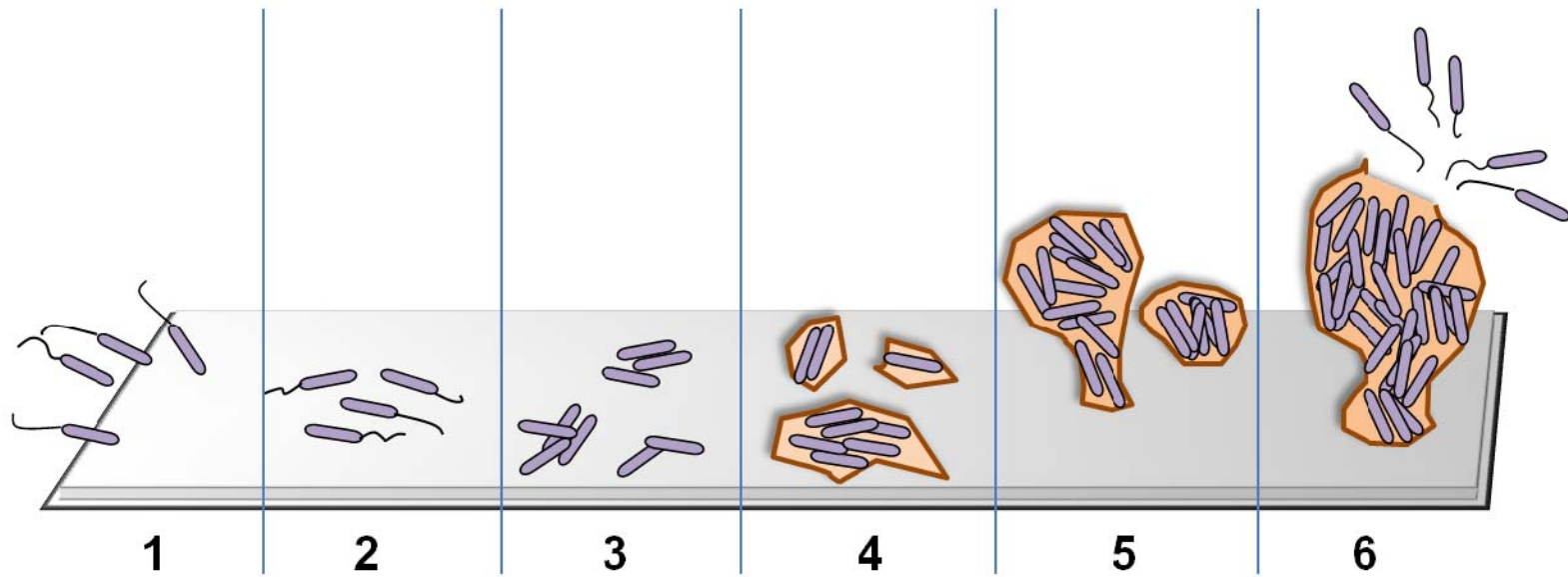
Figure 2.1 Biofilm development (Wood, 2009). (1) bacteria move to the solid surface; (2) reversible attachment; (3) irreversible attachment; (4) small biofilm matrix; (5) matured biofilm matrix; (6) biofilm dispersal.

Table 2.1 Cell adhesins in *E. coli* K-12 strains.

Adhesins	Locus	Assays for detection
curli	*csgBA*	Congo red assay (Zhang et al., 2007)
flagella	*flh*, *flg*, *fli*, and *mot* operons	swimming and swarming motility (Wood et al., 2006; Inoue et al., 2007)
type 1 fimbriae	*fimA*	yeast agglutination assay (García-Contreras et al., 2008)
putative fimbriae	*ycb, yad, sfm, yeh,* and *ybg* operons	electron microscopy (for *ycb, yad,* and *sfm*) fimbriae isolation and SDS-PAGE (*yeh* and *ybg*) (Korea et al., 2010)
conjugative pilus	*traA*	electron microscopy (Grossman and Silverman, 1989)
Ag43	*flu*	Western blotting (Sherlock et al., 2006)
putative autotransporter	*yfaL, yeeJ, ypjA,* and *ycgV*	no direct evidence for their role as autotransporter (Roux et al., 2005)
cellulose	*bcs* operon*, ompA*	cellulose assay using Congo red, calcofluor, and cellulose method (Ma and Wood, 2009)
colanic acid	*wcaK*	colanic acid assay-using 6-deoxyhexose (Zhang et al., 2008)
PGA	*pgaABCD*	FPLC (Wang et al., 2005)

2.2.2 Biofilm formation and toxin/antitoxin systems

hha and *tomB* are contiguous genes with 30-fold increase in gene expression in biofilms (Ren et al., 2004a). Further research showed that Hha controls biofilm formation by decreasing fimbriae production and controlling cell death (García-Contreras et al., 2008). Hha binds to rare codon tRNAs, represses fimbriae production, and activates prophage lytic genes (García-Contreras et al., 2008). Hha works as a toxin and TomB works as an antitoxin which attenuates the toxicity by Hha (García-Contreras et al., 2008). Hha is also shown to be required for persister cell formation via MqsR overproduction by Kim et al. (Kim and Wood, 2010).

mqsR is induced 8 fold in biofilms (Ren et al., 2004a). MqsR is a toxin and works as an RNase similar to RelE and YoeB (Brown et al., 2009). The antitoxin that works in conjunction with MqsR is MqsA which binds DNA via its helix-turn-helix (HTH) motif in the C-terminal domain and binds the toxin via its N-terminal zinc-binding domain (Brown et al., 2009). The MqsR/MqsA complex represses *cspD*, which encodes another toxin CspD (Kim et al., 2010). The MqsR and MqsA TA system are unique since they control much more than just cell death (Wang et al., 2011). The genes encoding MqsR and MqsA are the first locus that upon its deletion, decreases the formation of persister cells (Kim and Wood, 2010). The toxins CspD, Hha, and HokA require MqsR to influence persister cell formation (Kim and Wood, 2010). MqsR/MqsA is also the first TA system found to be induced in biofilms (Kim and Wood, 2010), the first to be related to quorum sensing (Ren et al., 2004a), cell motility (Ren et al., 2004a), and biofilm formation (Ren et al., 2004a). In addition, MqsA is the first antitoxin that regulates more than its own transcription as it binds the *mqsRA, cspD*, *mcbR*, and *spy* promoters (Brown et al., 2009; Kim et al., 2010). Furthermore, the antitoxin MqsA represses *rpoS*, reducing the concentration of c-di-GMP, increasing motility, and decreasing biofilm formation (Wang et al., 2011). The connection between MqsA and RpoS showed that the novel role of antitoxin MqsA

as regulating the general stress response (Wang et al., 2011). MqsA is degraded rapidly upon the addition of oxidative stress (Wang et al., 2011). This degradation leads to the switch from high motility to low motility, which is also the shift from planktonic state to biofilm state (Wang et al., 2011).

2.2.3 Biofilm formation via cell signaling related genes

Acylhomoserine lactones (AHL)

Cell signaling plays a role in biofilm formation. The AHLs are common quorum sensing signals in Gram-negative bacteria (Jayaraman and Wood, 2008). *E. coli* is not capable of synthesizing AHLs because it does not have an AHL synthase (Van Houdt et al., 2006). However, it can sense AHL signals with the AHL receptor SdiA (Van Houdt et al., 2006). In addition, the addition of exogenous AHLs represses *E. coli* biofilm formation via SdiA (Lee et al., 2007a).

Indole

Indole is a quorum-sensing compound which can inhibit *E. coli* biofilm formation (Lee et al., 2007a). It is produced from tryptophan by the tryptophanase TnaA (Wood, 2009). Indole was initially reported to enhance biofilm formation in *E. coli* S17-1 (Di Martino et al., 2003). However subsequent research showed that indole inhibits biofilm formation for 9 non-pathogenic *E. coli* strains (Domka et al., 2006; Lee et al., 2007a; Zhang et al., 2007) and the pathogenic *E. coli* O157: H7 strain (Lee et al., 2007b). Interestingly, the AHL signal receptor SdiA is also required for indole to control biofilm formation (Lee et al., 2007a). Indole decreases *E. coli* biofilms by inhibiting motility, repressing acid resistance genes, repressing chemotaxis, and decreasing attachment to epithelial cells (Wood, 2009).

AI-2

The addition of AI-2 increases biofilm formation in *E. coli* (González Barrios et al., 2006b). AI-2 is a non-specific signal in both Gram-negative and Gram-positive bacteria. It is synthesized by *S*-ribosylhomocysterine lyase (LuxS), which converts the *S*-ribosylhomocysteine to homocysteine and (*S*)-4,5-dihydroxy-2,3-pentanedione (DPD) then DPD simultaneously changes into AI-2 molecules (Wood, 2009).

Cell signaling is influenced by temperature. Indole has a more significant effect on cell physiology and biofilm formation at low temperatures (25 and 30°C) compared with 37°C (Lee et al., 2008). In contrast, AI-2 addition has better effect at 37°C than 30°C (Lee et al., 2008). Hence it is quite possible that indole works primarily outside human host (relative lower temperature) while AI-2 works primarily inside the host (37°C) (Wood, 2009). This is the first time that the reason for redundant signals was figured out (Lee et al., 2008).

Many proteins change biofilm formation by affecting cell signaling. MqsR increases motility through quorum sensing signal AI-2 and QseBC (two-component motility regulatory system) and motility (González Barrios et al., 2006b) and by its RNase activity which results in conditions that degrade antitoxin MqsA which induces production of RpoS (Wang et al., 2011). In addition, MqsR induces *yncC* expression (González Barrios et al., 2006b). YncC (renamed to McbR) increases biofilm formation by repressing the production of colanic acid which is responsible colony mucoidy. YncC is also shown to work by repressing the predicted periplasmic protein-encoding gene *ybiM* (Zhang et al., 2008).

yliH and *yceP* are induced in biofilm cells vs. the planktonic cells (Schembri et al., 2003; Ren et al., 2004a). These two proteins are related to biofilm formation through catabolite repression by regulating the synthesis of quorum sensing signal indole and the stress response (Domka et al., 2006).

Another uncharacterized protein important for biofilm formation is TqsA (previously YdgG) (Herzberg et al., 2006). The expression of *tqsA* is induced in biofilms after 7 h (Ren et al., 2004a). The deletion of *tqsA* leads to a 7,000-fold increase in biofilm thickness and 574-fold increase in biomass in flow cells (Herzberg et al., 2006). The mechanism for TqsA controlling biofilm formation is that TqsA works as a transporter of the signal molecule AI-2 (Herzberg et al., 2006), which is tightly related to biofilm formation and exists both intercellular and intracellular.

2.2.4 Biofilm formation via stress-related genes

The expression of *bhsA* is induced 12 fold in *E. coli* biofilm cells compared to planktonic cells (Ren et al., 2004a). BhsA decreases biofilm formation in the presence of glucose. BhsA works as a multiple stress resistance protein which increases the cell resistance to acid, heat, hydrogen peroxide, and cadmium (Zhang et al., 2007). In addition, deleting *bhsA* changes cell hydrophobicity since it affects outer membrane proteins (Zhang et al., 2007).

The expression of the *ymg* locus is induced in biofilms in several DNA microarrays (Ren et al., 2004b; Herzberg et al., 2006; Domka et al., 2007; Lee et al., 2007a). The gene cluster *ymgABC* is important for cell acid resistance (many acid resistance-related genes are repressed in biofilms, such as *gadABC* and *hdeABD*) (Lee et al., 2007c). Critically, the 3D structure of YmgB is similar to the toxin Hha, while these two proteins have only 5% sequence identity. Thus YmgB (renamed to AriR) regulates acid-resistance and biofilm-related genes (Lee et al., 2007c).

2.3 Engineering biofilm formation and dispersal

2.3.1 Overview

Engineered biofilms have applications in many different fields including bioremediation, wastewater treatment, biofuels, specialty/bulk chemicals, biocorrosion control, disease treatment,

bioMEMS, and pharmaceutical testing (Wood et al., 2011). Progress has been making in controlling biofilm formation and dispersal to make biofilms useful.

The first engineered biofilm was for the inhibition of sulfate-reducing bacteria biofilm formation which causes corrosion on steels (Jayaraman et al., 1999a). The biocorrosion of the 304 stainless steel and 1018 mild steel by *Desulfovibrio vulgaris* was inhibited by expressing the antimicrobial peptides indolicidin and bactenecin from *Bacillus subtilis* BE1500 and *B. subtilis* WB600 (Jayaraman et al., 1999a).

Similar work was done by utilizing the *Bacillus brevis* 18 biofilm to produce Gramicidin S in situ and inhibit the corrosion by *D. vulgaris* on stainless steel (Jayaraman et al., 1999c). The pitting corrosion of aluminum 2024 was also reduced by secretion of anionic peptides by engineered and natural *Bacillus* biofilms (Örnek et al., 2002). The axenic aerobic biofilms of either *Pseudomonas fragi* K or *B. brevis* 18 also inhibit corrosion of copper and aluminum by *D. vulgaris* (Jayaraman et al., 1999b).

The first engineered biofilm using a genetic circuit to control biofilm formation by an external stress (UV light) was in *E. coli* (Kobayashi et al., 2004). The stress from UV light converts double-stranded DNA into single-stranded DNA while the RecA protease is activated at the same time. The active RecA then degrades a phage λ cI repressor (this repressor represses *traA* expression) and thus the *traA* expression is induced. The *traA* gene is directly related to conjugation so enhanced *traA* expression increases conjugation and biofilm formation.

The first synthetic circuit utilizing quorum sensing to control biofilm formation was performed with indole (Lee et al., 2007a). In a dual-species biofilm system with both *E. coli* and *Pseudomonas fluorescens*, The *P. fluorescens* cells were engineered to express toluene *o*-monooxygenase which converts indole to insoluble indigoid. The decrease of extracellular indole led to an increase of *E. coli* biofilm since indole inhibits biofilm formation (Lee et al., 2007a).

2.3.2 Protein engineering

SdiA

AHL and indole control *E. coli* biofilm formation via SdiA (Lee et al., 2007a; Lee et al., 2008). Protein engineering on SdiA was performed to obtain variants with altered biofilm formation (Lee et al., 2009a). With endogenous indole, two variants of SdiA1E11 (F7L, F59L, Y70C, M94K, and K153X) and SdiA14C3 (W9R, P49T, N87T, frameshift at N96, and L123X) were obtained that reduce biofilm formation 5 to 20 fold compared to wild-type SdiA (Lee et al., 2009a). SdiA1E11 induced indole synthesis compared with wild-type SdiA. This result was confirmed by indole assay which showed 9-fold more indole production by SdiA1E11; this result also confirms the importance of both indole and SdiA in *E. coli* biofilm formation. In addition, another variant SdiA2D10 increases biofilm formation 7 fold in the presence of *N*-octanoyl-*DL*-homoserine lactone and *N*-(3-oxododecatanoyl)-*L*-homoserine lactone. Hence SdiA can be evolved to both increase and decrease biofilm formation.

H-NS

H-NS is a global regulator in *E. coli* which controls genes related to stress response, biofilm formation and virulence (Hong et al., 2010a). By protein engineering via error-prone PCR, over two thousand mutants were screened for changed biofilm formation, and one mutant, H-NS K57N, is able to reduce biofilm formation dramatically (Hong et al., 2010a). The wild-type H-NS increases biofilm formation and the H-NS K57N reduces biofilm formation. DNA microarray shows that H-NS K57N represses biofilm formation by interacting with nucleoid-associated proteins Cnu and StpA. Critically, H-NS K57N enhances the excision of defective prophage Rac. The excision of Rac prophage affects biofilm formation and cell lysis (by increasing the toxin HokD production). Hence the function of H-NS in biofilm formation may be engineered by only a one amino acid replacement.

Hha

Hha is a global regulator which can decrease initial biofilm formation by repressing rare codon tRNAs and fimbrial genes transcription (García-Contreras et al., 2008). Hha is toxic and leads to cell lysis as well as biofilm dispersal. Protein engineering of Hha was performed to control biofilm dispersal and a variant Hha 13D6 (D22V, L40R, V42I, and D48A) was obtained (Hong et al., 2010b). Without changing initial biofilm formation, this mutant causes 96% biofilm dispersal in flow cells by increasing cell lysis.

2.3.3 Engineering bacteriophage for biofilm dispersal

Bacteriophage may be engineered to express biofilm-degrading enzymes during infection to bacterial cells (Lu and Collins, 2007). Lu et al. cloned *dspB* (encodes an enzyme that degrades the biofilm adhesin β-1,6-*N*-acetyl-*D*-glucosamine) into a T7 phage. The expression of DspB enzyme during the infection significantly improves the ability for removing biofilms (almost 100% dispersal).

2.4 Interkingdom signaling

2.4.1 Overview

Communication between prokaryotes and eukaryotes, no matter if it is beneficial or detrimental, has existed for millions of years (Hughes and Sperandio, 2008). An example is that there are 10^{13} human cells and 10^{14} bacterial cells in the human body. The existence of bacteria in human intestine helps nutrient assimilation while the intestine also maintains a proper living environment for these bacteria. Bacteria-host communication is definitely required for this beneficial mutual association. The medium for the communication between bacteria and the host are various hormones and hormone-like chemical compounds (Hughes and Sperandio, 2008), and several mechanisms are used for the hormonal communication between bacteria and hosts. The location of receptors usually coordinates with the structure of the hormone. More

specifically, amine and peptide hormones usually bind to cell-surface receptors (since they cannot penetrate the cell membrane) while steroid hormones usually bind to intracellular receptors (since they cannot cross the plasma membrane).

Bacteria and flies may have a symbiotic relationship. For example, the nematode *Howardula aoronymphium*, a destructive macroparasite which can parasitize at least 10 mushroom-feeding species of *Drosophila*, infects the female larvae of the fruit fly *Drosophila neotestacea* and prevents the eggs from developing (Jaenike et al., 2010). However, a maternally transmitted bacterium *Spiroplasma* sp. seems to be able to rescue female flies from the ill effects of the worm infection (Jaenike et al., 2010). The *Spiroplasma* sp. spreads in North American populations of *D. neotestacea* and this endosymbiont is spreading from east to west (Jaenike et al., 2010).

The house fly has been considered a potential agent for disease transmission for long periods (Nazni et al., 2005). The habitual movement of the house fly makes it an ideal candidate for the transmission of various diseases such as cholera, shigellosis, and salmonellosis. There are three modes for bacterial transmission by flies, including the fecal-oral route of transmission (Thomas et al., 1992; Kelly et al., 1994), mechanical transmission of rotavirus by legs and wings (Tan et al., 1997), and fly landing which can contaminate clean surfaces with around 0.1 mg food each time (De Jesus et al., 2004). The close relationship between bacteria and flies requires communication between these two organisms using interkingdom signaling as the medium.

Molecules constantly diffuse into the surrounding medium no matter it is the gas or liquid. These compounds can behave as attractants or repellents for insects (Dethier, 1947); hence, we are interested in the interkingdom signaling between insects and bacteria. The decomposition products of carrion, feces, and animal secretions such as sweat can be powerful attractants. Blowflies are attracted by the hydrolysis products (including sodium sulfide) from

keratin, egg albumin, lecithin, and butter; any kind of ammoniacal decomposition; mercaptans, indole, and skatole; several fatty acids; trimethylamine and isobutylamine; some organic sulfides, hydrogen sulfide, inorganic sulfides, and organic substances

Initial exploration of the attraction of bacterial culture to blowflies has been made by R. L. Emmens (Emmens and Murray, 1982). Blowflies lay eggs in response to the odours from the cultures of *Pseudomonas aeruginosa*, *Bacillus subtilis, Proteus mirabilis* and *Enterobacter cloacae*. *P. aeruginosa and E. cloacae* were not able to produce stimulants for oviposition with fleece components while *B. subtilis* was. In addition, *P. mirabilis* degraded wool fibres for sulphurous compounds.

2.4.2 Insects and biofilms

Maggot therapy is a type of biotherapy by which live and disinfected maggots are introduced into the non-healing skin and soft tissue wounds of humans or animals to selectively clean the necrotic tissue within a wound and promote the healing (Whitaker et al., 2007). Although this is an ancient method for healing infected wounds, it has been reintroduced into many hospitals in the twenty-first century after the appearance of bacterial antibiotic resistance (Jaklič et al., 2008). Maggot therapy is more simple and safe compared with antibiotic treatment. Hence the practice of this therapy is increasing around the world. The most often used flies are the facultative calliphorids and the most widely used species is the greenbottle fly *Lucilia sericata* (Whitaker et al., 2007). As described in above, bacteria gain a thousand-fold increase in antibiotic resistance in biofilms compared with free living cells. The advantage of maggot therapy over antibiotic therapy is that there is no need to worry about bacterial antibiotic resistance with the maggot therapy strategy. Hence the effect of maggots on the biofilm formation of pathogens is being studied by us. Cazander et al. have discovered that maggot excretions and secretions can inhibit the biofilm formation of PAO1 on polyethylene, titanium,

stainless steel surfaces (Cazander et al., 2009). It can even break down existing biofilms (Cazander et al., 2009). In addition, the maggot excretions and secretions still have activity even after 1 month storage at room temperature (Cazander et al., 2009).

2.5 Post-translational modification

Post-translational modification is the chemical modification of a protein after the translation step (Krishna and Wold, 1993). This kind of modification occurs in the last step of protein synthesis while some biochemical functional groups (acetate, phosphate, lipids, and carbohydrates) are attached to the amino acids in protein. Post-translational modification is crucial and more frequently found for regulating the functions of many eukaryotic proteins (Wold, 1981). However, more and more reports show that post-translational modification, especially phosphorylation, is also important in prokaryotes (Cozzone, 1988). In addition, recent studies also found that the acetylation works in prokaryotes (Escalante-Semerena, 2010). The post-translational modification of acetylation occurs for all three domains of life and regulates diverse aspects of metabolism in that 2700 proteins in mammals are acetylated related to central metabolism, mRNA splicing, protein synthesis, cell morphology, and cell cycle (Linda I et al., 2010). Although identified in 1963 for eukaryotes (Linda I et al., 2010), in bacteria, the role of acetylation has not been well characterized even though this modification is relatively common in that at least 91 proteins are acetylated in *E. coli*.

CHAPTER III

OMPA INFLUENCES *ESCHERICHIA COLI* BIOFILM FORMATION BY

REPRESSING CELLULOSE PRODUCTION THROUGH THE CPXRA TWO-

COMPONENT SYSTEM

3.1 Overview

Previously we discovered that OmpA of *Escherichia coli* increases biofilm formation on polystyrene surfaces (González Barrios et al., 2006a). Here we show OmpA influences biofilm formation differently on hydrophobic and hydrophilic surfaces since it represses cellulose production which is hydrophilic. OmpA increased biofilm formation on polystyrene, polypropylene, and polyvinyl surfaces while it decreased biofilm formation on glass surfaces. Sand column assays corroborated that OmpA decreases attachment to hydrophilic surfaces. The *ompA* mutant formed sticky colonies, and the extracellular polysaccharide that caused stickiness was identified to be cellulose. A whole-transcriptome study revealed that OmpA induces the CpxRA two-component signal transduction pathway that responds to membrane stress. CpxA phosphorylates CpxR and results in reduced *csgD* expression. Reduced CsgD production represses *adrA* expression and results in reduced cellulose production since CsgD and AdrA are responsible for 3,5-cyclic diguanylic acid synthesis and cellulose production. Real-time polymerase chain reaction confirmed *csgD* and *adrA* are repressed by OmpA. Biofilm and cellulose assays with double deletion mutants *adrA ompA*, *csgB ompA*, and *cpxR ompA* confirmed OmpA decreased cellulose production and increased biofilm formation on polystyrene

surfaces through CpxR and AdrA. Further evidence of the link between OmpA and the CpxRA system was that overproduction of OmpA disrupted the membrane and led to cell lysis. Therefore, OmpA inhibits cellulose production through the CpxRA stress response system, and this reduction in cellulose increases biofilm formation on hydrophobic surfaces.

3.2 Introduction

Cell appendages promote biofilm formation for *E. coli*. For example, flagella and type 1 pili are required for biofilm formation (Pratt and Kolter, 1998). In addition, the outer membrane protein antigen 43 increases biofilm formation in a fimbriae-independent way and facilitates multispecies biofilm formation (Danese et al., 2000b). Curli is another outer surface appendage that increases biofilm formation (Vidal et al., 1998).   In curli-producing strains, other outer surface appendages, such as colanic acid and flagella, no longer influence biofilm formation (Prigent-Combaret et al., 2000). Similarly, the conjugation pilus acts as an adhesion factor for cell-cell and cell-surface interactions which promotes biofilm formation, and this appendage overrides the importance of flagella, type 1 fimbriae, antigen 43, and curli (Reisner et al., 2003). Furthermore, exopolysaccharides (EPS), as well as its components such as colanic acid and cellulose, also affect biofilm formation (Sutherland, 2001). Although colanic acid is critical for biofilm three dimensional structure formation based on the research of Danese et al (Danese et al., 2000a), overproduction of colanic acid inhibits biofilm formation in *E. coli* BW25113 strains (Zhang et al., 2008). Cellulose synthesis is also required for *E. coli* 1094 biofilm formation on glass slides (Da Re and Ghigo, 2006). However, in a *csgD*-overexpressing strain of *E. coli* MG1655, cellulose production negatively affects curli-mediated surface adhesion and aggregation on hydrophobic polypropylene microtitre plates (Gualdi et al., 2008).

OmpA is a major protein of the outer membrane in *E. coli* K-12 strains (Chai and Foulds, 1977) with ~100,000 copies per cell (Smith et al., 2007). It is a representative protein

for outer membrane protein assembly and structure (Kleinschmidt, 2003), is a receptor for bacteriophage including K3, Ox2, and M1, acts as an immune target and is involved in adhesion (Smith et al., 2007). Due to its abundance in the bacterial outer membrane, and its interesting structure with four short loops that protrude from the cell (Smith et al., 2007), we hypothesized that it may play a role in bacterial biofilm formation. Previously, we identified that OmpA promotes biofilm formation in *E. coli* K-12 on polystyrene surfaces (González Barrios et al., 2006a), and Orme *et al.* found that OmpA is overproduced during biofilm formation using both laboratory and clinical strains of *E. coli* (Orme et al., 2006). OmpA binds to silicon nitride surfaces (Lower et al., 2005), and we found OmpA participates in the regulation pathway through which conjugative plasmids increase biofilm formation (Yang et al., 2008).   In *Acinetobacter baumannii*, OmpA plays a role in biofilm formation on plastic as well as in the bacterial attachment to biotic surfaces such as *Candida albicans* filaments and A549 human alveolar epithelial cells (Gaddy et al., 2009). At the genetic level, OmpA is negatively regulated by the σ^E-dependent small RNA MicA (Johansen et al., 2008).

Cpx stress response system is a two-component signal transduction system that includes a sensor kinase CpxA and a response regulator CpxR (DiGiuseppe and Silhavy, 2003). CpxA kinase autophosphorylates at His248 using ATP after sensing envelope stress, then transfers this phosphate to a conserved Asp51 of CpxR to form phosphorylated CpxR (CpxR-P) (Albert Siryaporn and Goulian, 2008). The Cpx system has been linked to biofilm formation since the expression of Cpx-regulated genes are induced during initial adherence of *E. coli* to abiotic surfaces (Otto and Silhavy, 2002). Mutations in *cpxA* also reduce biofilm formation by affecting microbial adherence to solid surfaces (Dorel et al., 1999), and the mechanism for this biofilm reduction is inactivation of the Cpx pathway which results in induction of CsgD which promotes curli synthesis as well as cellulose production under low temperatures (Dorel et al., 1999;

Prigent-Combaret et al., 2001; Gualdi et al., 2008).

The regulation of cellulose production by CsgD is complex. CsgD stimulates transcription of *adrA* (Zogaj et al., 2001), which encodes a putative transmembrane protein with a GGDEF domain (Römling et al., 2000). AdrA then activates cellulose production post-transcriptionally by interacting with the cellulose synthesis operons *bcsABZC* and *bcsEFG*, as well as producing an activator of cellulose biosynthesis (Gerstel and Römling, 2003). In addition to the CsgD/AdrA pathway, there are alternative pathways for cellulose production in both *E. coli* (Da Re and Ghigo, 2006) and *Salmonella* sp. (García et al., 2004) that also involve 3,5-cyclic diguanylic acid (c-di-GMP). For example, *E. coli* 1094 uses YedQ for regulating cellulose production (Da Re and Ghigo, 2006), and in *Salmonella* sp., cellulose synthesis is independent of AdrA, but dependent on STM1987 (García et al., 2004). In the probiotic *E. coli* strain Nissle 1917, neither the CsgD/AdrA pathway nor YedQ is required for cellulose production, although cellulose production is still regulated by c-di-GMP (Monteiro et al., 2009).

After discovering that OmpA increases biofilm formation on plastic surfaces (González Barrios et al., 2006a), we find here that OmpA influences biofilm formation in a surface-dependent manner (increases biofilm formation on plastic but decreases biofilm formation on glass). Hence, our goal was to explore the genetic basis of how OmpA influences biofilm formation in this divergent manner. Whole-transcriptome analyses were performed to identify pathways influenced by OmpA in biofilm formation, and we found the Cpx system might be activated by OmpA. In addition, we found cellulose production increases upon deletion of *ompA*, which in turn leads to the surface-dependent biofilm formation due to the hydrophilic nature of this polymer.

3.3 Results

3.3.1 OmpA increases biofilm formation on hydrophobic surfaces and decreases biofilm formation/attachment on hydrophilic surfaces

We investigated whether deletion of *ompA* would affect biofilm formation on different surfaces (hydrophilic and hydrophobic surfaces) after discovering that this deletion decreased biofilm formation on hydrophobic polystyrene (PS) surfaces (González Barrios et al., 2006a). Here, upon deleting *ompA*, a 10- to 20-fold reduction of biofilm formation was found on polystyrene, polyvinyl chloride (PVC), and polypropylene (PP) surfaces (Fig. 3.1A). This dramatic reduction in biofilm formation on hydrophobic surfaces was complemented by expressing OmpA from pCA24N_*ompA* with 0.2 mM isopropyl-β-*D*-thiogalactopyranoside (IPTG) (Fig. 3.1A) under conditions where these results were not influenced by cell density differences.

In contrast, under the same conditions, the *ompA* mutant made ~10-fold more biofilm than the wild-type strain on glass (hydrophilic) surfaces (Fig. 3.1B). We also tested the impact of deleting *ompA* via sand columns in order to study attachment to a hydrophilic surface (Fig. 3.2); deleting *ompA* increased the percentage of attached cells by as much as 10 fold at 21 min. As expected, the *fimA* mutant (negative control) had less attachment than the wild-type strain (Van Houdt and Michiels, 2005) (Fig. 3.2). Hence, OmpA reduces cell attachment to hydrophilic surfaces.

Furthermore, the deletion of *ompA* did not change cell growth; the specific growth rate for the *ompA* mutant was 1.65 ± 0.04 h^{-1} while that of the wild-type strain was 1.63 ± 0.04 h^{-1}. The effect of adding IPTG was also tested and 0.1 mM IPTG did not affect cell growth or biofilm formation for the *ompA* mutant. Hence, OmpA influences biofilm formation in a surface-dependent fashion that is not related to growth but instead is dependent on the

hydrophobicity of the abiotic surface.
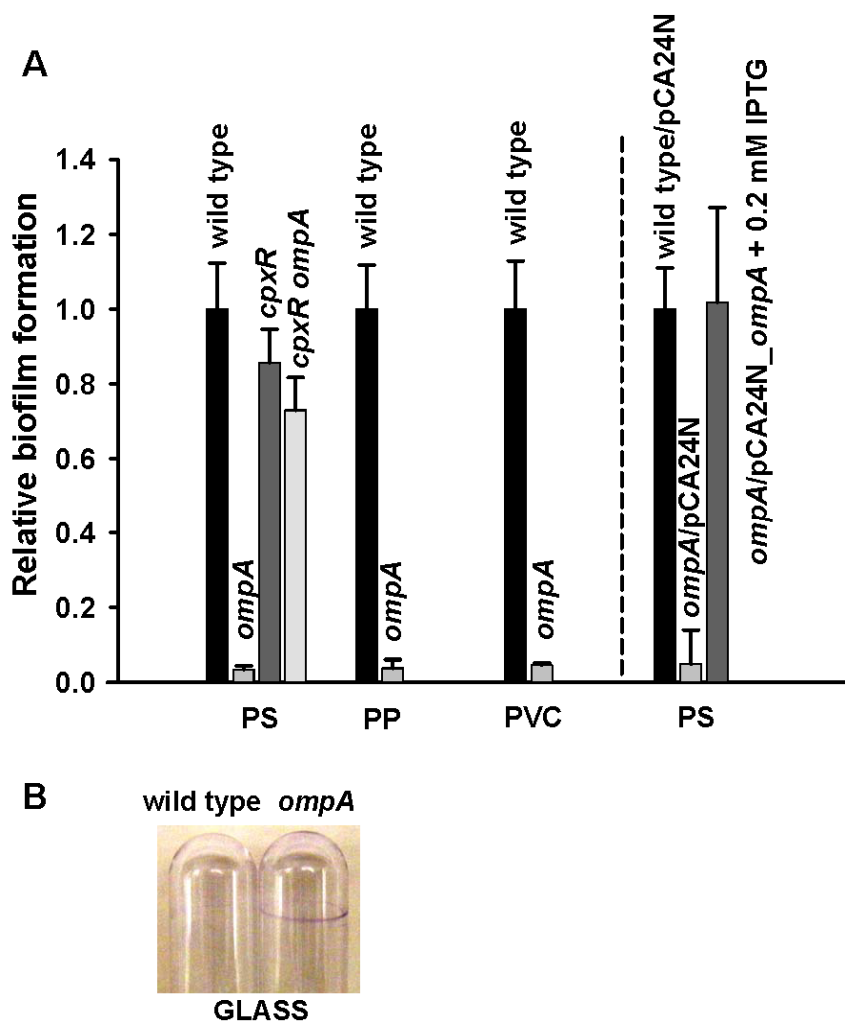
Figure 3.1 Biofilm formation on different surfaces. Relative normalized biofilm formation (total biofilm/growth) in Luria-Bertani medium (LB) at 37°C after 24 h for the *ompA* mutant *vs.* the BW25113 wild-type strain in 96-well plates constructed of polystyrene (PS), polyvinyl chloride (PVC), and polypropylene (PP), for the *cpxR* and *cpxR ompA* mutants in 96-well plates constructed of polystyrene, and for the wild-type/pCA24N, *ompA*/pCA24N, and *ompA*/pCA24N_*ompA* strains with 0.2 mM IPTG in 96-well plates constructed of polystyrene (A). Data are the average of 10 replicate wells from two independent cultures, and one standard deviation is shown. Biofilm formation for the BW25113 wild-type strain and the *ompA* mutant in LB at 37°C after 48 h in glass culture tubes (B).
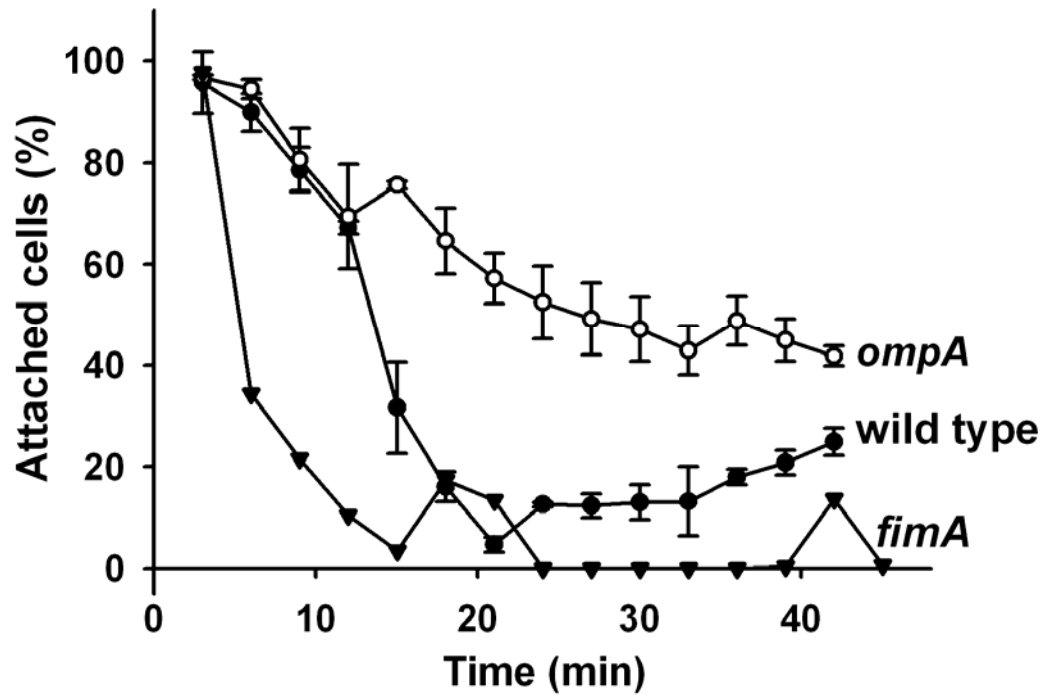
Figure 3.2 Attachment to sand columns. The percentage of attached cells was measured for the wild-type strain and the BW25113 *ompA* mutant at 37°C in LB medium. The BW25113 *fimA* mutant was used as fimbriae minus negative control. Data for the wild-type strain and the *ompA* mutant are the average of two independent cultures, and one standard deviation is shown.

3.3.2 Overproduction of OmpA leads to cell lysis

While deleting *ompA* did not affect cell growth, overproducing OmpA in shake flasks led to cell lysis (Fig. 3.3), which indicates OmpA expression increases envelope stress. With the same level of induction (0.1 mM IPTG), cells aggregated in overnight cultures of *ompA*/pCA24N_*ompA* while no cell clumping was seen in the *ompA*/pCA24N strain (vector control).

To corroborate the lysis seen upon visual inspection, cell lysis was quantified by measuring the genomic DNA released into the culture supernatants by the BW25113 *ompA*/pCA24N and *ompA*/pCA24N_*ompA* strains. Upon overproducing OmpA using 0.1 mM IPTG for 12.5 h, $48 \pm 5\%$ cell lysis occurred with *ompA*/pCA24N_*ompA* vs. $2.5 \pm 0.9\%$ cell lysis for the *ompA*/pCA24N strain. Hence, overproduction of OmpA leads to a 20-fold increase in cell lysis. These results were verified using an independent measure of cell lysis, via release of intracellular β-galactosidase activity. Since *E. coli* BW25113 does not have β-galactosidase activity due to mutated *lacZ,* we used *E. coli* MG1655/pCA24N and MG1655/pCA24N_*ompA*. Upon overproducing OmpA using 0.05 mM IPTG β-galactosidase activity increased 250 fold in the supernatant compared to that of the MG1655/pCA24N strain and similar levels of cell lysis were found compared to the genomic DNA method ($25 \pm 9\%$ cell lysis compared to $0.1 \pm 0.1\%$ cell lysis).

In addition, we also checked the influence of OmpA on other phenotypes. No differences between the wild-type strain and the *ompA* mutant were found for cell swimming motility, pH of planktonic cultures, EPS production, and colanic acid formation.

A

B
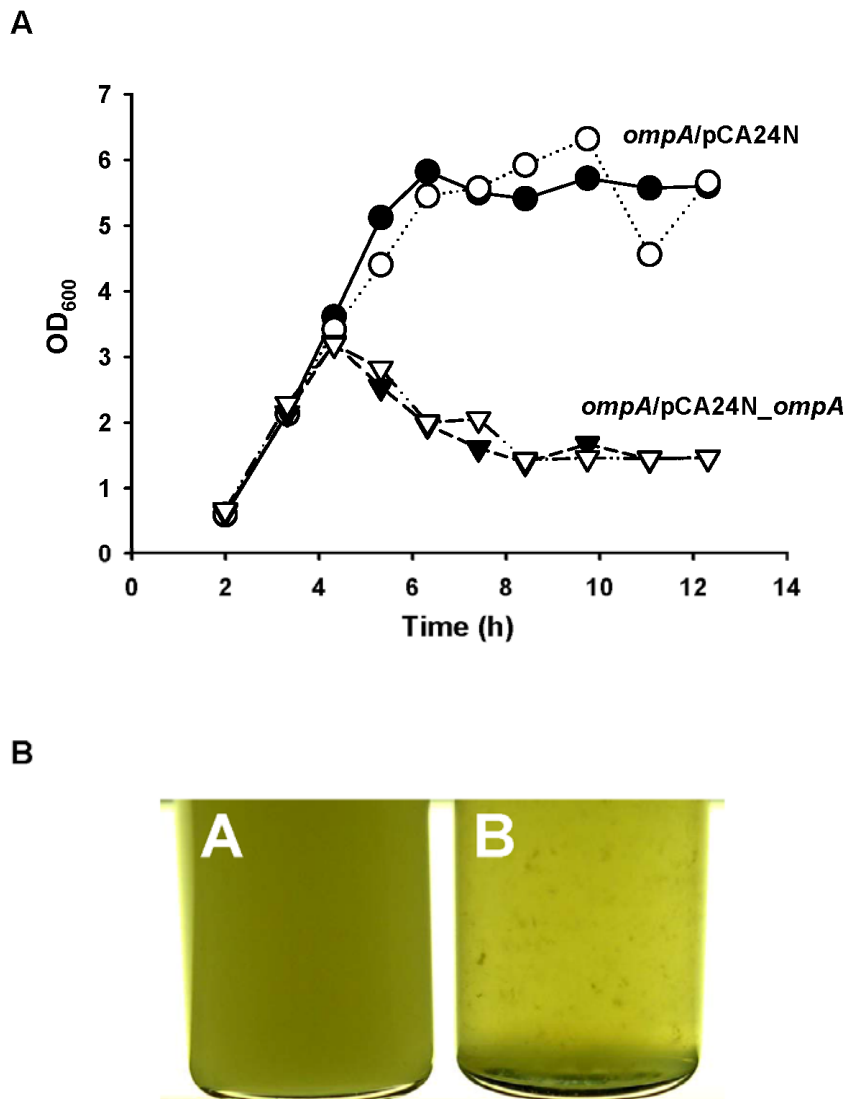
Figure 3.3 OmpA leads to cell lysis. Growth for the BW25113 *ompA*/pCA24N and *ompA*/pCA24N_*ompA* strains in LB at 37°C. Data are from two independent cultures (A). Cell clumping for *ompA*/pCA24N and *ompA*/pCA24N_*ompA* overnight cultures in LB at 37°C after 15 h (B). IPTG (0.1 mM) was added to each culture at 2.5 h to induce *ompA* expression.

3.3.3 OmpA induces *cpxP* expression

To further explore the role of OmpA in biofilm formation, a whole-transcriptome analysis of the *ompA* mutant *vs.* the wild-type strain was performed using biofilm cells collected from a hydrophobic (polystyrene) surface after 15 h of incubation (Table 3.1). *cpxP* was found to be the most repressed gene by deleting *ompA* (1.9 fold and 3.3 fold based on the two independent experiments). This result was corroborated by quantitative, reverse-transcription polymerase chain reaction (qRT-PCR) with biofilm cells from a third independent culture which showed *cpxP* was repressed by 2.7 fold. Hence, OmpA induces *cpxP* expression.

3.3.4 OmpA represses cellulose production

Colonies of the *ompA* mutant were found to be sticky compared to the wild-type strain, which indicated that the composition of the extracellular matrix may be changed by deleting *ompA*. Thus we tested colony morphology for the *ompA* mutant relative to the wild-type strain on Congo red plates at 37°C (Fig. 3.4) and found a red circle was formed around the *ompA* colony, which indicates deleting *ompA* may lead to the overproduction of some extracellular matrix that binds Congo red.

In *E. coli*, Congo red binds to both cellulose and curli (Da Re and Ghigo, 2006). To distinguish whether it is cellulose or curli that was overproduced in the *ompA* mutant, double mutants *adrA ompA* and *csgB ompA* (*csgB* encodes the curlin nucleator protein) were constructed by P1 transduction, and colony morphologies for these two strains were also tested with Congo red plates at 37°C. The *csgB ompA* mutant formed the same red EPS circle <u>outside</u> the colony as the *ompA* single mutant formed (Fig. 3.4), which indicates that without the curli gene *csgB*, the *ompA* mutation still increases Congo red-binding to substances around its colony. Hence, the Congo red-binding substance formed upon deleting *ompA* was not curli. The *adrA ompA* mutant lacked the outer red EPS circle, which indicates deleting *adrA* decreased Congo

red-binding. Hence, deleting *ompA* increases primarily cellulose production.

At 30°C (Fig. 3.4), the *ompA* mutant had a red, rough surface, which was due to the overproduction of primarily curli at this low temperature (Gualdi et al., 2008) since the wild-type strain, *ompA*, *adrA,* and *adrA ompA* all had red colonies due to curli formation whereas the curli-deficient strains *csgB*, *csgB ompA*, and *csgD* mutants had white colonies. Only the *ompA* mutant had a rough surface while the wild-type strain, the *adrA* mutant, and the *adrA ompA* mutant all had red, smooth surfaces which indicate increased cellulose production leads to a rough surface when curli are expressed at the same time.

Congo red-binding and calcofluor-binding assays were then performed for quantification of the cellulose production in planktonic cultures at 37°C, a temperature where curli is not generally formed (Fig. 3.5). Congo red was indicative of both curli formation and cellulose production while calcofluor was indicative for cellulose production (Da Re and Ghigo, 2006). Both assays showed the consistent result that the *ompA* mutation increases cellulose production by 6 to over 7 fold. Also from this assay we can see that cellulose production for the wild-type strain and the *adrA* mutant were similar, which means cellulose production in the wild-type strain is usually repressed under these conditions (Gualdi et al., 2008).

To confirm that the cellulose production in the *ompA* mutant was indeed much higher than in the wild-type strain, we detected cellulose on the exterior of the cells directly by measuring the glucose evolved upon its digestion with cellulase. Upon addition of cellulase, the glucose generated by digesting cellulose from the *ompA* mutant was 12 ± 4-fold higher than from the wild-type strain. The amount of cellulose produced by the wild-type strain in this assay was 0.011 ± 0.001 mg cellulose/mg protein, which is consistent with our calcofluor-binding result (0.02 ± 0.01 mg cellulose/mg protein).

Table 3.1   Partial whole-transcriptome profiles to determine the impact of OmpA on biofilm formation. Fold changes between polystyrene biofilm samples of the BW25113 *ompA* mutant *vs.* the BW25113 wild-type strain at 37°C after 15 h of incubation in LB are shown with two biological replicates PS-1 and PS-2. The GEO accession number is GSE14064. Important fold changes are shown in bold.

Gene	b #	Fold changes		Description
		PS-1	PS-2	
Signal transduction pathway				
cpxP	**b3913**	**-1.9**	**-3.3**	regulator of the Cpx response and possible chaperone involved in resistance to extracytoplasmic stress
Membrane proteins				
ompA	**b0957**	**-1097.5**	**-4096.0**	outer membrane protein A
htpX	b1829	-1.7	-1.6	heat shock protein, integral membrane protein
Metabolism				
fldA	b0684	-1.5	-2.5	flavodoxin 1
iscA	b2528	-1.5	-2.5	recruit and deliver Fe for Fe-S cluster assembly in IscU; possibly an alternative scaffold for Fe-S cluster assembly
iscU	b2529	-1.4	-3.0	NifU-like protein
iscS	b2530	-1.4	-2.3	cysteine desulfurase used in synthesis of Fe-S cluster
csrA	b2696	-1.4	-2.6	carbon storage regulator
ribB	b3041	-1.4	-2.1	3,4-dihydroxy-2-butanone 4-phosphate synthase
mgtA	b4242	2.1	2.1	magnesium transporter
Unknown				
ybeL	b0643	-1.2	-3.3	conserved hypothetical protein
ybjX	b0877	2.8	1.3	putative enzyme
ycfJ	b1110	2.0	1.3	putative periplasmic protein
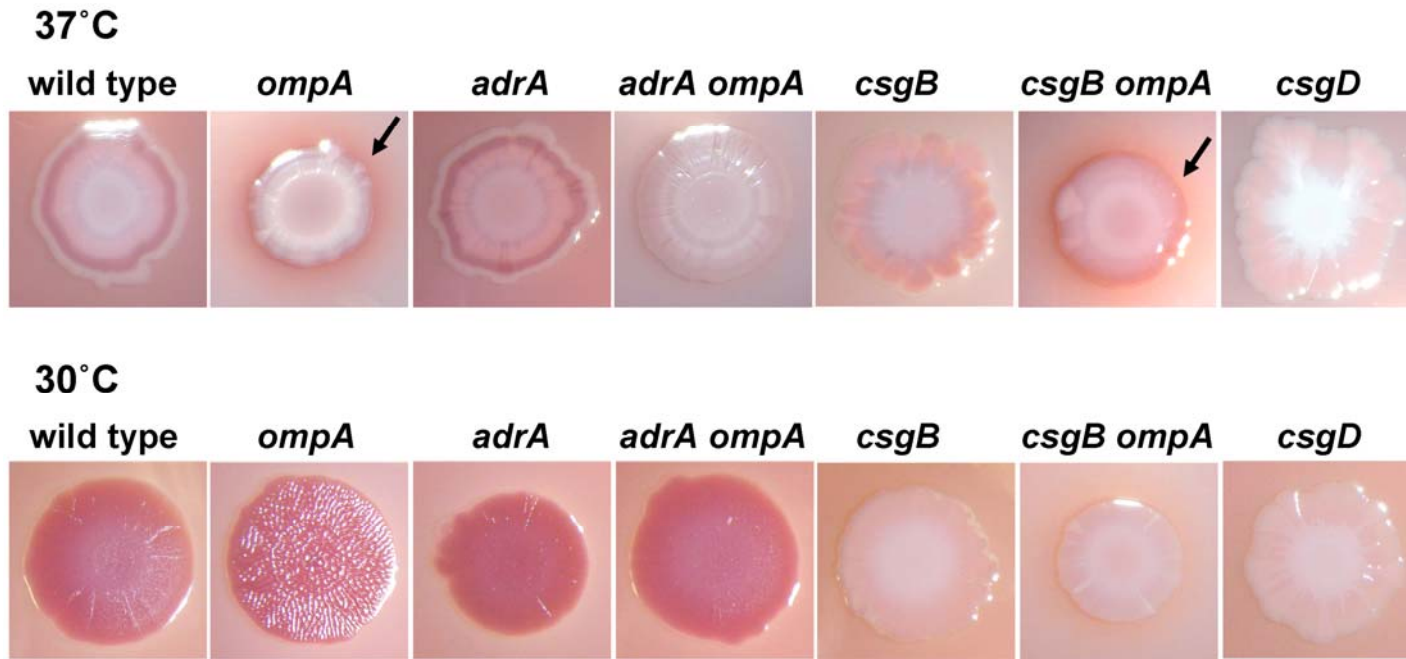
Figure 3.4 Colony morphology. The BW25113 wild-type strain, the *ompA* mutant, the *adrA* mutant, the *adrA ompA* mutant, the *csgB* mutant, the *csgB ompA* mutant and the *csgD* mutant were grown on Congo red plates at 37°C and 30°C. Black arrows point to the red zone of cellulose production around the *ompA* and *csgB ompA* mutants. Each panel is 2 cm by 2 cm in actual size on agar plates.
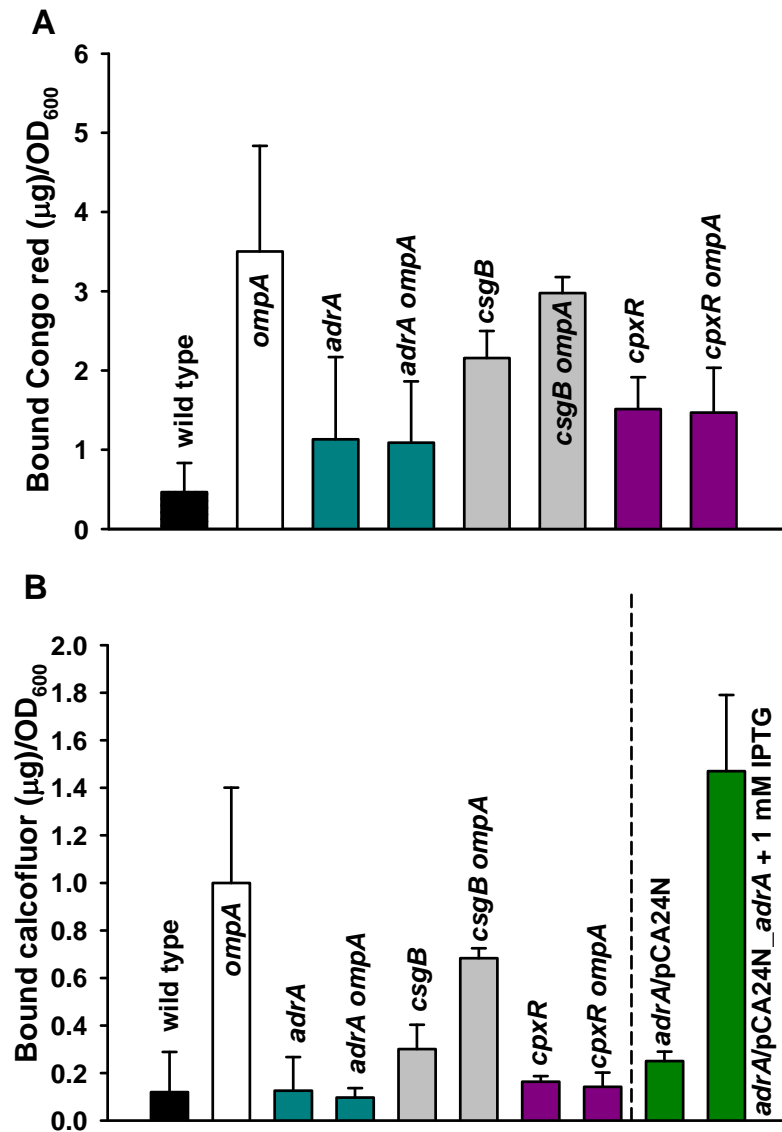
Figure 3.5 Quantification of cellulose production. Cellulose production quantification using Congo red for the wild-type strain, the BW25113 *ompA* mutant, the *adrA* mutant, the *adrA ompA* mutant, the *csgB* mutant, the *csgB ompA* mutant, the *cpxR* mutant, and the *cpxR ompA* mutant at 37°C in LB (A). Cellulose production quantification using calcofluor for the wild-type strain, the *ompA* mutant, the *adrA* mutant, the *adrA ompA* mutant, the *csgB* mutant, the *csgB ompA* mutant, the *cpxR* mutant, the *cpxR ompA* mutant, the *adrA*/pCA24N strain, and the *adrA*/pCA24N_*adrA* strain at 37°C in LB (B). *adrA* was induced with 1 mM IPTG. Data are the average of two independent cultures, and one standard deviation is shown.

To verify that the increase in cellulose upon deletion of *ompA* cellulose seen for planktonic cells also holds for biofilm cells, we repeated these three cellulose assays using biofilm cells collected from glass wool. As with planktonic cells, we found the biofilm cells of the *ompA* mutant had much higher cellulose production than the wild-type strain: ~4 fold using the Congo red-binding assay, ~6 fold using the calcofluor-binding assay, and ~22 fold using the cellulase digestion assay.

3.3.5 Short time induction of OmpA represses *csgD* and *adrA* expression

Since cellulose production was induced by deleting *ompA* but none of the cellulose-related genes had their expression changed in the whole-transcriptome studies with 15 h-old biofilm cells from polystyrene surfaces, we hypothesized that the expression of cellulose genes may be induced in the exponential phase *ompA* culture and change back to the wild-type levels after entering stationary phase, so they were not detected to have any transcription level difference in the whole-transcriptome studies performed with stationary-phase cells. Thus we performed qRT-PCR using exponential phase cultures of *ompA*/pCA24N_*ompA* and *ompA*/pCA24N (OmpA was induced with 0.1 mM IPTG for 30 min in exponential phase cultures with the turbidity at 600 nm around 0.5) and found expression of gene *csgD* and *adrA* was repressed 4.0 fold and 3.5 fold due to the expression of *ompA*. We used housekeeping gene *rrsG* as an internal reference for the qRT-PCR and calculated the changes of gene *csgD* and *adrA* expression based on the *rrsG* expression level. CsgD and AdrA synthesize c-di-GMP (Da Re and Ghigo, 2006), which binds to BcsAB (cellulose synthase) to increase cellulose production (Zogaj et al., 2001). Hence, OmpA represses *csgD* and *adrA* expression which should result in increased cellulose production as was seen upon deleting *ompA* (Fig. 3.4 & 3.5).

OmpA expression was only induced for 30 min with IPTG in this qRT-PCR experiment and the cell viability was not changed within this short time since Fig. 3.3A shows that the

turbidity at 600 nm for the OmpA overproduction strain starts to decrease after 2 h of induction with IPTG (IPTG was added at 2.5 h and the turbidity at 600 nm started to decrease after 4.5 h). This result was confirmed by a time-course β-galactosidase activity measurement using culture supernatants of the MG1655/pCA24N and MG1655/pCA24N_ompA strains that showed significant cell lysis occurred after 2 h induction with 0.05 mM IPTG (data not shown). Hence, OmpA causes cell lysis only when cell density and OmpA expression reaches some threshold level (after 2 h of induction by IPTG). Therefore, this qRT-PCR result was not affected by cell viability.

3.3.6 Cellulose inhibits biofilm formation on polystyrene plates

To corroborate our hypothesis that cellulose inhibits biofilm formation on plastic due to its hydrophilic nature, we overproduced AdrA with the *adrA*/pCA24N_*adrA* strain and assayed biofilm formation on polystyrene plates. With 1 mM IPTG, overproducing AdrA decreased biofilm formation by more than 10 fold on hydrophobic surfaces (Fig. 3.6). This reduction in biofilm formation was accompanied by a 5-fold increase in cellulose production upon inducing AdrA (Fig. 3.5B). Hence, cellulose inhibits biofilm formation on polystyrene plates.
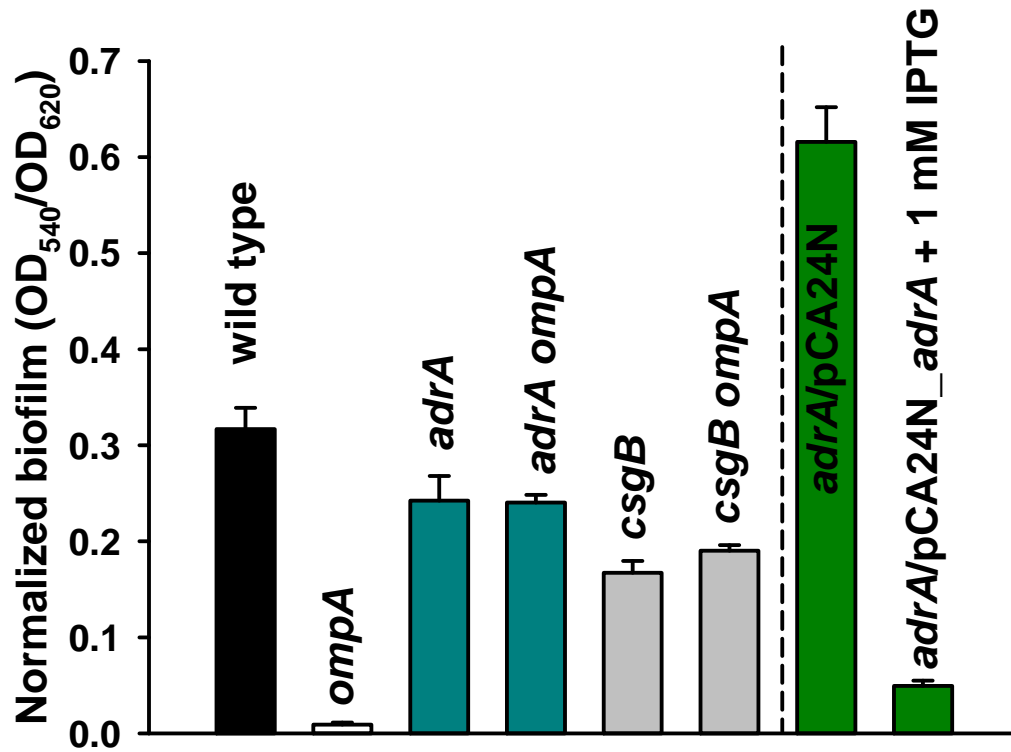
Figure 3.6 Biofilm formation for double mutants with both *ompA* and cellulose genes deleted. Normalized biofilm formation (total biofilm/growth) with polystyrene 96-well plates in LB at 37°C after 15 h. Data are the average of 10 replicate wells from two independent cultures, and one standard deviation is shown. BW25113 *adrA* was induced with 1 mM IPTG.

3.3.7 OmpA influences cellulose production and biofilm formation through CpxR

Since *cpxP* transcription was repressed in the *ompA* mutant cells that formed biofilm on polystyrene (Table 3.1) and since *cpxP* transcription depends almost exclusively on CpxR activity (Danese and Silhavy, 1998), we hypothesized that OmpA production may activate the two-component CpxRA system which increases CpxR phosphorylation. To study the relationship between OmpA and the CpxRA system and also their relationship with cellulose production and biofilm formation, we constructed a *cpxR ompA* double mutant via P1 transduction and measured its cellulose production (Fig. 3.5) and biofilm formation (Fig. 3.1A). The results show that without CpxR, deletion of *ompA* does not change cellulose production or biofilm formation. Hence OmpA represses cellulose production and increases biofilm formation on polystyrene by activating CpxR.

3.4 Discussion

In this study, we show OmpA influences biofilm formation through the Cpx stress response system which reduces cellulose production (summarized in Fig. 3.7) and results in more biofilm formation on hydrophobic surfaces and less biofilm formation on hydrophilic surfaces. The lines of evidence that support this are: (i) OmpA increases biofilm formation on hydrophobic surfaces and decreases biofilm formation on hydrophilic surfaces without affecting growth (Fig. 3.1), (ii) OmpA reduces attachment on hydrophilic surfaces (Fig. 3.2), (iii) OmpA overproduction leads to cell lysis (Fig. 3.3) indicating envelope stress, (iv) OmpA induces *cpxP* expression (Table 3.1) and qRT-PCR corroborated that OmpA induces expression of *cpxP* indicating an activation of the CpxRA signal transduction pathway (Danese and Silhavy, 1998), (v) the BW25113 *cpxR ompA* double mutant has a bigger colony size than either the *cpxR* or *ompA* single mutants (this phenotype was also observed in our study) which indicates a positive relationship between CpxR and OmpA as Typas et al. (Typas et al., 2008) reported, (vi) OmpA

represses cellulose production around colonies on the Congo red plate (Fig. 3.4, 37°C) and in planktonic cells as well as glass wool biofilm cells as shown three ways: via a Congo red assay, a calcofluor assay (Fig. 3.5), and a cellulase-digestion assay in which glucose was measured, (vii) double mutant *csgB ompA* has similar colony morphology with the *ompA* mutant, indicating it is cellulose, not curli, that was induced by deleting *ompA* (Fig. 3.4), (viii) double mutants *adrA ompA* and *cpxR ompA* fail to increase cellulose production compared with the *ompA* single mutant, while the *csgB ompA* double mutant has more cellulose production than the *csgB* mutant (Fig. 3.5), indicating a connection among OmpA, AdrA, and CpxR for regulating cellulose production, (ix) qRT-PCR shows OmpA represses *csgD* and *adrA* transcription which should reduce cellulose, (x) overproduction of AdrA increases cellulose production (Fig. 3.5B) and decreases biofilm formation on polystyrene plates (Fig. 3.6) which matches the *ompA* mutant phenotype with high cellulose production and low biofilm formation on polystyrene plates, and (xi) double mutants *adrA ompA* (Fig. 3.6) and *cpxR ompA* (Fig. 3.1A) have no change in biofilm formation compared with the *adrA* and *cpxR* single mutants, which means OmpA functions through AdrA and CpxR for controlling biofilm formation.

The Cpx-signaling pathway responds to stress from misfolded proteins from the inner membrane (Raivio and Silhavy, 1999) as well as to a lipoprotein located on the outer membrane, NlpE (Otto and Silhavy, 2002). Here we discovered the Cpx-signaling pathway also responds to the most abundant outer membrane protein, OmpA. Expression of *cpxP* was repressed in the *ompA* mutant (Table 3.1) and these results were corroborated by qRT-PCR. Transcription of *cpxP* is a result of CpxRA system activity and CpxR phosphorylation (Danese and Silhavy, 1998; Wolfe et al., 2008). In addition, cell lysis by overproduction of OmpA clearly indicates membrane stress occurred. Hence we hypothesize that the production of OmpA can directly or indirectly activate the CpxRA two-component stress response system.
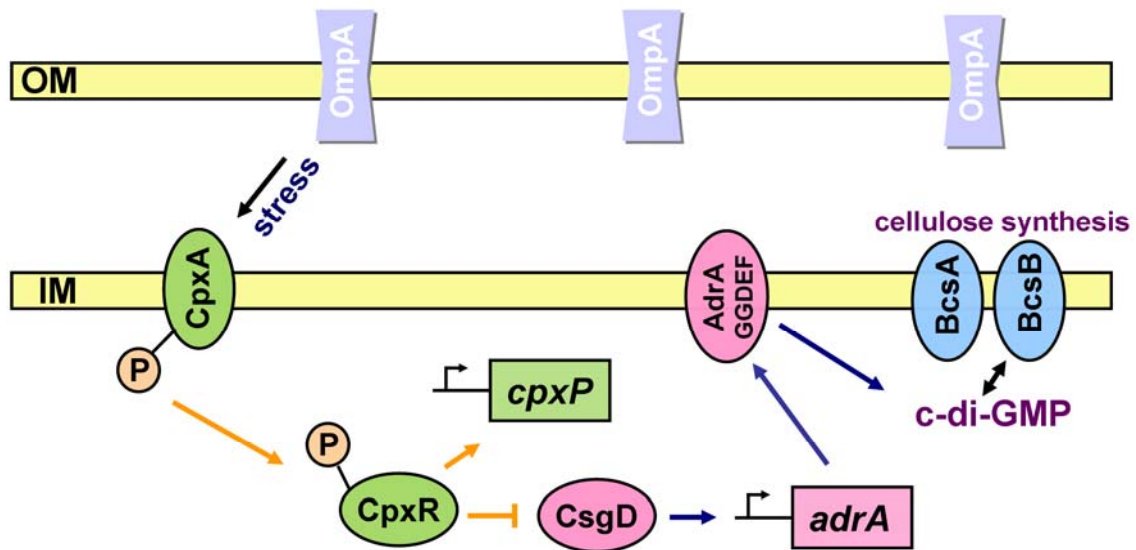
Figure 3.7 Hypothesized mechanism for cellulose production via OmpA. OmpA may activate the CpxRA two-component system which forms CpxR-P. CpxR-P induces *cpxP* transcription and represses *csgD* which leads to the repression of *adrA*. AdrA is responsible for c-di-GMP expression and cellulose production. → indicates induction and ⊥ indicates repression.

CpxR negatively regulates expression of *csgB* and *csgD* (Dorel et al., 2006). For the regulation of *csgD*, OmpR binds to the *csgD* promoter and activates *csgD* expression, whereas CpxR-P binds to its own recognition site on the *csgD* promoter which overlaps the OmpR-binding site and represses the *csgD* expression; thus, CpxR-P negatively affects *csgD* expression (Jubelin et al., 2005). This repression is triggered by osmolarity and curli overproduction (Prigent-Combaret et al., 2001). CsgD also regulates AdrA, a protein with a GGDEF domain, which is responsible for c-di-GMP synthesis and which is required for cellulose production (Zogaj et al., 2001; Gualdi et al., 2008). Since cellulose biosynthesis genes *bcsABZC* are constitutively transcribed, cellulose synthesis depends only on AdrA for synthesizing c-di-GMP which can control cellulose production by binding with BcsB (works with BcsA as cellulose synthase) and regulating the cellulose synthase activity (Zogaj et al., 2001; Gualdi et al., 2008). Our qRT-PCR result for *csgD* and *adrA* shows that with overproduction of OmpA, expression of *csgD* and *adrA* were both repressed, resulting in a reduction of cellulose production. Hence OmpA decreases cellulose production by inhibiting the CsgD/AdrA pathway. There may also be some alternative regulation pathways (Da Re and Ghigo, 2006) such as YedQ for cellulose production that are influenced by OmpA.

OmpA increases biofilm formation on hydrophobic surfaces (PS, PVC, and PP), decreases biofilm formation on hydrophilic surfaces (glass), and decreases attachment to sand by decreasing cellulose production. We explain this interesting observation based on the hydrophilic property of cellulose, a polysaccharide consisting of a linear chain of several hundred to over ten thousand β (1→4) linked *D*-glucose units. Previously, Römling *et al.* found AdrA is required for *Salmonella typhimurium* attachment to glass surfaces (Römling et al., 2000). In *S. enteritidis,* cellulose also increases biofilm formation on glass tubes (Solano et al., 2002). Therefore, cellulose promotes biofilm formation on glass, and we saw this with the *ompA*

mutant that produces more cellulose in that there was more biofilm formation on glass (Fig. 3.1B) and more attachment to sand (Fig. 3.2). We also found that increasing cellulose production by overproducing AdrA (Fig. 3.5B) decreases biofilm formation on hydrophobic polystyrene plates (Fig. 3.6). Hence, cellulose decreases biofilm formation on polystyrene, and it is repression of cellulose synthesis that causes OmpA to work differently on different surfaces.

Factors other than cellulose production can also influence biofilm formation, including curli formation, which is also regulated by CsgD (Römling et al., 2000). The interaction between cellulose and curli makes their influence on biofilm formation complex. Cellulose decreases curli-mediated biofilm formation on polypropylene microtitre plates (Gualdi et al., 2008), which can be explained by the hydrophilic property of cellulose; however, similar results were obtained also on glass, a hydrophilic surface. Curli helps adherence of *E. coli* to intestinal epithelial cells, and cellulose alone has no effect, but co-expression of cellulose and curli decreases this adherence (Wang et al., 2006). In addition, with pure water contact angle measurements, co-expression of cellulose and thin aggregative fimbriae leads to formation of a highly hydrophobic network while cellulose alone shows hydrophilic properties in *S. typhimurium* (Zogaj et al., 2001). In our biofilm and cellulose studies, we found the *csgB* mutant, deficient for curli formation, produces more cellulose than the wild-type strain and other mutants such as *cpxR* and *adrA* (Fig. 3.5). The *csgB ompA* double mutant produced high amounts of cellulose, lost the ability to decrease biofilm on polystyrene plates (Fig. 3.6), and its phenotype became similar to the *csgB* single mutant for biofilm formation. Hence we can make two hypotheses: (i) the deficiency of curli formation can lead to more cellulose production, or (ii) cellulose cannot decrease biofilm on polystyrene surfaces in the absence of curli.

OmpA exists in *E. coli* and in many enterobacteria. It is located on the outer membrane of bacterial cells, and functions as an adhesin and as an invasin (Smith et al., 2007). The

position of OmpA indicates its importance for adhesion and biofilm formation and also indicates that the regulation of OmpA may occur post-transcriptionally, which cannot be detected using transcription-level genetic tools such as whole-transcriptome studies and qRT-PCR. Hence, in addition to CpxRA, whose activation by OmpA is reflected in an increase in *cpxP* transcription, there may be additional regulatory pathways that OmpA works through to alter biofilm formation.

3.5 Experimental procedures

3.5.1 Bacterial strains, media, growth conditions, and growth rate assay

All the strains and plasmids used in this study are listed in Table 3.2. *E. coli* K-12 BW25113 and its isogenic mutants (Baba et al., 2006) were obtained from the Genome Analysis Project in Japan (Mori et al., 2000) and were used for all experiments except the β-galactosidase cell lysis experiments in which *E. coli* MG1655 was used. Plasmid pCA24N_*ompA*, carrying *ompA* under control of the $P_{T5\text{-}lac}$ promoter with tight regulation via the *lacI*^{q} repressor, as well as the empty plasmid pCA24N, were also obtained from the Genomic Analysis Project in Japan (Kitagawa et al., 2005). Expression of *ompA* and *adrA* was induced by 0.05 to 1 mM IPTG (Sigma, St. Louis, MO).

LB (Sambrook et al., 1989) was used to culture all the *E. coli* cells. Kanamycin (50 μg/mL) was used for pre-culturing the isogenic knock-outs. Chloramphenicol (30 μg/mL) was used for the strains harboring pCA24N and its derivatives. The specific growth rates of the *E. coli* wild-type strain and the *ompA* mutant were determined by measuring the turbidity at 600 nm for two independent cultures of each strain as a function of time with values less than 0.7. All experiments were performed at 37°C if not especially indicated.

Table 3.2 *E. coli* **strains and plasmids used in this study.** Km^r, Cm^r, and Ap^r denote kanamycin, chloramphenicol, and ampicillin resistance, respectively.

Strain/Plasmid	Genotype	Source
Strain		
BW25113	*lacI*^{q} *rrnB*$_{T14}$ *ΔlacZ*$_{WJ16}$ *hsdR514* *ΔaraBAD*$_{AH33}$ *ΔrhaBAD*$_{LD78}$	(Datsenko and Wanner, 2000)
MG1655	F$^-$ λ$^-$ *ilvG rfb-50 rph-1*	(Blattner et al., 1997)
BW25113 *ompA*	BW25113 Δ*ompA* Ω Km^r	(Baba et al., 2006)
BW25113 *cpxR*	BW25113 Δ*cpxR* Ω Km^r	(Baba et al., 2006)
BW25113 *adrA*	BW25113 Δ*adrA* Ω Km^r	(Baba et al., 2006)
BW25113 *csgB*	BW25113 Δ*csgB* Ω Km^r	(Baba et al., 2006)
BW25113 *csgD*	BW25113 Δ*csgD* Ω Km^r	(Baba et al., 2006)
BW25113 *fimA*	BW25113 Δ*fimA* Ω Km^r	(Baba et al., 2006)
BW25113 *cpxR ompA*	BW25113 Δ*cpxR* Δ*ompA* Ω Km^r	This study
BW25113 *adrA ompA*	BW25113 Δ*adrA* Δ*ompA* Ω Km^r	This study
BW25113 *csgB ompA*	BW25113 Δ*csgB* Δ*ompA* Ω Km^r	This study
Plasmid		
pCP20	Ap^r, Cm^r; temperature-sensitive replication and thermal induction of FLP recombinase	(Cherepanov and Wackernagel, 1995)
pCA24N	Cm^r; *lacI*^{q}, pCA24N	(Kitagawa et al., 2005)
pCA24N_*ompA*	Cm^r; *lacI*^{q}, pCA24N p$_{T5-lac}$::*ompA*	(Kitagawa et al., 2005)
pCA24N_*adrA*	Cm^r; *lacI*^{q}, pCA24N p$_{T5-lac}$::*adrA*	(Kitagawa et al., 2005)

3.5.2 Crystal violet biofilm assay

The biofilm assay was performed in 96-well PS, PP, and PVC plates as reported previously (Kim et al., 2009). Briefly, cells were inoculated at an initial turbidity at 600 nm of 0.05 and grown for 15 or 24 h without shaking, and then the cell density and total biofilm were measured using crystal violet staining. Each data point was averaged from at least twelve replicate wells (six wells from each of two independent cultures). For biofilm formation on glass, 1 mL of culture at a turbidity of 0.05 at 600 nm was loaded into 85 mm sterile glass culture tubes and incubated for 48 h without shaking, and then 1 mL 0.1% crystal violet was added for 20 min to stain the biofilm. At least two independent cultures were used with at least three tubes used for each strain.

3.5.3 EPS and colanic acid assays

The amount of total EPS and colanic acid was determined as described previously (Zhang et al., 2008). Briefly, about 60 mg of cell colony mass from overnight agar plates was boiled in water for 10 min. The supernatant were then used for an anthrone-H_2SO_4 assay to determine EPS concentrations, and colanic acid was determined by measuring the amount of fucose using sulfuric acid and cysteine hydrochloride as reagents. Each assay was performed with two independent cultures.

3.5.4 Sand column assay

The sand column assay was performed as described previously (Landini and Zehnder, 2002) with modifications to prevent damage to fimbriae (Kim et al., 2009). Rather than resuspending in PBS buffer, cells were directly inoculated into 250 mL LB medium with an initial turbidity of 0.05 at 600 nm and grown to a turbidity of 0.5 to 0.6. Then cells were added directly to the sand column (a 12 cm syringe column filled with 18 g of sterile sea sand) at a flow rate of 0.5 mL/min. Fourteen fractions (1.5 mL each) were collected, and the fraction of attached

cells was calculated as 1 - efflux turbidity/input turbidity. The fimbriae minus strain BW25113 *fimA* mutant was used as negative control.

3.5.5 Cell swimming motility assay and pH

Cell swimming motility was performed as previously described (Sperandio et al., 2002; Domka et al., 2006). Overnight cultures were used to inoculate into the plates. At least five plates were used for each independent culture, and two independent cultures were used for each strain. The pH of the supernatants of the overnight cultures was measured after removing cells by centrifuging at 16,000 g for 10 min.

3.5.6 P1 transduction

Transduction with P1 bacteriophage was used to construct the *cpxR ompA*, *adrA ompA*, and *csgB ompA* mutants using the Rapid Gene Knockout method (Maeda, 2008). Briefly, the kanamycin resistance gene (Km^r) was first removed by FLP recombinase (expressed from pCP20) from the $\Delta cpxR$ Ω Km^r, $\Delta adrA$ Ω Km^r, and $\Delta csgB$ Ω Km^r mutants, then bacteriophage P1 was grown with BW25113 $\Delta ompA$ Ω Km^r and the lysate was used for transduction into the three resulting kanamycin-sensitive strains. All six of the mutations were verified by colony PCR with primer sites located upstream and downstream of the deleted gene (Table 3.3). Single mutants were used as positive controls.

3.5.7 Cellulose assay using Congo red and calcofluor

To detect curli/cellulose production in the *ompA* mutant using bacterial colonies, 2 µL of overnight culture (with 50 μg/mL kanamycin for mutants) was spotted onto LB plates (no NaCl) containing 0.004% Congo red and 0.002% brilliant blue (Da Re and Ghigo, 2006). Plates were incubated for 24 h at 37°C and 48 h at 30°C. Red colonies indicate the binding of Congo red.

To quantify cellulose production for planktonic cells, the Congo red method of Lee et al. (Lee et al., 2007d) was used with some modifications; similarly, calcofluor was also used to

measure cellulose. Cells from two mL of a 14 to 15 h culture were centrifuged and resuspended in 1 mL 1% tryptone with 40 µg/mL Congo red or 16 µg/mL calcofluor and incubated for 2 h at 250 rpm. Bacterial bound Congo red or calcofluor were removed by centrifugation for 5-10 min at 17,000 g, and the amount of unbound Congo red or calcofluor was determined by measuring the absorbance of the supernatant at 490 nm for Congo red and at 350 nm for calcofluor.

3.5.8 Cellulose assay using cellulase

Colonies of the wild-type strain and the *ompA* mutant were collected from the surface of LB agar plates after overnight incubation at 37°C. For each strain, around 50 mg of cells were transferred into 400 µL 2.5M 2-(*N*-morpholino)-ethanesulfonic acid (MES) buffer (pH 5.5) with or without 6 U/mL cellulase (*Aspergillus niger*, MP Biomedicals) and incubated at 37°C for 16 h. Each sample was adjusted with 2.5 mM MES buffer to a turbidity of 40 at 600 nm and centrifuged. The glucose amount in the supernatant was measured using the glucose (HK) assay kit (Sigma-Aldrich) and compared to the signal obtained with no cellulase treatment.

3.5.9 Cellulose assay using biofilm cells

To quantify cellulose production in biofilm cells of the *ompA* mutant, cells were grown in 250 mL LB medium with 7 g glass wool for 14 to 15 h. The glass wool was washed twice with 0.85% NaCl and sonicated 2 min at 22 W (FS3 sonicator, Fisher Scientific Co.) in 100 mL of cold 0.85% NaCl buffer to release the cells which were centrifuged at 10,000 g for 2 min (J2-HS centrifuge, Beckman, Palo Alto, CA, USA). The Congo red-binding assay, calcofluor-binding assay, and cellulase treatment + glucose determination assay were then performed with these glass wool biofilm cells as indicated above.

Table 3.3   Primers used for qRT-PCR and double mutant verification.

Name	Sequence
qRT-PCR	
adrA	Forward: 5'- ACGGCATGACGGGCGTGTATAACC -3'
	Reverse: 5'- CGCAGGGTAATTTGTAACTGTCGGG -3'
csgD	Forward: 5'- ATACGCCTGAAGATTACCCGTACCG -3'
	Reverse: 5'- AGTAAGGAGGGCTGATTCCGTGC -3'
cpxP	Forward: 5'- GAACATCAGCGTCAGCAGATGCGAG -3'
	Reverse: 5'- GGTTGCGGACTTTTGCCATCTCAAC-3'
ybjX	Forward: 5'- TATGTCGCAGCTAACTGAACGGACC -3'
	Reverse: 5'- CCAGTGGGAAAGTTCGTTCATCCAC-3'
prpB	Forward: 5'- GCCGCTGTTTACCACCGACG AATTA -3'
	Reverse: 5'- GATGCTTTCGTACAGCTCGTTGCGG -3'
Verification of double mutations	
adrA	Forward: 5'- TATGAGTGCCTGCCTCAAGAAAGC -3'
	Reverse: 5'- GCGTACTGGAAGAGAAAGGCTTC -3'
csgB	Forward: 5'- CGCAGACATACTTTCCATCGTAACGC -3'
	Reverse: 5'- CGCTACCGGAGAATACGATTGCTG -3'
cpxR	Forward: 5'- CGTCTGATGACGTAATTTCTGCC -3'
	Reverse: 5'- GTGAATCGAGCTTGGGTAACATC -3'
ompA	Forward: 5'- GTTGTAGACTTTACATCGCCAGG -3'
	Reverse: 5'- GCTGGGTAAGGAATAACTGACG -3'

3.5.10 Cell lysis assays

Genomic DNA was used as in indicator of cell lysis. BW25113 *ompA*/pCA24N and *ompA*/pCA24N_*ompA* were inoculated into 25 mL of LB medium with an initial turbidity of 0.05 at 600 nm, and IPTG (0.1 mM) was added to both cultures after incubating for 2.5 h at 37°C with 250 rpm shaking. After a total of 15 h of incubating, 1.8 mL was sampled and centrifuged. The supernatant was purified with phenol/chloroform/isoamyl alcohol followed by precipitating with an equal volume of isopropanol in 1/10 volume 3 M NaOAc. The genomic DNA concentration was measured by quantitative PCR using primers for *purA* (encodes the subunit of adenylosuccinate synthetase), and the percentage of cell lysis was calculated as the ratio of genomic DNA concentration in the supernatant relative to that of the sonicated sample in which all genomic DNA was released. This experiment was performed with two independent cultures for each strain.

β-galactosidase was also used as in indicator of cell lysis. This assay was performed as described previously (Rice et al., 2007) except the β-galactosidase was generated from a chromosomal copy of *lacZ*[+] by the addition of IPTG. MG1655/pCA24N and MG1655/pCA24N_*ompA* were inoculated into 25 mL LB medium with an initial turbidity of 0.05 at 600 nm, and IPTG (0.05 mM) was added to both cultures after incubating for 2.5 h at 37°C with 250 rpm shaking. One mL of culture was harvested after 15 h and centrifuged for 2 min at 17,000 *g*. The β-galactosidase activity of the supernatant and sonicated cell pellet was measured as previously described (Wood and Peretti, 1991), and the percentage of cell lysis was calculated as the ratio of β-galactosidase activity in the supernatant relative to that of the sonicated cell pellet. This experiment was performed with four independent cultures for each strain.

3.5.11 RNA isolation from biofilms

Thirty g of polystyrene foam shavings of approximately 1 mm diameter was submerged in 250 mL medium and autoclaved. 2.5 mL overnight culture of the wild-type strain and the *ompA* mutant were inoculated into 250 mL of medium. After 15 h of incubation at 37°C, the polystyrene foam was washed twice in 200 mL of cold 0.85% NaCl buffer to remove planktonic cells, and the biofilm cells were removed by sonication at 22 W (FS3 sonicator, Fisher Scientific Co.) in 200 mL of cold 0.85% NaCl buffer. The buffer containing biofilm cells was then centrifuged at 10,000 g for 2 min at -2°C (J2-HS centrifuge, Beckman, Palo Alto, CA, USA). This cell pellet was resuspended in RNA*later* (Ambion) or RNAprotect (Qiagen), transferred to pre-chilled bead beater tubes, and centrifuged for 15 sec. Cells were lysed with 0.1 mm Zirconia/Silica beads (Biospec Products, Inc., OK) in a bead beater (Ren et al., 2004a), and total RNA was isolated using a Qiagen RNeasy Mini Kit.

3.5.12 Whole-transcriptome analysis

The *E. coli* GeneChip Genome 2.0 array (Affymetrix, P/N 900551) was used to analyze differential gene expression for the *ompA* mutant *vs*. the wild-type strain for biofilm cells on polystyrene. The *E. coli* GeneChip Genome 2.0 array contains 10,208 probe sets for open reading frames, rRNA, tRNA, and intergenic regions in four *E. coli* strains (MG1655, CFT073, O157:H7-Sakai, and O157:H7-EDL933). The cDNA synthesis, fragmentation, and hybridizations were performed as described previously (González Barrios et al., 2006b). Fragmented and labeled cDNA was hybridized for 16 h at 45°C, and global scaling was applied to make the average signal intensity 500. The probe array images were inspected for any image artifacts. Background values, noise values, and scaling factors of both arrays were examined and were comparable. The intensities of polyadenosine RNA controls were used to monitor the labeling process, and signals of the *araA* and *rhaA* deleted genes of BW25113 (Table 3.2) were

low. If the gene with the larger transcription rate did not have a consistent transcription rate based on the 11-15 probe pairs (*P*-value less than 0.05), these genes were discarded. A gene was considered differentially expressed when the *P*-value for comparing two chips was lower than 0.05 (to assure that the change in gene expression was statistically significant and that false positives arise less than 5%) and if their fold change is higher than standard deviation for the whole genome (Ren et al., 2004b). The expression data were deposited in the NCBI Gene Expression Omnibus and are accessible through accession number GSE14064.

3.5.13 qRT-PCR

qRT-PCR was performed using the StepOne™ Real-Time PCR System (Applied Biosystems, Foster City, CA). Total RNA (200 ng) was used for the qRT-PCR reaction using the SuperScriptTM III Plantinum® SYBR® Green One-Step qRT-PCR Kit (Invitrogen, Carlsbad, CA). Primers used are listed in Table 3.3. The housekeeping gene *rrsG* was used to normalize the gene expression data. The annealing temperature was 60°C for all of the genes in this study.

CHAPTER IV

ENGINEERING A NOVEL C-DI-GMP-BINDING PROTEIN FOR BIOFILM

DISPERSAL

4.1 Overview

Bacteria prefer to grow attached to themselves or an interface, and it is important for an array of applications to make biofilms disperse. Here we report simultaneously the discovery and protein engineering of BdcA (formerly YjgI) for biofilm dispersal using the universal signal 3,5-cyclic diguanylic acid (c-di-GMP). The *bdcA* deletion reduced biofilm dispersal, and production of BdcA increased biofilm dispersal to wild-type levels. Since BdcA increases motility and extracellular DNA production while decreasing exopolysaccharide, cell length, and aggregation, we reasoned that BdcA decreases the concentration of c-di-GMP, the intracellular messenger that controls cell motility through flagellar rotation and biofilm formation through synthesis of curli and cellulose. Consistently, c-di-GMP levels increase upon deleting *bdcA,* and purified BdcA binds c-di-GMP but does not act as a phosphodiesterase. Additionally, BdcR (formerly YjgJ) is a negative regulator of *bdcA*. To increase biofilm dispersal, we used protein engineering to evolve BdcA for greater c-di-GMP binding and found that the single amino acid change E50Q causes nearly complete removal of biofilms via dispersal without affecting initial biofilm formation.

4.2 Introduction

Biofilm dispersal is the last stage of biofilm development in which cells detach from the biofilm and disperse into the environment (Kaplan, 2010). The ability to control biofilm

_____

formation is important, since bacteria in biofilms are responsible for most infectious diseases (Romero et al., 2008), and biofilms need to be controlled for engineering applications such as biocorrosion (Jayaraman et al., 1999a). Dispersal occurs by two mechanisms: active dispersal which is initiated by the bacteria themselves and passive dispersal mediated by external forces such as fluid shear and abrasion (Kaplan, 2010).

Biofilm dispersal occurs both in unfavorable and favorable conditions. As biofilms grow, cells inside the biofilm may not be able to access nutrients and may not be able to release toxic compounds quickly, so biofilm dispersal allows cells to escape from the unfavorable conditions. Hence, a change in environmental conditions (e.g., nutrition level and oxygen depletion) can lead to the removal of biofilms (Karatan and Watnick, 2009). For example, *Pseudomonas aeruginosa* biofilms undergo dispersal in response to a sudden decrease/increase of substrates (Hunt et al., 2004; Sauer et al., 2004). Even when conditions are favorable, cells may leave the biofilm and attach to a new surface, where they can make more colonies. Therefore, biofilm dispersal is important for the survival of the species as it allows the bacterial population to expand (Kaplan, 2010). For example, reproducible, periodic dispersal occurs in *Actinobacillus actinomycetemcomitans* (Kaplan, 2010), *Pseudomonas putida* (Gjermansen et al., 2010), and *Serratia marcescens* (Rice et al., 2005). In addition, for many pathogenic bacteria, biofilm dispersal plays a critical role in the transmission of bacteria from environmental reservoirs to human hosts, in the transmission of bacteria between hosts, and in the exacerbation and spread of infection within a single host (Kaplan, 2010).

Biofilms may be dispersed by several mechanisms including by (i) degrading or repressing production of adhesive components in the biofilm matrix, (ii) degrading the substrate on which the biofilm colony is growing, (iii) lysing a subpopulation of cells (e.g., phage-mediated cell lysis), (iv) inducing motility, (v) producing extracellular surfactants such as

rhamnolipids, (vi) modulating fimbrial adherence, and (vii) increasing cell division at the outer surface of the biofilm colony (Kaplan, 2010). Proteins that increase biofilm removal upon their production include CsrA which represses synthesis of the adhesin poly-β-1,6-*N*-acetyl-*D*-glucosamine (Wang et al., 2005) in *Escherichia coli,* although it does not disperse biofilms in the presence of glucose (Jackson et al., 2002). Other proteins have been identified that, upon inactivation, prevent dispersal including DspB of *A. actinomycetemcomitans,* which degrades a linear polymer of *N*-acetylglucosamine (Kaplan et al., 2003), BdlA of *P. aeruginosa,* which decreases adhesiveness by decreasing c-di-GMP (Morgan et al., 2006), and AlpP of *Pseudoalteromonas tunicate,* which kills cells by producing hydrogen peroxide from L-lysine (Mai-Prochnow et al., 2008). In addition, NirS (Barraud et al., 2006) of *P. aeruginosa* produces, via BdlA, nitric oxide that is important for biofilm dispersal although nitric oxide alone removes 63% of biofilms but the combination of nitric oxide and chlorine can remove 85-90% of biofilms (Barraud et al., 2009).

Active dispersal based on motility is regulated by the universal intracellular signal c-di-GMP (Fig. 4.1A). c-di-GMP is synthesized by diguanylate cyclases, enzymes that are identified by a typical GGDEF motif, from two guanosine-5'-triphosphate molecules and degraded by phosphodiesterases (PDEs) which are characterized by an EAL or a HD-GYP domains (Dow et al., 2006). *E. coli* has 29 putative c-di-GMP related proteins, including 12 proteins with a GGDEF domain, 10 proteins with an EAL domain, and 7 proteins with both domains (Sommerfeldt et al., 2009). As an important intracellular signal, c-di-GMP affects many phenotypes including extracellular polysaccharide (EPS) production, biofilm formation, rugose colony development in *Vibrio vulnificus* (Nakhamchik et al., 2008) and *P. aeruginosa* (Ueda and Wood, 2009), and biofilm formation, cell length, and swimming motility in *E. coli* (Méndez-Ortiz et al., 2006).
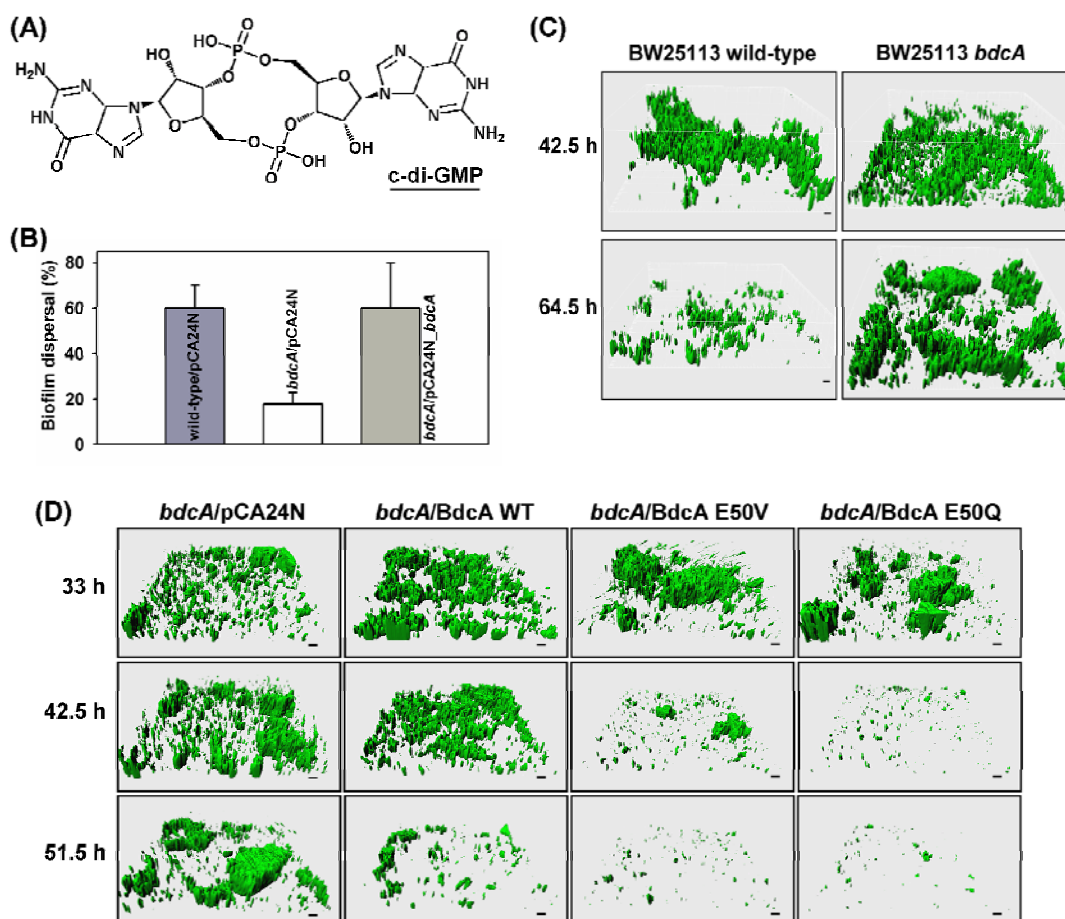
Figure 4.1 BdcA increases biofilm dispersal. Chemical structure of c-di-GMP (A). Relative normalized biofilm dispersal after 42 h with static biofilms formed in 96-well polystyrene plates **(B)**. Biofilms were formed with Luria-Bertani medium (LB) and 30 μg/mL chloramphenicol at 37°C using BW25113/pCA24N, *bdcA*/pCA24N, and *bdcA*/pCA24N_*bdcA*. Isopropyl-β-*D*-thiogalactopyranoside (IPTG) (0.1 mM) was added to each strain after 19 h of incubation. Biofilm formation after 23 h of IPTG induction (42 h total) is compared to the biofilm formation after 12 h of IPTG induction (31 h total) to obtain biofilm dispersal. Data are the average of 12 replicate wells from two independent cultures, and one standard deviation is shown. Representative Imaris images of flow cell biofilms after 42.5 h and 64.5 h of incubation with LB medium **(C)**. Each strain has pCM18 for producing GFP to visualize the biofilms, and erythromycin (300 μg/mL) was added to retain pCM18. Imaris images of flow cell biofilms of BW25113 *bdcA* producing evolved BdcA from pCA24N **(D)**. After forming biofilms in LB for 24 hr, IPTG (0.5 mM) was added to induce BdcA production for 9 h (33 h total), 18.5 h (42.5 h total), and 27.5 h (51.5 h). Each strain has the pCM18 plasmid for producing GFP. Chloramphenicol (30 μg/mL) was used to retain the pCA24N-based plasmids, and erythromycin (300 μg/mL) was used to retain pCM18. BdcA WT indicates native BdcA, BdcA E50V is the epPCR evolved BdcA, BdcA E50Q is the best saturation mutant. Scale bars represent 10 μm.

In this study, we focused on creating an engineered protein that causes bacteria to disperse. Using a biofilm screen for uncharacterized genes related to biofilm formation and the transport of the quorum-sensing (QS) signal autoinducer 2 (AI-2) (Herzberg et al., 2006), we identified that YjgI (renamed BdcA for biofilm dispersal via c-di-GMP) is a positive factor for removing biofilms. We explored the mechanism of how BdcA influences biofilm dispersal by a series of phenotype assays and determined that BdcA is a c-di-GMP-binding protein. In addition, we evolved BdcA by random mutagenesis and saturation mutagenesis of *bdcA* to obtain a more effective biofilm dispersal protein. Hence, we evolved the first protein for the enhanced biofilm dispersal, BdcA E50Q, resulting in nearly complete biofilm removal.

4.3 Results

4.3.1 BdcA increases biofilm dispersal

To identify proteins that may be used to remove biofilms, we screened biofilm formation with knockout mutants for 32 uncharacterized genes whose expression is altered by a *tqsA* deletion (Herzberg et al., 2006) (Table 4.1); TqsA is the putative exporter of QS signal AI-2, which enhances biofilm formation in *E. coli* (González Barrios et al., 2006b). We found that the *bdcA* mutant decreased biofilm dispersal by 3 ± 1 fold compared with the wild-type strain in a static biofilm assay with 96-well polystyrene plates (Fig. 4.1B), which suggested BdcA controls biofilm removal. To corroborate this biofilm result with a more rigorous assay and to further investigate the function of BdcA under other conditions (e.g., glass surface and continuous flow), we performed a flow cell assay and again found the *bdcA* mutant showed 6 ± 2-fold decreased biofilm dispersal (Fig. 4.1C and Table 4.2). The lack of biofilm dispersal was complemented by expressing *bdcA* in trans (Fig. 4.1B); hence, BdcA increases biofilm dispersal.

Table 4.1 List of biofilm formation. Normalized biofilm formation ($OD_{540\,nm}/OD_{620\,nm}$) in LB medium at 37°C for mutations in uncharacterized genes that are related to AI-2 transporter TqsA (Herzberg et al., 2006).

Strains	7 h	15 h	24 h
wild-type	0.052 ± 0.003	0.34 ± 0.01	0.1083 ± 0.0007
oxc	0.97 ± 0.05	0.26 ± 0.03	0.071 ± 0.008
ves	1.00 ± 0.02	0.42 ± 0.04	0.06 ± 0.02
yadS	0.98 ± 0.09	0.21 ± 0.03	0.06 ± 0.01
yafX	0.53 ± 0.03	0.27 ± 0.02	0.09 ± 0.02
ybaW	0.91 ± 0.03	0.25 ± 0.03	0.069 ± 0.004
ybfE	0.58 ± 0.02	0.25 ± 0.02	0.10 ± 0.01
ybfG	0.02 ± 0.01	0.20 ± 0.02	0.16 ± 0.01
ybfP	0.70 ± 0.05	0.25 ± 0.03	0.11 ± 0.02
ybhM	1.10 ± 0.04	0.39 ± 0.04	0.06 ± 0.01
ybjI	0.66 ± 0.03	0.28 ± 0.05	0.08 ± 0.02
yceO	0.03 ± 0.01	0.18 ± 0.01	0.17 ± 0.01
yciE	0.85 ± 0.03	0.37 ± 0.03	0.069 ± 0.005
yddJ	0.03 ± 0.01	0.25 ± 0.01	0.11 ± 0.01
yecT	0.015 ± 0.003	0.09 ± 0.01	0.1 ± 0.1
yfaA	0.80 ± 0.04	0.50 ± 0.03	0.085 ± 0.008
yfaE	0.55 ± 0.01	0.18 ± 0.02	0.12 ± 0.02
yfjR	0.47 ± 0.01	0.18 ± 0.03	0.20 ± 0.01
ygfF	0.74 ± 0.04	0.38 ± 0.03	0.12 ± 0.01
yghG	0.38 ± 0.01	0.46 ± 0.02	0.10 ± 0.01
yhaC	0.05 ± 0.01	0.22 ± 0.04	0.06 ± 0.01
yibE	0.75 ± 0.02	0.27 ± 0.03	0.10 ± 0.01
yicF	0.77 ± 0.01	0.33 ± 0.03	0.09 ± 0.02
yjbL	1.02 ± 0.04	0.30 ± 0.02	0.100 ± 0.009
yjfM	1.28 ± 0.05	0.32 ± 0.02	0.06 ± 0.01
yjgI (bdcA)	0.04 ± 0.01	0.12 ± 0.01	0.18 ± 0.02
yjgN	0.026 ± 0.005	0.40 ± 0.07	0.27 ± 0.04
yjiP	0.63 ± 0.02	0.40 ± 0.02	0.13 ± 0.02
ykiB	0.77 ± 0.05	0.30 ± 0.05	0.12 ± 0.06
ylbE	0.08 ± 0.01	0.31 ± 0.01	0.10 ± 0.01
yoga	0.68 ± 0.02	0.37 ± 0.03	0.11 ± 0.05
yodC	0.44 ± 0.01	0.040 ± 0.004	0.015 ± 0.004
ytfA	0.20 ± 0.01	0.53 ± 0.04	0.11 ± 0.02

Table 4.2 Flow cell statistical analysis of biofilms via COMSTAT for biofilms formed at 37°C. For the wild-type strain and the *bdcA* mutant, cultures were grown in LB for 24 h, 33 h, 42.5 h, 51.5 h, and 64.5 h. For *bdcA*/pCA24N, *bdcA*/BdcA, *bdcA*/BdcA E50V, and *bdcA*/BdcA E50Q, cultures were grown in LB with 30 μg/mL chloramphenicol for 24 h, and then *bdcA* expression was induced by adding 0.5 mM IPTG. Data were collected at 33 h, 42.5 h, and 51.5 h. BdcA is the native protein, BdcA E50V is the epPCR variant, and BdcA E50Q is the saturation mutagenesis variant.

COMSTAT values	Time	wild-type	*bdcA*	*bdcA*/pCA24N	*bdcA*/BdcA	*bdcA*/BdcA E50V	*bdcA*/BdcA E50Q
Biomass ($\mu m^3/\mu m^2$)	24 h	0.5 ± 0.8	0.4 ± 0.4				
	33 h	2 ± 3	2 ± 4	3 ± 3	3 ± 2	4 ± 3	4 ± 2
	42.5 h	2 ± 4	3 ± 2	4 ± 2	3 ± 1	0.8 ± 0.5	0.17 ± 0.07
	51.5 h	0.4 ± 0.3	2 ± 1	3.7 ± 0.8	1.7 ± 0.8	0.2 ± 0.3	0.16 ± 0.08
	64.5 h	0.3 ± 0.2	3 ± 2				
Surface coverage (%)	24 h	5 ± 2	5 ± 2				
	33 h	6 ± 6	8 ± 3	10 ± 3	13 ± 6	13 ± 7	11 ± 5
	42.5 h	5 ± 5	15 ± 9	13 ± 5	12 ± 4	5 ± 2	2.2 ± 0.7
	51.5 h	3 ± 1	14 ± 6	12 ± 4	10 ± 5	2 ± 1	3.0 ± 0.9
	64.5 h	2.6 ± 0.9	18 ± 9				
Average thickness (μm)	24 h	1 ± 1	0.8 ± 0.8				
	33 h	3 ± 5	3 ± 6	4 ± 4	5 ± 4	5 ± 3	4 ± 2
	42.5 h	4 ± 7	4 ± 3	5 ± 2	4 ± 2	1.1 ± 0.6	0.2 ± 0.1
	51.5 h	0.6 ± 0.4	3 ± 2	4 ± 1	2.3 ± 0.9	0.3 ± 0.4	0.2 ± 0.1
	64.5 h	0.5 ± 0.3	3 ± 2				
Roughness coefficient	24 h	1.89 ± 0.07	1.8 ± 0.1				
	33 h	1.8 ± 0.3	1.7 ± 0.2	1.6 ± 0.1	1.5 ± 0.2	1.5 ± 0.2	1.7 ± 0.1
	42.5 h	1.7 ± 0.3	1.5 ± 0.2	1.6 ± 0.2	1.6 ± 0.2	1.80 ± 0.07	1.92 ± 0.02
	51.5 h	1.89 ± 0.05	1.5 ± 0.1	1.60 ± 0.06	1.6 ± 0.2	1.91 ± 0.06	1.89 ± 0.04
	64.5 h	1.90 ± 0.04	1.5 ± 0.2				

4.3.2 BdcA increases cell motility and extracellular DNA (eDNA) while decreasing EPS production, cell size, and cell aggregation

To provide insights into the mechanism by which BdcA increases biofilm dispersal, we tested other biofilm-related phenotypes for the *bdcA* mutant and the *bdcA*-expressing strain. BdcA increased cell swimming motility by 2.2 ± 0.4 fold (Fig. 4.2A) and eDNA production by 3.05 ± 0.02 fold (Fig. 4.2B), while it decreased EPS production by 3 ± 2 fold (Fig. 4.2C), cell size by 2 ± 1 fold (Fig. 4.2D), and cell aggregation by 2.2 ± 0.7 fold (Fig. 4.2E). All five phenotypes seen upon producing BdcA are consistent with decreasing c-di-GMP concentrations (D'Argenio and Miller, 2004; Méndez-Ortiz et al., 2006; Nakhamchik et al., 2008; Ueda and Wood, 2010). Furthermore, the deletion of *bdcA* has the opposite effect on all these five phenotypes (Fig. 4.2), and production of BdcA from a plasmid complemented each of these phenotypes. Hence we hypothesized that BdcA may activate biofilm dispersal by decreasing the c-di-GMP concentrations in *E. coli*.

Importantly, four of the five phenotype changes found here (eDNA production, EPS production, cell aggregation, and cell size) were obtained with cells grown in biofilms. Planktonic cultures did not show differences in eDNA production, cell aggregation, and EPS production (cell size was not tested under this condition). This indicates that the physiological role of BdcA is strongly linked to biofilm formation.
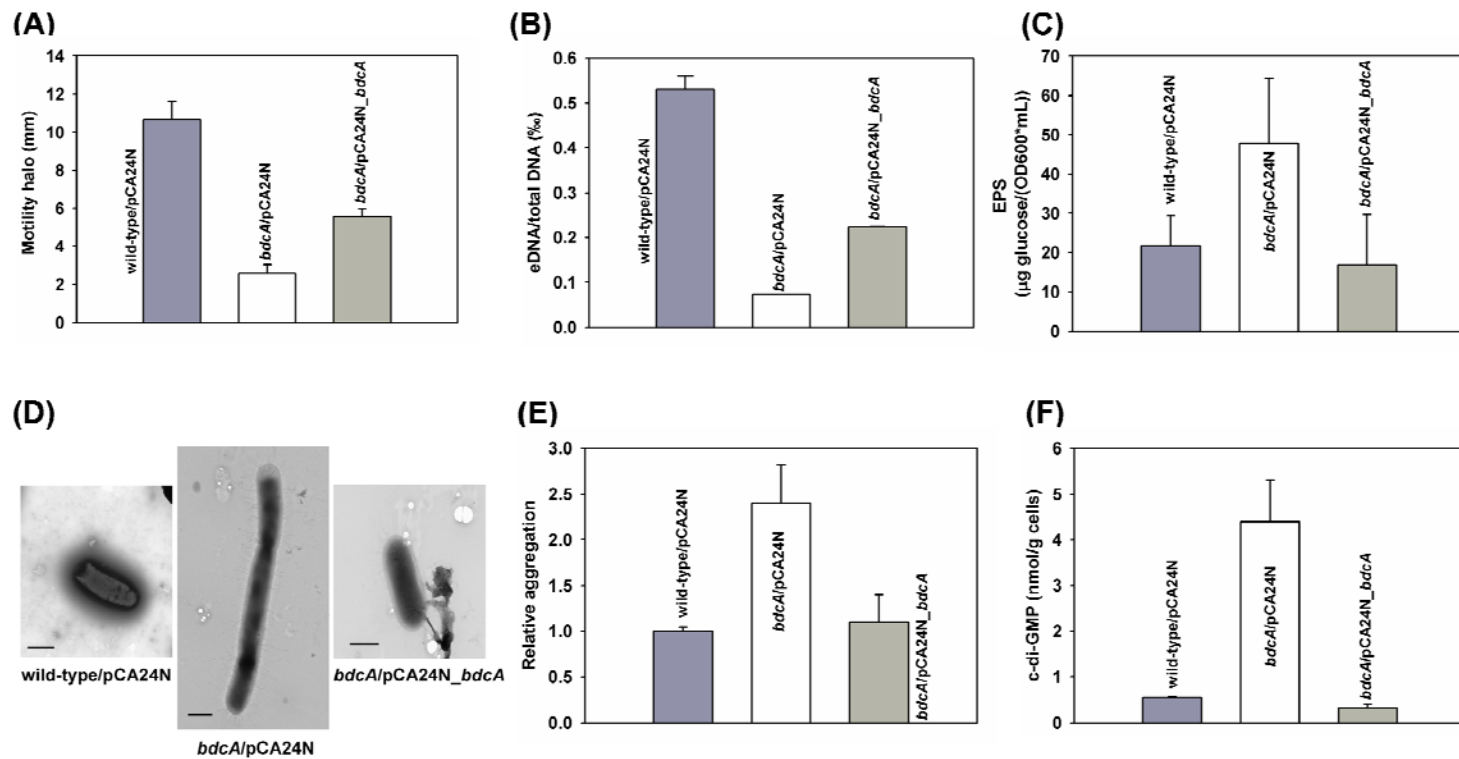
Figure 4.2 BdcA binds c-di-GMP to alter swimming, eDNA, EPS, cell morphology, and aggregation. Swimming motility after 15 h of growth on motility agar plates **(A)**. eDNA production after 24 h in 96-well plates **(B)**. EPS production after 24 h in 96-well plates **(C)**. Cell length after 24 h in 96-well plates **(D)**. Cell aggregation after 24 h in 96-well plates **(E)**. c-di-GMP concentration after 24 h (static cultures) **(F)**. All experiments were conducted in LB medium at 37ºC. *bdcA* was induced from pCA24N_*bdcA* via 0.1 mM IPTG, and 30 μg/mL chloramphenicol was used to retain the pCA24N-based plasmids. Data are the average of at least two independent cultures, and one standard deviation is shown.

4.3.3 BdcA binds c-di-GMP to control phenotypes

To confirm that BdcA can change the c-di-GMP level, we performed high performance liquid chromatography (HPLC) as previously described (Ueda and Wood, 2009) and measured the concentrations of c-di-GMP upon deleting *bdcA* and upon producing BdcA from plasmid pCA24N_*bdcA* via 0.1 mM IPTG. We found that deleting *bdcA* increased the c-di-GMP concentration 8 fold compared to the wild-strain and that producing BdcA decreased c-di-GMP concentrations back to the wild-type levels (Fig. 4.2F). Hence BdcA is directly or indirectly related to c-di-GMP levels in *E. coli*.

There are several ways BdcA may affect c-di-GMP concentrations. However, since BdcA has no DNA-binding motif and since there was no significant change in gene expression in the whole-transcriptome for the *bdcA* mutant vs. the wild-type strain (results not shown), BdcA is not likely to be a regulator that can change the transcription of c-di-GMP-related genes. Furthermore, since BdcA was annotated as putative enzyme, it seemed more plausible that BdcA controlled c-di-GMP concentrations as a phosphodiesterase or as a c-di-GMP-binding protein. Hence, we tested BdcA for PDE activity by purifying the His-tagged protein. HPLC indicated BdcA reduces c-di-GMP; however, we could not detect the traditional c-di-GMP degradation products 5′-phosphoguanylyl-(3′→5′)-guanosine (Rao et al., 2010) and guanosine monophosphate (GMP) (Schmidt et al., 2005) (Fig. 4.3). Therefore, BdcA decreases the concentration of c-di-GMP probably by binding rather than by catalyzing the degradation of c-di-GMP as a PDE. These results also show that no other effector is required for the binding of c-di-GMP by BdcA.

To prove that BdcA acts as a c-di-GMP-binding protein, not a PDE, we used ^{31}P nuclear magnetic resonance (NMR) spectroscopy since it shows a peak for c-di-GMP whether it is bound or unbound; hence, it may be used to quantify the amount of c-di-GMP after contact with BdcA.

Using NMR, we found the amount of c-di-GMP was not altered by treatment with purified BdcA (Fig. 4.4). Furthermore, BdcA was found to have a binding constant of 11.7 μM for c-di-GMP (Fig. 4.5), and unaltered c-di-GMP was recovered from BdcA after digestion with trypsin. Therefore, BdcA is not a PDE but instead alters phenotypes by changing c-di-GMP concentrations in the cell.

4.3.4 BdcR (YjgJ) regulates *bdcA*

We performed quantitative, reverse transcription-polymerase chain reaction (qRT-PCR) to check the transcription of *bdcA* in biofilms at different time points (from 2 h to 24 h). Gene expression of *bdcA* increases with incubation time and is maximum at 8 h (4.9 ± 0.3-fold more compared to 2 h) and decreases at 24 h (2.0 ± 0.2-fold less compared to 2 h). In addition, to investigate the regulation of *bdcA*, we measured *bdcA* transcription via qRT-PCR for the *yjgJ* mutant (*yjgJ* is upstream of *bdcA*) and the *yjgH* mutant (*yjgH* is downstream of *bdcA*) relative to the wild-type strain with 8 h cultures since this was the maximum for *bdcA* induction. *bdcA* expression in the *yjgJ* mutant was increased 7.3 ± 0.9 fold comparing to the value in the wild-type strain while *bdcA* expression in the *yjgH* mutant was not changed significantly (1.4 ± 0.2 fold vs. the wild-type strain). In addition, YjgJ is predicted to be a putative regulator with a helix-turn-helix motif, which is the most common DNA-binding motif in prokaryotic transcription factors (Ramos et al., 2005). Hence we conclude that the transcription of *bdcA* is time-dependent in biofilms and is controlled by a repressor YjgJ. We renamed the YjgJ as BdcR for its regulation of BdcA.
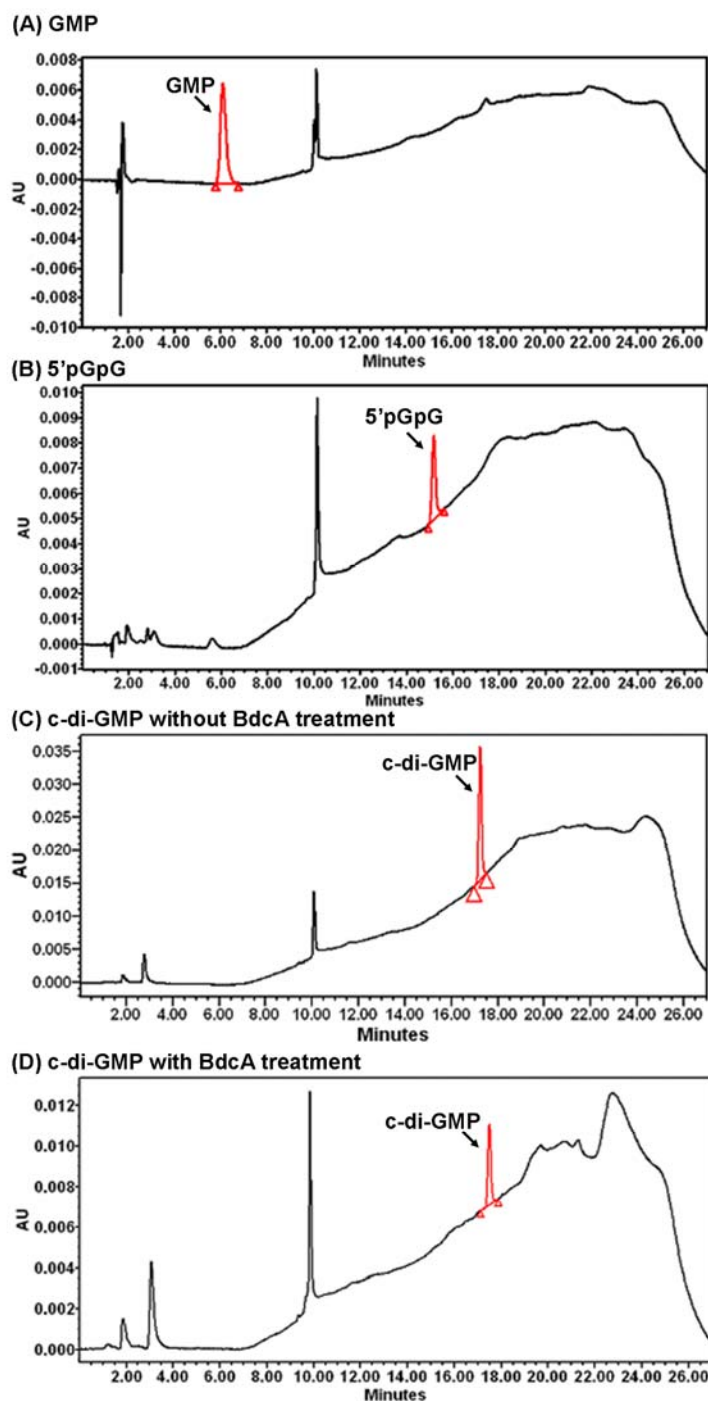
Figure 4.3 BdcA decreases free intracellular c-di-GMP. HPLC chromatogram for 10 μM guanosine monophosphate (GMP) **(A)**. HPLC chromatogram for 2.5 μM 5′-phosphoguanylyl-(3′→5′)-guanosine (5'pGpG) produced by treating 2.5 μM c-di-GMP with 2 μM of known phosphodiesterase YahA for 2 h at 37°C **(B)**. HPLC chromatogram for 10 μM c-di-GMP **(C)**. HPLC chromatogram after treating 10 μM c-di-GMP with 5 μM BdcA for 2 h at 37°C **(D)**.

³¹P NMR Spectrum of GMP

3.77

³¹P NMR Spectrum of c-di-GMP

-1.31

³¹P NMR spectrum of reaction mixture after incubation with BdcA E50Q

-1.31
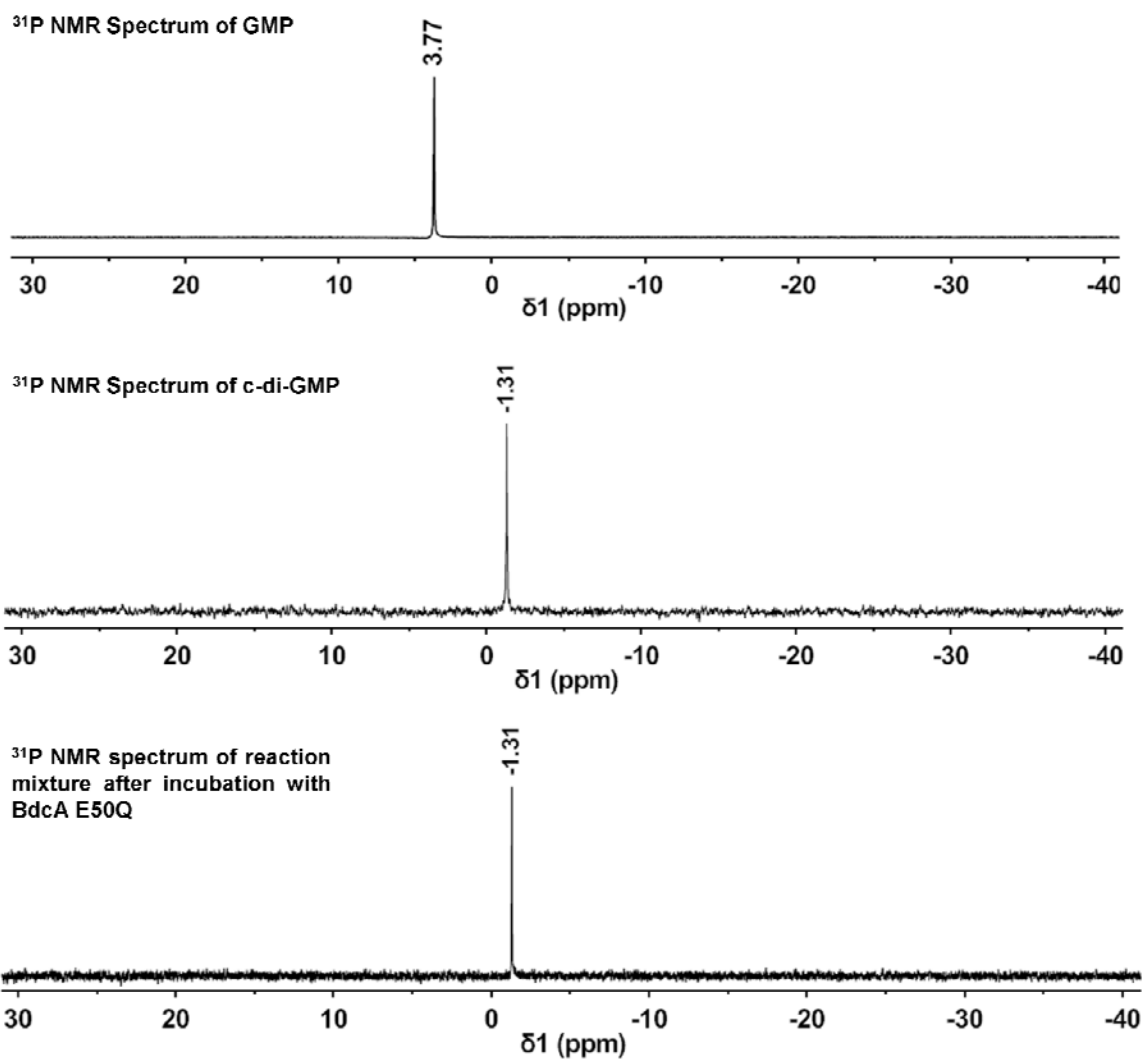
Figure 4.4   BdcA does not catalyze c-di-GMP degradation. ³¹P NMR spectrum for GMP and for c-di-GMP with and without BdcA E50Q. 85% phosphoric acid was used as an external standard for the chemical shift at 0 ppm.
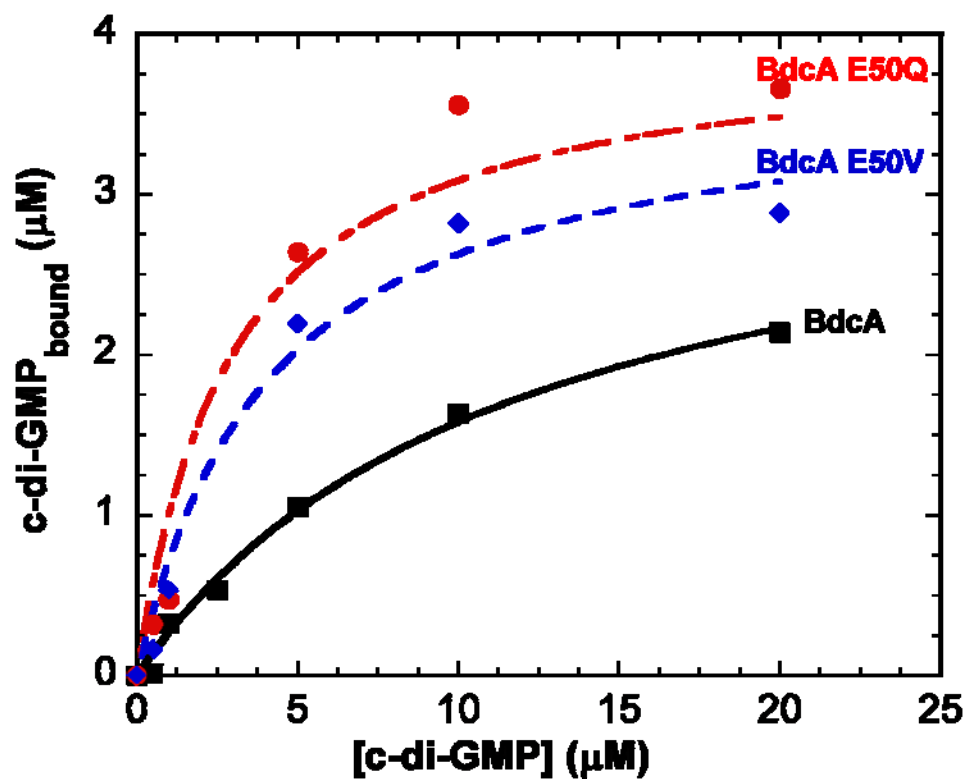
Figure 4.5 BdcA binds c-di-GMP. Binding curves for 10 μM BdcA, BdcA E50V, and BdcA E50Q with 0.5 to 20 μM c-di-GMP.

4.3.5 Protein engineering of BdcA for biofilm dispersal

After we indentified that BdcA reduces c-di-GMP concentrations, we used a novel protein engineering screen, based on higher motility (high motility indicates better dispersal due to reduction of c-di-GMP), to engineer superior biofilm dispersal. This screen was used rather than measuring biofilm removal directly, since it is much more efficient than a comparison of biofilms formed on two plates at two different time points.

Using random *bdcA* mutagenesis and expression of these mutant *bdcA* genes using BW25113 *bdcA*/pCA24N_*bdcA*, we screened ~6000 colonies for enhanced swimming motility. From the motility screen, we obtained 13 alleles with better motility and sequenced them. Among them, the strain producing BdcA E50V showed 2.8 ± 0.4-fold higher swimming motility and 6 ± 2-fold increased biofilm dispersal in 96-well plates compared to native BdcA. With only one amino acid changed (E50V), the binding constant of BdcA for c-di-GMP was reduced from 11.7 μM (native BdcA) to 4.2 μM (BdcA E50V) (Fig. 4.5), which indicates the BdcA E50V variant has higher affinity for c-di-GMP.

Since a single mutation randomly placed in codons generates on average only 5.6 out of 19 possible substitutions (Rui et al., 2004), we performed saturation mutagenesis on the codon of E50 and screened for mutants with higher motility than the *bdcA*/BdcA E50V strain. Over 400 colonies were screened to ensure the probability of trying all the possibilities is nearly 100% (Rui et al., 2004). By substituting all 20 amino acids into this position, we obtained the *bdcA*/BdcA E50Q mutant with 2.0 ± 0.2-fold higher swimming motility and 2 ± 1-fold increased biofilm dispersal ability compared to E50V. The binding constant of BdcA E50Q was measured as 3.0 μM (Fig. 4.5), which is smaller than BdcA E50V, indicating a further improved binding affinity to c-di-GMP.

Improved biofilm dispersal for strains producing the BdcA E50V and BdcA E50Q

protein engineering variants was confirmed using the flow cell assay (Fig. 4.1D and Table 4.2). After 33 h, biofilm formation was similar for the strains that lacked BdcA, that produce wild-type BdcA, that produce error-prone PCR (epPCR) variant BdcA E50V, and that produce saturation mutagenesis variant BdcA E50Q, indicating the four strains produce initially about the same amounts of biofilm. After IPTG induction for 18.5 h (42.5 h), the strains that produce BdcA E50V and BdcA E50Q showed 3.8-fold and 18-fold less biomass than the strain that produces native BdcA. This trend was consistent after IPTG induction for 27.5 h (51.5 h). Hence, the E50V and E50Q amino acid replacements (Fig. 4.6) dramatically increased the ability of BdcA to cause biofilm dispersal, and biofilm formation is almost completely removed.

4.4 Discussion

Protein engineering and recombinant engineering are promising strategies to control biofilm formation, but they have not been applied previously for enhancing biofilm dispersal. The first report for engineering biofilm formation via a genetic circuit used external stress from DNA-damaging agents to control the biofilm formation of *E. coli* (Kobayashi et al., 2004). Previously, we created the first synthetic circuit utilizing quorum-sensing signals to control biofilm formation by manipulating concentrations of the signal indole via toluene *o*-monooxygenase in a consortium of *Pseudomonas fluorescens* and *E. coli* (Lee et al., 2007a). In addition, we controlled *E. coli* biofilm formation by evolving the quorum-sensing regulator SdiA; upon addition of the extracellular signal *N*-acylhomoserine lactone, biofilm formation was increased with SdiA variant 2D10, and SdiA variant 1E11 was created that reduced biofilm formation by increasing concentrations of the inhibitor indole (Lee et al., 2009a). We also engineered the global regulator H-NS to control biofilm formation via prophage excision and cell death (Hong et al., 2010a). These results showed that bacterial biofilm formation may be controlled by manipulating key regulatory proteins and enzymes. Here we created the first

engineered protein for biofilm dispersal.
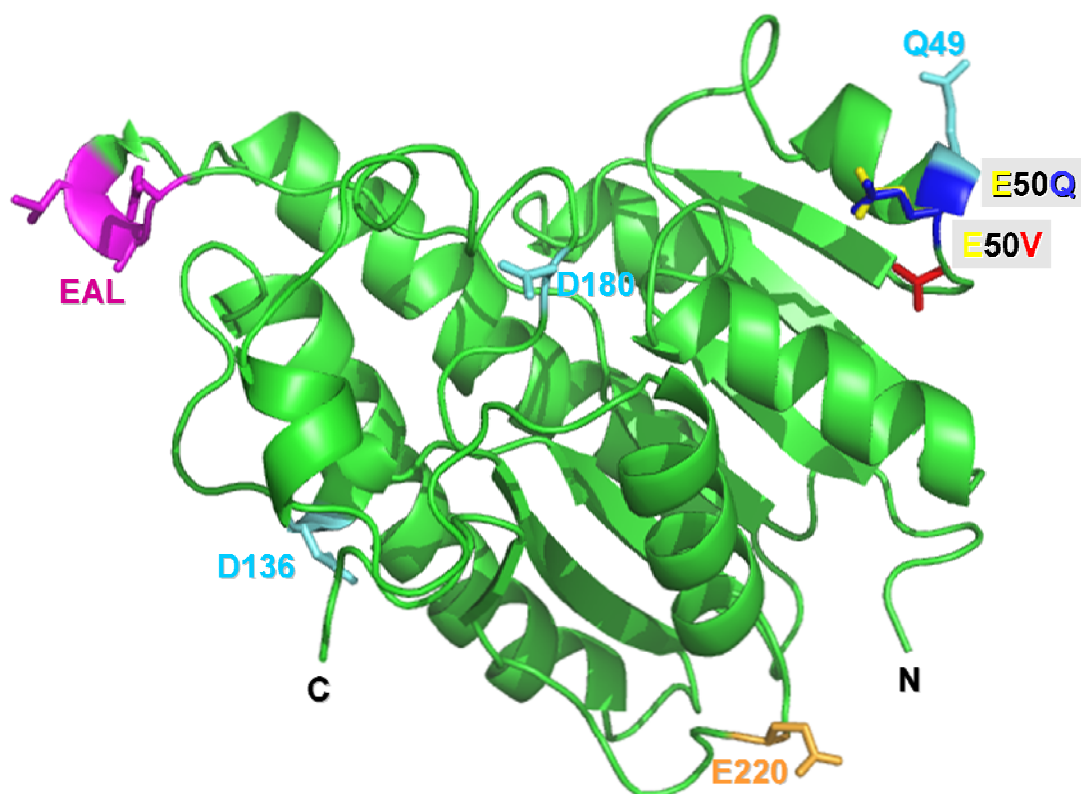
Figure 4.6   Swiss-model for evolved BdcA. The E50 residue is indicated in yellow, the E50V variant is indicated in red, and the E50Q variant is indicated in blue. The typical phosphodiesterase for c-di-GMP contains EALXR for coordinating Mg^{2+}, Q/R/D/D for c-di-GMP binding, and T/E for catalysis. The degenerate phosphodiesterase domains of BdcA are indicated: EAL in pink as part of the EALXR motif, Q49/D136/D180 in turquoise as part of the Q/R/D/D motif, and E220 in orange as part of the T/E motif. The amino and carboxy termini are marked as N and C.

BdcA is predicted to be an oxidoreductase with a Rossmann fold to bind nucleotides (Gherardini et al., 2010). Unlike PDEs, BdcA does not have complete amino acid domains for enzymatic activity as it lacks R of EALXR for coordinating Mg^{2+}, lacks R of Q/R/D/D for c-di-GMP binding, lacks T of the T/E catalytic domain (Sommerfeldt et al., 2009), and lacks completely HD-GYP (Dow et al., 2006) for catalysis (Fig. 4.6). BdcA is also smaller (237 aa) than most PDEs. Hence, BdcA does not catalyze c-di-GMP degradation. Intracellular measurements show that BdcA decreases c-di-GMP concentrations, and the *in vitro* studies indicate BdcA directly reduces unbound c-di-GMP concentrations. Since ^{31}P NMR spectroscopy showed that c-di-GMP is not degraded, since the usual c-di-GMP degradation products were not detected, and since we recovered fully c-di-GMP from BdcA after trypsin digestion, we conclude that BdcA controls biofilm removal and many other biofilm-related phenotypes (motility, EPS, eDNA, cell length, and aggregation) through its direct binding of c-di-GMP. Also, our estimate is that upon producing BdcA from pCA24N_*bdcA,* BdcA levels are 200-fold greater than c-di-GMP on a molar basis; hence, binding of c-di-GMP by BdcA is reasonable to explain the phenotypes seen.

It is not necessary for BdcA to interact with other proteins to control these phenotypes; for example, by decreasing the concentration of free c-di-GMP, motility is enhanced by releasing the brake on motility via YcgR. YcgR reduces bacterial swimming by binding c-di-GMP and interacting with MotA to act as a brake that limits individual stator complexes (Boehm et al., 2010) as well as interacts with flagellar proteins FliG and FliM in the presence of c-di-GMP to reduce torque (Paul et al., 2010).

c-di-GMP also controls many other vital processes in bacteria; however, the mechanisms by which c-di-GMP affects these phenotypes are diverse and our understanding is not always complete. c-di-GMP riboswitches bind the second messenger to control complex physiological

processes such as biofilm formation, virulence gene expression, and persistence of infection in *V. cholerae* (Kulshina et al., 2009). Alternatively, the transcriptional regulator VpsT in *V. cholerae* directly senses c-di-GMP by oligomerizing upon c-di-GMP binding to control extracellular matrix production, motility, and biofilm formation (Krasteva et al., 2010). LapD of *Pseudomonas fluorescens* regulates surface attachment via LapA by binding to intracellular c-di-GMP (Newell et al., 2009). Our results show we have identified a novel class of protein that controls cellular activity (i.e., biofilm dispersal) by binding c-di-GMP.

Without knowing the detailed mechanism about how c-di-GMP affects biofilm formation in *E. coli*, we evolved BdcA to create a better biofilm-dispersing protein. These results provide further evidence of the tight relationship between c-di-GMP and biofilm dispersal. The most important amino acid replacements occurred at the E50 position. By replacing glutamic acid with valine (E50V) and glutamine (E50Q), these one amino acid changes progressively increase the binding affinity of BdcA for c-di-GMP, which subsequently reduces, in a corresponding manner, the intracellular c-di-GMP concentrations. Supporting increased c-di-GMP binding, the E50 position is adjacent to the Q49 position of the remnant Q/R/D/D motif for c-di-GMP binding by PDEs.

With BdcA, we demonstrate that we can control the final stage in biofilm development, dispersal, by performing protein engineering on a single regulator. Therefore, although there are myriad genetic paths leading to biofilm formation, biofilm dispersal may be triggered via a single engineered protein. Furthermore, this work is promising in terms of broad applications since c-di-GMP is utilized by diverse bacteria (D'Argenio and Miller, 2004) and in nearly all these strains it controls motility; hence, reduction of c-di-GMP concentrations may be a universal mechanism for increasing bioiflm dispersal. Also, *bdcA* shows high sequence conservation with other species with the highest similarity to a homolg in *Shigella* sp. (98%).

Furthermore, the genera *Klebsiella, Salmonella, Xanthomonas, Citrobacter, Sphingopyxis, Pantoea, Roseomonas* show *bdcA* sequence conservation above 70%. In addition, 17 other bacteria show over 50% protein sequence identity with BdcA in the *E. coli* BW25113 strain (Fig. 4.7). Thus, BdcA is well conserved in many bacteria and may be used for biofilm dispersal by many strains.
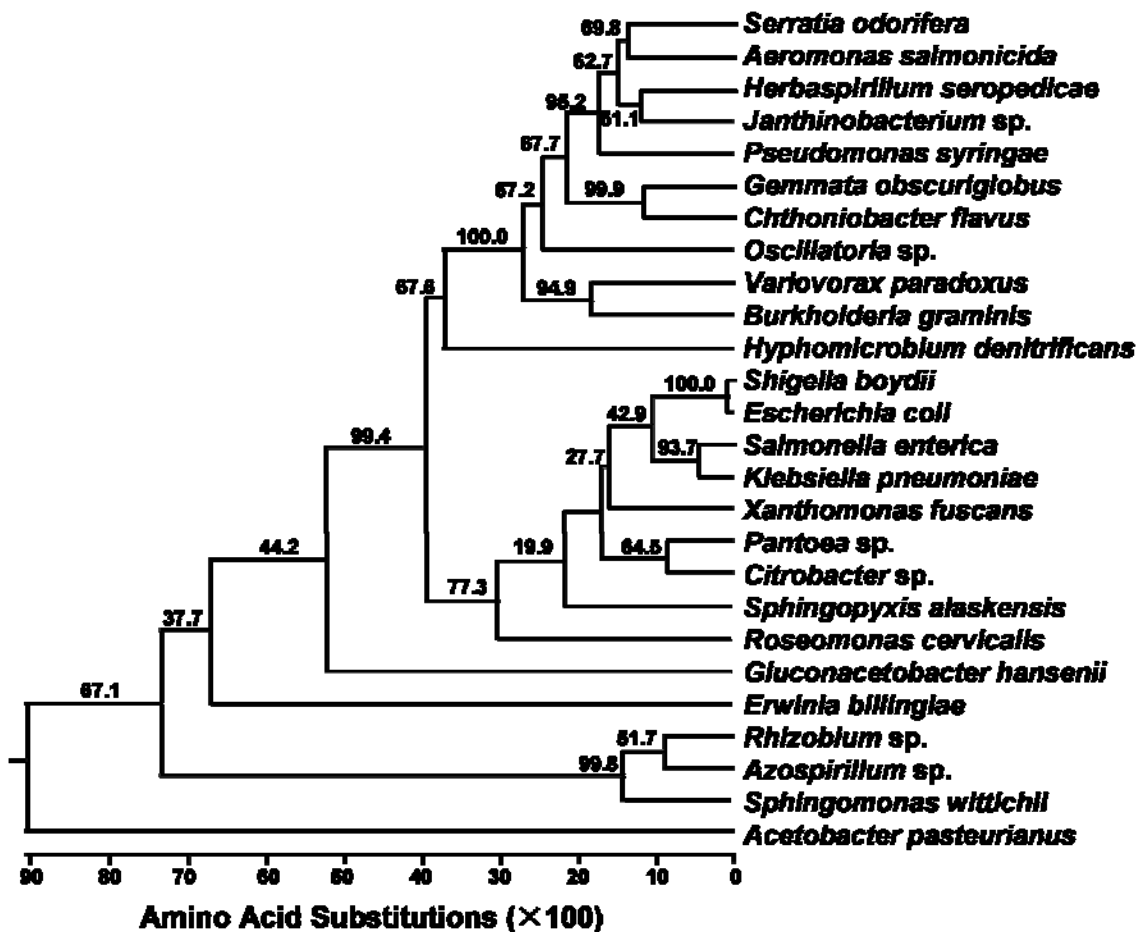
Figure 4.7   Phylogenetic tree of BdcA.

By discovering BdcA and creating the E50V and E50Q variants, we have also obtained important new tools that along with H-NS K57N (evolved to decrease biofilm formation through cell lysis by inducing cryptic prophage Rac) (Hong et al., 2010a), SdiA 1E11 (evolved to decrease biofilm formation by increasing indole concentrations) (Lee et al., 2009a), and SdiA SD10 (evolved to increase biofilm with the addition of homoserine lactone signals) (Lee et al., 2009a), allow the control of biofilm formation for various applications. These applications include decreasing biocorrosion on carbon steel (Jayaraman et al., 1999a) and performing biocatalysis for producing biofuels, chemicals, and food additives (Rosche et al., 2009). Therefore our study here shows the feasibility of controlling biofilm development via protein engineering using *E. coli* K-12 as a model organism. Extrapolating these results, one can imagine that with similar strategies, each stage of biofilm development may be controlled by synthetic biology using these and other engineered biofilm proteins. This would allow multi-species biofilms to be formed and dissolved and even controlled temporally and spatially (including at various depths and lengths) to expedite chemical transformations in biofilm reactors.

4.5 Experimental procedures

4.5.1 Bacterial strains, media, growth conditions, and growth rate assay

The strains and plasmids used in this study are listed in Table 4.3. *E. coli* K-12 BW25113 and its isogenic mutants (Baba et al., 2006) were obtained from the Genome Analysis Project in Japan. Plasmid pCA24N_*bdcA*, carrying *bdcA* under control of the P$_{T5-lac}$ promoter with tight regulation via the *lacI*^{q} repressor, and the empty plasmid pCA24N were also obtained from the Genomic Analysis Project in Japan (Kitagawa et al., 2005). Expression of *bdcA* was induced by 0.1 mM IPTG (Sigma, St. Louis, MO) unless otherwise indicated.

LB (Sambrook et al., 1989) and 37°C were used for all the experiments. Kanamycin (50 μg/mL) was used for pre-culturing the isogenic knock-outs. Chloramphenicol (30 μg/mL) was used for the strains harboring pCA24N and its derivatives, and 300 μg/mL erythromycin was used for pCM18.

4.5.2 Static biofilms for screening biofilm dispersal

Biofilm formation was assayed in 96-well polystyrene plates using 0.1% crystal violet staining (Corning Costar, Cambridge, MA) as previously described (Fletcher, 1977) with small modifications. Briefly, each well was inoculated with overnight cultures at an initial turbidity at 600 nm of 0.05 and grown without shaking for 19 h with 30 μg/mL chloramphenicol, then 0.1 mM IPTG was added to the culture to induce *bdcA*. The mixture was shaken at 150 rpm for 1 min and incubated for another 12 to 23 h (42 h total). Biofilm formation after 12 h of IPTG induction (31 h total) was used to establish the extent of mature biofilm formation. Biofilm dispersal was determined after 23 h of IPTG induction (43 h total). Comparison of these two values gave the percentage of biofilm dispersal. At least two independent cultures were used for each strain.

Table 4.3 *E. coli* **strains and plasmids used in this study.** Km^r, Cm^r, and Em^r denote kanamycin, chloramphenicol, and erythromycin resistance, respectively.

Strain/Plasmid	Genotype	Source
Strain		
BW25113	*lacI*^{q} *rrnB*$_{T14}$ *ΔlacZ*$_{WJ16}$ *hsdR514 ΔaraBAD*$_{AH33}$ *ΔrhaBAD*$_{LD78}$	(Datsenko and Wanner, 2000)
BW25113 *bdcA*	BW25113 Δ*bdcA* Ω Km^r	(Baba et al., 2006)
Plasmid		
pCA24N	Cm^r; *lacI*^{q}, pCA24N	(Kitagawa et al., 2005)
pCA24N_*bdcA*	Cm^r; *lacI*^{q}, pCA24N $p_{T5\text{-}lac}$::*bdcA*	(Kitagawa et al., 2005)
pCA24N_*yahA*	Cm^r; *lacI*^{q}, pCA24N $p_{T5\text{-}lac}$::*yahA*	(Kitagawa et al., 2005)
pCM18	Em^r; pTRKL2-P_{CP25}RBSII-*gfp*mut3*-T_0-T_1	(Hansen et al., 2001)

4.5.3 Flow cell biofilms and image analysis

The flow cell experiments were performed as previously described (Yang et al., 2008). pCM18 (Hansen et al., 2001) was used to produce the green fluorescent protein (GFP) for imaging each strain. The flow cells were inoculated with cultures at an initial turbidity at 600 nm of 0.05 at a flow rate of 10 mL/min for 2 h, and then fresh medium was added at 10 mL/min. For the wild-type strain and the *bdcA* mutant, biofilm images were taken after 24 h, 33 h, 42.5 h, 51.5 h, and 64.5 h. For *bdcA*/pCA24N, *bdcA*/pCA24N_*bdcA*, *bdcA*/BdcA E50V, and *bdcA*/BdcA E50Q, 0.5 mM IPTG was added to each flow cell system after 24 h, and images were taken 9 h, 18.5 h, and 27.5 h after IPTG addition (i.e., at 32, 42.5, and 51.5 total h). Biofilm images from nine random positions were taken and analyzed with Imaris confocal software (Bitplane, Zurich, Switzerland) and COMSTAT confocal software, respectively, as previously described (Yang et al., 2008).

4.5.4 EPS, swimming motility, aggregation, and eDNA assays

The amount of total EPS was determined as described previously (Zhang et al., 2008) with slight modifications. Briefly, cell cultures grown in 96-well plates for 24 h without shaking were collected and boiled in water for 10 min. The supernatant were then used for an anthrone-H_2SO_4 assay to determine EPS concentrations. This assay was performed with two independent cultures.

Swimming motility was performed as previously described (Sperandio et al., 2002). Single colonies or overnight cultures were used to inoculate the plates. The swimming halo was measured after 15 h. At least five plates were used for each independent culture, and two independent cultures were used for each strain.

Cell aggregation was assayed by comparing the cell turbidity at 600 nm near the surface of cultures in 96-well plates after 24 h of growth without shaking. This assay was performed

with two independent cultures.

eDNA was measured as previously described (Ma and Wood, 2009) using cultures grown in 96-well plates for 24 h without shaking. This assay was performed with two independent cultures.

4.5.5 RNA isolation from biofilms

To analyze differential gene expression for the *bdcA* mutant *vs*. the wild-type strain in biofilms, overnight cultures (2.5 mL) of the wild-type strain and the *bdcA* mutant were inoculated into 250 mL of LB medium with 10 g glass wool (Corning Glass Works, Corning, NY). After 15 h, the biofilm cells on the glass wool were collected as previously described (Ren et al., 2004a). To determine temporal *bdcA* expression, overnight cultures of the wild-type strain were inoculated into 130 mL of LB medium with 5 g of glass wool, and biofilm cells were collected from the glass wool after 2 h, 4 h, 8 h, 15 h, and 24 h. For the qRT-PCR for *bdcA* expression with the *yjgJ* deletion and the *yjgH* deletion, overnight cultures of the wild-type strain, the *yjgJ* mutant, and the *yjgH* mutant were inoculated into 130 mL LB medium with 5 g glass wool, and biofilm cells were collected after 8 h incubation. Cell pellets were resuspended in RNA*later* (Ambion Inc., Austin, TX), and total RNA was isolated using the RNeasy Mini Kit (Qiagen Inc., Valencia, CA) (Ren et al., 2004a).

4.5.6 Whole-transcriptome analysis

The *E. coli* GeneChip Genome 2.0 array (Affymetrix, P/N 900551) was used, and cDNA synthesis, fragmentation, and hybridizations were performed as described previously (González Barrios et al., 2006b). If the gene with the larger transcription rate did not have a consistent transcription rate based on the 11-15 probe pairs (*P*-value less than 0.05), these genes were discarded. A gene was considered differentially expressed when the *P*-value for comparing two chips was lower than 0.05 (to assure that the change in gene expression was statistically

significant and that false positives arise less than 5%) and if their fold change is higher than standard deviation for the whole genome (Ren et al., 2004b). The expression data were deposited in the NCBI Gene Expression Omnibus and are accessible through accession number GSE22057.

4.5.7 Quantification of c-di-GMP

c-di-GMP was quantified using HPLC as described previously (Ueda and Wood, 2009). Strains were grown from overnight cultures in 1 L of medium with 30 μg/mL chloramphenicol and 0.1 mM IPTG for 24 h without shaking. A photodiode array detector (Waters, Milford, MA) was used to detect nucleotides at 254 nm after the HPLC separation step. Commercial c-di-GMP (BIOLOG Life Science Institute, Bremen, Germany) was used as the standard. The c-di-GMP peak was verified by spiking the *bdcA*/pCA24N sample with the commercial c-di-GMP. This experiment was performed with two independent cultures.

4.5.8 PDE assay

PDE activity was assayed as previously described (Schmidt et al., 2005). His-tagged proteins (BdcA, BdcA E50V, and BdcA E50Q) were purified with Ni-NTA agarose (Qiagen) and contacted with 5 to 80 μM c-di-GMP in PDE assay buffer (50 mM Tris-HCl, 5 mM $MgCl_2$, 0.5 mM EDTA, 50 mM NaCl, pH ~6.0) for 0.5 h and 1 h. The reaction was stopped by heating at 95°C for 5 min after the addition of 10 mM $CaCl_2$. After centrifugation, the c-di-GMP concentration in the supernatant was analyzed by HPLC. Phosphodiesterase YahA from *E. coli* was used as a positive control and to generate the 5′-phosphoguanylyl-(3′→5′)-guanosine (Schmidt et al., 2005) from c-di-GMP. Guanosine monophosphate was obtained from Sigma. These data also provided rough estimates of the binding constants.

4.5.9 ^{31}P NMR

BdcA E50Q (5 μM) was incubated with 200 μM c-di-GMP for 8 h in PDE assay buffer. The ^{31}P NMR spectrum was obtained using a Varian INOVA 400 spectrometer and a broad band probe (proton decoupled, acquisition time 1.6 s, first delay 1.0 s, 90º pulse width 8.5 μs, line broadening 2 Hz, and number of transients 2000). 85% phosphoric acid was used as an external standard for the chemical shift 0 ppm. The ^{31}P NMR spectrum for GMP was obtained in the same manner.

4.5.10 c-di-GMP binding assays

Purified His-tagged proteins (10 μM) were incubated with 0.5 to 20 μM c-di-GMP for 0.5 h. Free c-di-GMP and BdcA-bound c-di-GMP were separated using a 10 kDa protein filter unit (Millipore, Cork, Ireland). The amount of free c-di-GMP for each sample was measured with HPLC (Schmidt et al., 2005). BdcA-bound c-di-GMP was recovered using 1.6 μg trypsin (Agilent Technologies, Inc., Santa Clara, CA) for 16 h to remove the protein and release c-di-GMP from BdcA. The released c-di-GMP was measured via HPLC to confirm the c-di-GMP was bound to the protein.

4.5.11 Random mutagenesis and saturation mutagenesis

bdcA expressed from pCA24N_*bdcA* was mutated by epPCR using primers epPCR-f and epPCR-r (Table 4.4). A 100 μL reaction contained 7.5 mM MgCl$_2$, 0.7 mM MnCl$_2$, 1 M betaine, 100 ng template DNA, 0.2 mM dATP and dGTP, 1 mM dCTP and dTTP, 5U *Taq* DNA polymerase (New England Biolabs, Beverly, MA), and 0.3 μM of each primer in 1X epPCR buffer (Sigma). The PCR program was set as 94°C for 5 min, followed by 30 cycles at 94°C for 1 min, 55°C for 1 min, and 72°C for 2 min, with a final extension step of 72°C for 7 min. The epPCR product was cloned into pCA24N_*bdcA* using restriction enzymes BseRI and HindIII after treating the plasmid with Antarctic phosphatase (New England Biolabs). The ligation

mixture was electroporated into BW25113 *bdcA*. Screening based on swimming motility was performed by inoculating single colonies into 150 x 15 mm 0.3% agar plates (1% tryptone, 0.25% NaCl, and 0.3% agar) with autoclaved toothpicks. At least one control sample (*bdcA*/pCA24N_*bdcA*) was used on each plate (no IPTG was required for induction of *bdcA*). The plates were incubated for 15 h, and colonies with increased motility were selected for a second round of screening based on motility. Plasmids were isolated, re-electroporated into BW25113 *bdcA*, and the best strains were re-tested for motility to ensure the changes in motility were due to mutated *bdcA* rather than chromosomal changes. Biofilm dispersal ability was then tested with these mutants. Over 6000 colonies were screened in this experiment. Plasmids that resulted in improved BdcA activity were sequenced by a BigDye Terminator Cycle Sequencing Kit (Applied Biosystems, Foster City, CA).

Saturation mutagenesis of *bdcA* at the E50 codon was performed in a 50 μL system with 125 ng of primers BdcASM-f and BdcASM-r (Table 4.4), 1 μL dNTP mix, 2.5 U *Pfu* polymerase, 30 ng template plasmid, and 1X *Pfu* reaction buffer (10 mM KCl, 6 mM $(NH_4)_2SO_4$, 20 mM Tris-HCl (pH 8.8), 2 mM $MgSO_4$, 0.1% triton X-100, and 0.1 mg/mL BSA). The PCR program was 95°C for 1 min, followed by 16 cycles of 95°C for 50 sec, 60°C for 1 min, and 68°C for 6 min, with a final extension step of 68°C for 6 min. The PCR product was treated with 10 U *Dpn* I restriction enzyme (New England Biolabs) for 3 h, and the mixture was directly used for electroporation. PCR Screening was based on motility.

4.5.12 Electron microscopy

Electron microscopy was performed using cultures grown in 96-well plates for 24 h without shaking. Each sample was diluted in LB to a turbidity at 600 nm of 0.2-0.5, stained in ammonium molybdate, and checked under JEOL 1200EX electron microscopy. This assay was performed with two independent cultures.

Table 4.4 DNA oligonucleotides used in this study. N represents A, T, G, or C, while S represents G and C.

Name	Primer sequence
epPCR-f	5'-GCCCTTTCGTCTTCACCTCG-3'
epPCR-r	5'-GAACAAATCCAGATGGAGTTCTGAGGTCATT-3'
BdcASM-f	5'-CCGCTAAACGCCTGGCACAA<u>NNS</u>ACTGGAGCGACAGCA G-3'
BdcASM-r	5'-CTGCTGTCGCTCCAGT<u>SNN</u>TTGTGCCAGGCGTTTAGCGG-3'
bdcA-rt-f	5'-GGGCGCTTTTACAGGTAAGACA-3'
bdcA-rt-r	5'-CGTCTCTGTCAGCACTATCTGTG-3'

4.5.13 qRT-PCR

qRT-PCR was performed as previously described (Ma and Wood, 2009). Primers used are listed in Table 4.4 as *bdcA*-rt-f and *bdcA*-rt-r. The housekeeping gene *rrsG* was as the internal reference, and the annealing temperature was 60°C.

4.5.14 Protein modeling

The three-dimensional model was obtained using the SWISS-MODEL server (http://swissmodel.expasy.org/) (Peitsch, 1995; Arnold et al., 2006; Kiefer et al., 2009) using L-xylulose reductase from *E. coli* (PDB 3d3w), which has 24% sequence identity. The protein image was made with PyMOL (http://pymol.sourceforge.net/).

4.5.15 Phylogenetic tree construction

The phylogenetic tree was constructed with the DNASTAR-Lasergene MegAlign software (DNASTAR, Madison, WI). The Kimura distance formula was used to calculate distance values. The values computed are the mean number of differences per site and fall between 0-1. Zero represents complete identity and 1 represent no identity. The phylogenetic tree scale uses these values multiplied by 100. The bootstrap analysis was performed with number of trials as 1000 and random seed as 111.

CHAPTER V

QUORUM-SENSING SWARMING SIGNALS FOR *PROTEUS MIRABILIS* AND THEIR RELATION TO BLOWFLIES

5.1 Overview

Flies transport specific bacteria for their larvae, at the same time the bacteria gain a wider range of nutrients. This symbiotic interaction of the two organisms may depend on interkingdom signaling. Two kinds of bacteria were identified by us in the salivary gland extracts of the blowfly *Lucilia sericata*: *Proteus mirabilis* and *Providencia stuartii.* Here, we focus on *P. mirabilis* since it aggressively out-competed both *Pseudomonas aeruginosa* and *Escherichia coli* during biofilm formation, since it swarmed significantly, and since it is expected that the swarming phenotype depends on quorum sensing. In addition, *P. mirabilis* produces a strong smell during its growth, which probably attracts blowflies. We performed transposon mutagenesis with the *P. mirabilis* strain and screened ~3000 swarming-deficient mutants to identify seven genes related to swarming (*rfaL*, *ureR*, *fis, hybG, zapB, fadE* and *PROSTU_03490*); among these, *ureR, fis, hybG, zapB, fadE* and *PROSTU_03490* are novel. Furthermore, swarming was tested with these mutants in the presence of eight chemicals (at 10 μM and 250 μM) which were previously identified as attractants for blowflies (benzoic acid, butyric acid, indole, lactic acid, *p*-cresol, phenol, KOH, and NaOH), and two other chemicals important in *P. mirabilis* metabolism (putrescine and ammonia). We found lactic acid, phenol, NaOH, KOH, putrescine, and ammonia restore swarming motility of seven different mutants. Hence, these compounds are necessary for swarming, and 5 of these compounds have never been associated with swarming previously with this strain (NaOH, KOH, NH_3, phenol, and lactic acid). These mutants were also tested for their ability to attract blowflies. Hence, we have identified several potential interkingdom signals for *P. mirabilis* and blowflies.

5.2 Introduction

Bacteria consumed by immature blowflies (Diptera: Calliphoridae) feeding on a resource (Ahmad et al., 2006) survive larval molting and pupation, and are present in emergent adult insects which serve as a dispersal mechanism (Ahmad et al., 2006). These flies and their relatives disperse over 100 pathogens (Greenberg, 1973), many of which are responsible for the estimated 76 million food-borne illnesses occurring annually in the U.S. *E. coli* O157:H7, which is responsible for hemorrhagic colitis and hemolytic uremic syndrome (Sanderson et al., 2006), accounts for 73,000 illnesses and 61 deaths (FoodNet, June 2006).

Proteus species are Gram-negative bacteria belonging to the *Enterobacteriaceae* family and cause serious infection problem in humans (Liu, 2010). *Proteus mirabilis* causes 90% of *Proteus* infections. It serves as a common inhabitant of dogs, cows, and birds and causes nosocomial infections from the source of human feces. *Lucilia sericata* is a common blowfly existing in most areas of the world. It is typically one of the first organisms that get attracted by the odours produced by cadaver decomposition and arrive at a body after death (Clark et al., 2006). The larvae of *L. sericata* are the most commonly used ones in maggot therapy (Schmidtchen et al., 2003).

Flies may be attracted and repelled by various factors, including temperature, light, and odours (Dethier, 1947). Flies can sense and respond to attractants by receptors on eggs, cerci, and antennae. Odours by attractants in nature help recognize potential mates and kin, the oviposition site, and a food source. Odours as repellents usually help protect insects from danger. Proteins, fats, and oils are the major materials of living organisms. There is no odour by proteins and fats themselves. However, their decomposition products in carrion, feces, urine, animal secretions (sweat, decomposing plant material, fungi, and algae) are usually notably odorous. Among all the decomposition compounds from fats and proteins, ammonia appears to be the

most common single nitrogenous product. It is a major constituent of urine by acting as the primary excretion product as well as the secondary product by urea decomposition. Skatole, indole, mercaptans, and the sulfides are the most penetrating odours of putrefaction. Another large group of attractants are fatty acids, which are usually the fermentation products and decomposition components.

Quorum sensing (QS) is the regulation of gene expression in bacteria as a function of the concentration of secreted small molecules that reflect cell density (Miller and Bassler, 2001). Gram-positive and Gram-negative bacteria both use QS communication to regulate their physiology behavior including symbiosis, virulence, competence, conjugation, antibiotic production, motility, sporulation, and especially biofilm formation (Davies et al., 1998; González Barrios et al., 2006b). Acylhomoserine lactones (AHL) in Gram-negative bacteria, indole, and autoinducer 2 (AI-2) in both Gram-negative and Gram-positive bacteria (Jayaraman and Wood, 2008; Han et al., 2010) are typical QS signals. QS regulates swarming motility (Daniels et al., 2004).

Swarming is a flagella-driven movement of differentiated hyperflagellated, elongated, and multinucleated swarmer cells by which bacteria spread as a biofilm over a surface (Daniels et al., 2004). Glycolipid or lipopeptide biosurfactants work as wetting agents by reducing surface tension. The QS signal AHL enhances swarming motility in *Serratia liquefaciens* (Daniels et al., 2004), while indole diminishes *P. aeruginosa* swarming motility (Lee et al., 2009b). The quorum quenching signal brominated furanone inhibits *E. coli* swarming motility via inhibiting both AHL- and AI-2-mediated signaling (Ren et al., 2001).

Bacteria and fruit flies share a common cell-cell communication system (Waters and Bassler, 2005). The inner membrane protein AarA of *P. stuartii* is required for the release of an extracellular quorum-sensing signal whose structure has not been identified yet (Waters and

Bassler, 2005). The homolog of AarA in the fruit fly *Drosophila melanogaster* is a rhomboid protein RHO that controls fly wing vein development and eye organization. Expression of *P. stuartii aarA* in a *D. melanogaster rho* mutant rescued wing vein development while expression of *rho* in a *P. stuartii aarA* mutant complemented the QS signaling defect.

Interkingdom signals can help bacteria recognize activity of the host immune system (Hughes and Sperandio, 2008). For example, the *P. aeruginosa* OprF protein on the cell surface binds to host interferon-γ, activates the QS system by inducing *rhlI* (RhlI synthesizes the QS signaling molecule C_4-homoserine lactone), induces the expression of *lecA* (encodes virulence determinant type I *P. aeruginosa* lectin (PA-I lectin)), and increases the production of pyocyanin (Wu et al., 2005). *P. aeruginosa* also detects adenosine of injured host cells and activates its PA-1 lectin virulence factor (Patel et al., 2007). Indole works as a beneficial signal in intestinal epithelial cells by increasing epithelial-cell tight-junction resistance and attenuating inflammation indicators (Bansal et al., 2010).

The rationale for the work here is that since swarming is based on QS (Daniels et al., 2004), and since flies respond to compounds produced by bacteria, we hypothesized that bacterial strains deficient in swarming QS signals may also be deficient in interkingdom signaling with flies. After generating *P. mirablis* transposon mutants that are deficient in swarming, we tested 10 compounds which were previously reported to be able to attract flies (Table 5.1) for their ability to restore swarming and to restore interkingdom signaling between *P. mirabilis* and *L. sericata*. Using this approach we identified five new chemicals related to swarming, identified seven new pathways related to the synthesis of these compounds, and found the genetic basis for the interkingdom signaling.

Table 5.1   List of attractants used in *P. mirabilis* TN mutants swarming test. *Anastrepha ludens* is a Mexican fruit fly. The other insects are blowflies.

Attractants	Insects	References
indole	*L. sericata*	(Dethier, 1947)
	Cochliomyia/Chrysomya	(Monika Hilker, 2002)
sodium hydroxide	*L. cuprina*	(Dethier, 1947)
potassium hydroxide	*L. cuprina*	(Dethier, 1947)
lactic acid	*L. sericata* /Calliphora erythrocephala*	(Dethier, 1947)
ammonia	*L. sericata*	(Monika Hilker, 2002)
putrescine	*Anastrepha ludens*	(Robacker, 2001)
p-cresol	*Cochliomyia /Chrysomya*	(Monika Hilker, 2002)
benzoic acid	*Cochliomyia /Chrysomya*	(Monika Hilker, 2002)
butyric acid	*Cochliomyia*	(Broce, 1980)
phenol	*Cochliomyia /Chrysomya*	(Monika Hilker, 2002)

5.3 Results

5.3.1 *P. mirabilis* isolated from fly salivary glands

By adding *L. sericata* maggot salivary gland extracts to *E. coli* and *P. aeruginosa* cultures, we found that one bacterium had notable swarming motility ability that outcompeted the growth of both *E. coli* and *P. aeruginosa*. The bacteria from the fly salivary glands were then identified using both a biochemical test (the 20-test system API Rapid 20E from bioMérieux, Inc. for identifying *Enterobacteriaceae* members) and pyrosequencing (Roche 454 FLX pyrosequencing platform of 454 Life Science, Branford, CT). This bacterium with the enhanced swarming was identified as *P. mirabilis* and another bacterium from the salivary gland extracts was identified as *P. stuartii*.

It was expected to find bacteria associated intimately with flies. Previously *Providencia* sp., *E. coli* O157:H7, *Enterococcus faecalis* (Orla-Jensen), and *Ochrobactrum* sp. were isolated from the screw-worm fly *Cochliomyia macellaria* (Ahmad et al., 2006). *P. mirabilis* was also isolated from maggots of the blowfly *Calliphora vicina* (Erdmann, 1987).

5.3.2 Swarming deficient mutants

Transposon mutagenesis was performed by introducing the Tn*5* transposon randomly into the genome of *P. mirabilis*. Around 3,000 colonies were obtained, and 50 swarming deficient mutants were identified. After confirming the swarming phenotype, 23 mutations were sequenced to identify which genes were related to swarming in *P. mirabilis*.

Six groups of genes were identified to be related to swarming motility of *P. mirabilis* (Table 5.2), including genes related to metabolism (*hybG*, *proC*, *pdxA*, *adhE*, and *fadE*), regulation (*fis*, *PMI2857*, and *yojN*), transcription/translation (*PMIr001*, *pnp*, *rhlB*, *rpsM*, *rrfG*, *ugd*, and *ureR*), cell surface (*rfaL* and *zapB*), flagella (*flgK* and *flhD*), and uncharacterized functions (*PROSTU_03490*).

Table 5.2 Summary of sequencing results. Transposon insertion site and the relative insertion position is listed (middle indicates that the transposon is inserted in the coding portion of the gene, and upstream indicates that the transposon is inserted in the upstream intergenic region). The organism used for the Basic Local Alignment Search Tool (BLAST) is also listed. *P. mirabilis* HI4320 is the best fit organism for the sequence BLAST while *Providencia* strains are also used for the BLAST search since these two bacteria both exist in *L. sericata*.

Mutant name	Gene	Insertion position	Organism	Gene function
Metabolism				
Mutant A	*hybG*	middle	*P. mirabilis* HI4320	hydrogenase nickel incorporation protein
R20	*proC*	middle	*P. mirabilis* HI4320	pyrroline-5-carboxylate reductase
Mutant E&H	*pdxA*	upstream	*P. mirabilis* HI4320	4-hydroxythreonine-4-phosphate dehydrogenase
7_18&7_40&7_28	*adhE*	middle	*P. mirabilis* HI4320	bifunctional acetaldehyde-CoA/alcohol dehydrogenase
Mutant I	*fadE*	middle	*P. mirabilis* HI4320	acyl-CoA dehydrogenase
Regulator				
R5	*fis*	middle	*P. mirabilis* HI4320	DNA-binding protein Fis
R7	*PMI2857*	middle	*P. mirabilis* HI4320	helix-turn-helix XRE-family like proteins
Mutant F	*yojN*	middle	*Providencia rettgeri* DSM 1131	putative two-component sensor protein like YojN
Nucleotide related				
R18	*PMIr001*	middle	*P. mirabilis* HI4320	16S ribosomal RNA
R27	*pnp*	middle	*P. mirabilis* HI4320	polynucleotide phosphorylase/polyadenylase
R54	*rhlB*	middle	*P. mirabilis* HI4320	ATP-dependent RNA helicase
R11	*rpsM*	upstream	*P. mirabilis* HI4320	30S ribosomal protein S13
R51	*rrfG*	middle	*P. mirabilis* HI4320	dTDP-*D*-glucose-4,6-dehydratase
R39&O	*ugd*	middle	*P. mirabilis* HI4320	UDP-glucose 6-dehydrogenase
R30	*ureR*	middle	*P. mirabilis* HI4320	urease operon transcriptional activator

Table 5.2 continued

Mutant name	Gene	Insertion position	Organism	Gene function
Cell surface-related				
7 14	*rfaL*	middle	*P. mirabilis* HI4320	O-antigen ligase
R24	*zapB*	middle	*P. mirabilis* HI4320	cell division protein
Others				
R26	*PROSTU_03490*	middle	*P. stuartii* ATCC 25827	hypothetical protein
Flagellar				
R58	*flgK*	middle	*P. mirabilis* HI4320	flagellar hook-associated protein 1
R52&R15	*flhD*	upstream	*P. mirabilis* HI4320	transcriptional activator FlhD for flagellar

Three of these genes were previously identified to be related to *P. mirabilis* swarming motility; hence, our method was able to recover some known swarming-related mutations for *P. mirabilis*. The *flhDC* activator is the central component for regulating swarmer cell differentiation in *P. mirabilis* and other bacteria (Clemmer and Rather, 2007), and *P. mirabilis flhDC* mutants are unable to swarm. The *flgK* gene encodes the flagellar hook-associated proteins and is tightly associated with bacterial swarming motility (Fraser et al., 1999). In *P. mirabilis*, the ZapA protein (IgA-degrading metalloprotease) works as a virulence factor expressed specifically in swarmer cells although the *zapA* mutant does not show decreased swarming (Walker et al., 1999). The *zapB* gene that we identified is necessary for ZapA activity (Walker et al., 1999).

5.3.3 Complementation of swarming mutations via known fly attractants

To determine if any of the swarming mutations are part of interkingdom signaling with blow flies, ten known fly attractants (Table 5.1) were added to the swarming plates with the swarming mutants to see if swarming could be restored; i.e., to see whether the mutations that disrupted swarming also disrupted interkingdom signaling between the bacterium and the flies. The addition of six known fly attractants restored the swarming motility of different swarming deficient mutants. Hence, in addition to attracting flies, these attractants can also function as the molecules that control swarming of *P. mirabilis*. Therefore, we identified six chemicals (putrescine, NaOH, KOH, NH_3, phenol, and lactic acid) that function both as fly attractants and bacterial swarming signals. Furthermore, we identified seven (RfaL, UreR, Fis, HybG, ZapB, FadE, and PROSTU_03490) biochemical pathways these attractants work through by identifying the genes disrupted by the transposon mutagenesis. The motility complementation results are summarized in Tables 5.3, 5.4, and 5.5.

From Table 5.4, the *rfaL* mutant (7_14) has increased motility upon addition of 10 μg/mL and 250 μg/mL of NaOH, 250 μg/mL KOH, 10 μg/mL putrescine, 250 μg/mL putrescine,

Table 5.3 **Swarming complementation with indole (compared with DMF), benzoic acid (compared with ethanol), and *p*-cresol (compared with ethanol).** The values are swarming halos (mm) on Luria-Bertani (LB) plates (the ~ 4 mm colony size is not included). The swarming motility was tested after 10 h of incubation at 37°C.

Mutant name	Transposon insertion site	DMF	indole		Ethanol	Benzoic acid		*p*-cresol	
			10 μg/mL	250 μg/mL		10 μg/mL	250 μg/mL	10 μg/mL	250 μg/mL
WT		16 ±10	26±10	16 ±10	21 ± 9	16 ± 2	14 ± 1	21 ± 7	22 ± 7
7_18/40/28	*adhE*	1	2	1.4	0.8	1	1.6	0.6	1.3
I	*fadE*	0	0	0	0	0	0	0	0
R5	*fis*	0	0	0	1 ± 1	0	0	1 ± 2	1 ± 2
A	*hybG*	2.9	3.25	3	0	0	0	0.2	1 ± 2
E	*pdxA*	0	0	0	0	0	0	0	0
R7	*PMI2857*	0	0	0	0	0	0	0	0
R18	*PMIr001*	0	0	0	0	0	0	0	0
R27	*pnp*	0	0	0	0	0	0	0	0
R20	*proC*	7.6	8.4	5.5	7.3	7.5	6.1	8	8.4
R26	*PROSTU_03490*	0	0	0	2 ± 3	0	0	2	2 ± 2
7_14	*rfaL*	0	0	0	0	0	0	0	0
R54	*rhlB*	0	0	0	0	0	0	0	0
R51	*rrfG*	6.95	2.12	2.4	0	0	0	0	0
R39/O	*ugd*	0	0	0	0	0	0	0	0
R30	*ureR*	0	0	0	0	0	0	0	0
F	*yojN*	0	0	0	0	0	0	0	0
R24	*zapB*	0	0	0	0	0	0	0	0
R58	*flgK*	0	0	0	0	0	0	0	0
R52/R15	*flhD*	0	0	0	0	0	0	0	0

Table 5.4 Swarming complementation with NaOH, KOH, putrescine, and ammonia (compared with H₂O). The values are swarming halos (mm) on LB plates (the ~ 4 mm colony size is not included). The swarming motility was tested after 10 h incubation at 37°C. Interesting results are shown in bold.

Mutant name	Transposon insertion site	H₂O	NaOH		KOH		Putrescine		NH₃	
			10 μg/mL	250 μg/mL	10 μg/mL	250 μg/mL	10 μg/mL	250 μg/mL	2 μL	15 μL
WT		23 ± 7	25 ± 8	26 ± 10	26 ± 10	24 ± 7	22 ± 9	23 ± 7	20	10.1
7_18/40/28	*adhE*	6.7	8	1	11.9	2	10.2	8.9	0	0
I	*fadE*	0	4 ± 6	1.2	**7 ± 9**	1 ± 2	**4 ± 5**	**6 ± 10**	0	0
R5	*fis*	0.3 ± 0.3	0	0.2	0.1 ± 0.6	2 ± 3	0	**6 ± 4**	3.3	0
A	*hybG*	0	4 ± 6	9.7	6 ± 3	1 ± 2	0	0	0	0
E	*pdxA*	0	0	0	0	0	0	0	0	0
R7	*PMI2857*	0	1	0.2	1.4	2	0.3	0	0	0
R18	*PMIr001*	0	0	0	0	0	0	0	0	0
R27	*pnp*	0	0	0	0	0	0	0	0	0
R20	*proC*	4	1	2.1	2	2	2	2	0	0
R26	*PROSTU_03490*	1 ± 2	2 ± 3	3 ± 3	0	4 ± 1	**5 ± 5**	**7 ± 10**	1.5	0
7_14	*rfaL*	0	**16 ± 10**	**4 ± 5**	2.6 ± 0.3	**8 ± 8**	**7 ± 4**	**16 ± 10**	0	**4.8 ± 0.5**
R54	*rhlB*	0	1±2	1.2	0	1 ± 1	0	2 ± 3	0	0
R51	*rrfG*	5.55	9.89	6.7	11.72	4.45	5	5	5	2
R39/O	*ugd*	1.3 ± 0.4	1 ± 2	0	4.2 ± 0.7	3 ± 1	6 ± 3	5.5 ± 0.5	0	0
R30	*ureR*	6 ± 6	1 ± 2	0.3	1 ± 2	1 ± 2	0	0	**22 ± 4**	**14 ± 2**
F	*yojN*	0	0	0	0	0	0	0	0	0
R24	*zapB*	1 ± 1	0.4 ± 0.9	1.2	2 ± 3	3 ± 5	0	0	1.1	0
R58	*flgK*	0	0	0	0	0	0	0	0	0
R52/R15	*flhD*	0	0	0	0	0	0	0	0	0

Table 5.5 **Swarming complementation with phenol, butyric acid, and lactic acid (compared with H₂O).** The values are swarming halos (mm) on LB plates (the ~ 4 mm colony size is not included). The swarming motility was tested after 10 h incubation at 37°C. Interesting results are shown in bold.

Mutant name	Transposon insertion site	H₂O	Phenol		Butyric acid		Lactic acid	
			10 µg/mL	250 µg/mL	10 µg/mL	250 µg/mL	10 µg/mL	250 µg/mL
WT		23 ± 7	26 ± 10	26 ± 10	26 ± 10	31 ± 9	24 ± 7	21 ± 7
7_18/40/28	*adhE*	6.7	2	1.7	6	2	2	9.4
I	*fadE*	0	2.5	9.2	15	2	4 ± 6	4 ± 7
R5	*fis*	0.3 ± 0.3	0	2	0.9	2 ± 4	**8 ± 5**	**5 ± 5**
A	*hybG*	0	**6 ± 3**	**9 ± 3**	2 ± 7	3 ± 3	0	0
E	*pdxA*	0	0	0	0	0	0	0
R7	*PMI2857*	0	0	2	0.9	2	0.2	0.9
R18	*PMIr001*	0	0	0	0	0	0	0
R27	*pnp*	0	0	0	0	0	0	0
R20	*proC*	4	2	0	4.9	2	15.1	4.6
R26	*PROSTU_03490*	1 ± 2	0	0	0	0	2 ± 3	2 ± 3
7_14	*rfaL*	0	0	0	0	0	0	0
R54	*rhlB*	0	1.3	2.57	1.7	2.1	1 ± 1	1 ± 1
R51	*rrfG*	5.55	9.75	8.3	8.35	8.65	9.35	2.5
R39/O	*ugd*	1.3 ± 0.4	0	0	0.3 ± 0.8	1 ± 2	0	0.3 ± 0.8
R30	*ureR*	6 ± 6	2	1.5	0.9	2	0	0.4 ± 0.9
F	*yojN*	0	0	0	0	0	0	0
R24	*zapB*	1 ± 1	2	1.5	0.9	2	**10 ± 6**	**12 ± 7**
R58	*flgK*	0	0	0	0	0	0	0
R52/R15	*flhD*	0	0	0	0	0	0	0

92

and 15 µL ammonium hydroxide (by evaporation) (control sample did not swarm). The *ureR* (R30) mutant has 3.6-fold and 2.3-fold increased motility upon the addition of 2 µL and 15 µL ammonium hydroxide (by evaporation). Additionally, the *fadE* mutant (I) has increased swarming motility upon addition of 10 µg/mL KOH, 10 µg/mL and 250 µg/mL putrescine (control sample did not swarm), the *fis* mutant (R5) has 20-fold increased swarming motility upon addition of 250 µg/mL putrescine, and the *PROSTU_03490* mutant (R26) has 5-fold and 7-fold increased swarming motility upon addition of 10 µg/mL and 250 µg/mL putrescine. From Table 5.5, the *fis* mutant (R5) had increased swarming with 10 µg/mL and 250 µg/mL of lactic acid (26-fold and 16-fold increases, respectively), the *hybG* mutant (mutant A) had increased swarming with 10 µg/mL and 250 µg/mL phenol (fold change is infinity since control sample did not swarm), and the *zapB* mutant (R24) has 10-fold and 12-fold increased swarming with 10 µg/mL and 250 µg/mL lactic acid.

5.3.4 RfaL is required for fly attraction and oviposition

Initial tests for fly attraction and oviposition were performed with the *rfaL* mutant vs. the wild-type strain since the *rfaL* mutant has complemented swarming motility with the addition of known signaling molecule putrescine. The wild-type strain showed ~1.7-fold better fly attraction than the *rfaL* mutant based on the average of three replicates. In addition, the only oviposition we observed from four trials occurred in the wild-type strain. Therefore, RfaL is required for fly attraction and oviposition, it is necessary for swarming, and this swarming deficiency may be complemented by the addition of putrescine. Hence, putrescine may be interkingdom signals for this insect.

5.4 Discussion

P. mirabilis is a Gram-negative urinary tract pathogen for humans (Morgenstein et al., 2010). The prominent feature of this bacterium is its ability to swarm. The swarming behavior

involves a complex repeating cycle of differentiation between two cell types, the vegetative (swimmer) and swarmer cells (Janda and Abbott, 2005). The swimmer cells dominate in liquid and are Gram-negative rods. These cells change into the swarmer cells with longer cell length and more flagella after 3 to 4 h when they are placed on solid surfaces (Morgenstein et al., 2010). The flagellar rotation is inhibited during this conversion, and extracellular signal is required to control this multicellular behavior. Genes related to lipopolysaccharide, flagellar, cell wall synthesis, cell division, proteolysis (Belas et al., 1995), as well as virulence-related genes such as haemolysin, protease, and urease (Liaw et al., 2001) are involved in this conversion. Hence it is reasonable to consider that the swarming motility is tightly connected to the virulence of *P. mirabilis*. The host-bacterium interaction that virulence genes control and the bacterium-bacterium QS behavior that swarming requires are interrelated.

An initial test showed that *P. mirabilis* has significant swarming motility on LB plates regardless of the temperature (room temperature or 37°C, data not shown). So when this bacterium is brought onto the surface of a human wound, it can spread and cover the wound area quickly. The QS signal for *P. mirabilis* is produced and functions during the swarming. This signal may also work as an attractant for flies for oviposition on the wound surface. The fly eggs grow to maggots and eat the dead tissues in the wounds as well as perhaps the bacteria. Probably that is the reason that we can isolate *P. mirabilis* from the larvae salivary gland extract.

In this study we identified six chemicals (putrescine, NaOH, KOH, NH_3, phenol, and lactic acid) that are important for restoring swarming with seven mutants (*rfaL*, *ureR*, *fis, hybG*, *zapB*, *fadE* and *PROSTU_03490*). Except *rfaL*, the other six genes identified to be important for swarming are novel. Except putrescine, the other five chemicals (NaOH, KOH, NH_3, phenol, and lactic acid) that restored swarming are novel.

Along with the novel chemicals for swarming, putrescine was identified. Putrescine is an extracellular signal required for swarming in *P. mirabilis* (Sturgill and Rather, 2004). It belongs to the group of polyamines including putrescine, agmatine, and spermidine. Putrescine is a constituent of the outer membrane of *P. mirabilis*. In addition, the extracellular putrescine regulates gene expression in many organisms. Putrescine is the product of SpeB in *P. mirabilis* and it can repress its own expression (Sturgill and Rather, 2004). Mutation in *speA* (encoding arginine decarboxylase) or *speB* (encoding agmatine ureohydrolase) block the major pathway for putrescine production and results in a two to three hour delay in swarmer cell differentiation (Stevenson and Rather, 2006). Adding 25 µM exogenous putrescine can completely restore the swarmer cell differentiation of the *speA* mutant (Stevenson and Rather, 2006). In addition, the swarming motility of *speA* mutant can be restored by deleting its extragenic suppressor gene *disA* (Stevenson and Rather, 2006). Furthermore, putrescine showed the ability to attract Mexican fruit fly *Anastrepha ludens* (Robacker, 2001).

RfaL (WaaL) is the lipopolysaccharide O-antigen ligase. In *P. mirabilis* the deletion of *rfaL* causes disability lack of differentiating into swarmer cell (Morgenstein et al., 2010). The *rfaL* mutation also inhibits the *flhDC* operon expression (Morgenstein et al., 2010). In *P. aeruginosa*, the RfaL protein is a membrane protein with 11 potential transmembrane segments (Abeyrathne and Lam, 2007). We show for the first time that putrescine can restore the swarming of an *rfaL* mutant. In addition, we show the deletion of *rfaL* decreases fly attraction. Hence we propose that RfaL may work as a transporter for putrescine and putrescine may be the interkingdom signal that can be sensed by both blowfly *L. sericata* and the bacteria *P. mirabilis.*

Ammonia is another important chemical that is proposed to be the interkingdom signal molecule. Ammonia is produced by almost all organisms. It is one of the most characteristic odours in fresh manure (Richardson, 1916). It can attract blowfly *L. sericata* (Monika Hilker,

2002). Urease is the enzyme that catalyzes the hydrolysis of urea into carbon dioxide and ammonia (Nicholson et al., 1993). In *P. mirabilis*, urease is encoded by the *ure* operon which contains eight genes. UreR is the transcription regulator of *P. mirabilis* urease. The activation of urease causes the hydrolysis of urea to ammonia, which leads to the increase of pH and the formation of stones. Hence urease is the virulence factor (Mobley and Belas, 1995). Here we show for the first time that ammonia can complement the swarming deficiency that the *ureR* mutant causes. And we propose for the first time that ammonia may be the interkingdom signal that controls both blowfly *L. sericata* and bacteria *P. mirabilis* activity.

5.5 Future work

We will need to test the fly attraction and oviposition activity for all the mutants we obtained and identify those with increased fly attraction and oviposition. In addition, the complementation test for fly attraction and oviposition assay will need to be conducted by adding chemicals that complemented swarming motility back into mutant strains. The concentration of effective signal molecules should be tested in *P. mirabilis* wild-type and the corresponding mutants.

5.6 Experimental procedures

5.6.1 Maggot salivary gland extraction

L. sericata larvae were grown at room temperature on beef liver until the third instar. They were removed from the jar and checked to make sure the crop was full before each experiment. Each maggot was removed and quickly rinsed in diluted bleach solution (1.25% sodium hypochlorite) followed by two phosphate buffered saline solutions (0.8% NaCl, 0.02% KCl, 0.144% Na_2HPO_4, and 0.024% KH_2PO_4, pH 7.4) before dissection. The salivary gland was removed and put into the sterile microcentrifuge tube filled with appropriate volume of sterile PBS (20 µL per pair of salivary glands to be extracted).

5.6.2 *P. mirabilis* identification

Once the salivary glands were removed, the glands were collected in a microcentrifuge tube, mashed, and spread onto bacterial media. Trypticase soy agar plates with 5% sheep blood (TS-blood agar; BVA Scientific, San Antonio, TX) were used for the recovery of aerobic microbial species. Plates were incubated aerobically for 24 h at 37°C. Phenotypically distinct colonies were chosen and subcultured onto fresh media to attain cultural purity. Multiple subculturing was performed as necessary for isolation of bacterial species. *P. mirabilis* was identified using API Rapid 20E manual identification test strips. API RAPID 20E is a 4 hour identification kit for Gram-negative *Enterobacteriaceae* via biochemical analysis via 20 tests including those for glucose acidification, sucrose acidification, β-galactosidase, and indole production (Izard et al., 1984).

The microbial community members in the salivary glands were also evaluated using pyrosequencing. DNA samples were processed with FastDNA*SPIN (MP Biomedical LLC, Solon, OH) using a cell homogenizer (MP Biomedical, Solon, OH) according to the manufacturer's instructions and frozen at -80°C until pyrosequencing analysis. Each of the

combined samples was individually analyzed based upon the Roche 454 FLX pyrosequencing platform (https://www.roche-applied-science.com/sis/sequencing/flx/index.jsp) using the bacterial tag-encoded FLX amplicon pyrosequencing method previously described (Dowd et al., 2008c; Dowd et al., 2008a; Dowd et al., 2008b). Sequences from each sample assembled at 3% divergence were processed along with the number of reads integrated into each consensus. The resulting TC FASTA for each sample was evaluated using BLASTn against a custom SRDS database derived from the RDP-II database and GenBank (http://ncbi.nlm.nih.gov).

5.6.3 Transposon mutagenesis and swarming-based screening

Transposon mutagenesis was performed with the EX-Tn*5*™ <DHFR-1> Tnp transposome kit (Epicentre, Madison, WI). After electroporation with 50 μL of competent cells and 1 μL transposome supplied by the kit, we obtained around 3,000 colonies with Tn*5* transposon randomly inserted in the genome. Mueller-Hinton agar plates (Atlas, 2004) were used to select mutants with transposons inserted using 10 μg/mL trimethoprim. The agar concentration was adjusted to 3% to prevent swarming during this step. We then screened 3,000 colonies for swarming motility on LB agar plates with 1.5% agar at 37°C with after approximately 4 h. Fifty mutants with at least 3-fold decreased swarming were selected and confirmed as swarming deficient strains using the same condition.

5.6.4 DNA sequencing to identify transposon insertion positions

Genomic DNA was isolated from the swarming mutants via the UltraClean Microbial DNA isolation kit (MO BIO, Carlsbad, CA). For sequencing, arbitrary PCR was performed; the first round of arbitrary PCR reaction (PCR1) was performed using 100 ng genomic DNA, 0.5 μL 10 mM dNTP, 0.5 μL Pfu polymerase, 5 μL betaine, 2.5 μL 10X Pfu buffer, 0.75 μL 100 μM arbitrary primer 1 (5'-GGCCAGGCCTGCAGATGATGNNNNNNNNNNGTAT-3'), 0.75 μL 10 μM internal specific primer (5'-ACGGATTCGCAAACCTGTCACG-3'), and water for a 25

μL reaction. The PCR1 reaction conditions were 94°C 5 min; 6 cycles of 94°C 30 sec, 30°C 30 sec, 72°C 1 min; 30 cycles of 94°C 30 sec, 58°C 30 sec, 72°C 1 min; and 72°C 5 min. The second arbitrary PCR reaction (PCR2) was performed with 0.75 μL of PCR1 product, 0.5 μL 10 mM dNTP, 0.5 μL Pfu polymerase, 5 μL 5M betaine, 2.5 μL 10X Pfu buffer, 0.75 μL 10 μM arbitrary primer 2 (5'-GGCCAGGCCTGCAGATGATG-3'), 0.75 μL 10 μM external specific primer I (5'-AGGTGGCGGAAACATTGGATG-3'), and water for a 25 μL reaction . The PCR2 reaction conditions were 30 cycles of 94°C 30 sec, 55°C 30 sec, and 72°C 1 min. The third arbitrary PCR reaction was performed with 1 μL PCR2 product, 0.5 μL 10 mM dNTP, 0.5 μL Pfu polymerase, 5 μL 5M betaine, 2.5 μL 10X Pfu buffer, 0.75 μL 10 μM arbitrary primer 2 (5'-GGCCAGGCCTGCAGATGATG-3'), 0.75 μL 10 μM external specific primer II (5'-GGCGGAAACATTGGATGCGG-3'), and water to make it final 25 μL. The PCR3 reaction conditions were 30 cycles of 94°C 30 sec, 55°C 30 sec, and 72°C 1 min. The final PCR product after three sets of arbitrary PCR was purified and sequenced using Perkin Elmer ABI Big Dye Reaction Mix. The external specific primer II is also used here as sequencing primer. NCBI blast was used to compare sequences and identify the transposon insertion site.

5.6.5 Swarming complementation

For the swarming complementation test, 10 μg/mL and 250 μg/mL of each chemical were added to LB agar plates (1.5% agar). The stock solutions of indole and benzoic acid were dissolved in DMF. The *p*-cresol was dissolved in ethanol. The other chemicals phenol, butyric acid, lactic acid, NaOH, KOH, and putrescine were dissolved in H_2O. Two μL exponential phase cultures (OD600 ~1.0) were added on the surface of the agar plates and incubated at 37°C. For the swarming complementation test with ammonia, 2 μL and 15 μL ammonium hydroxide were dropped on the lid of Petri dishes because ammonium hydroxide can easily release

ammonia, and the evaporated ammonia can be sensed by bacteria in this way. Swarming halos were measured after 10 h.

5.6.6 Fly attraction and oviposition assay

The fly attraction assay was performed by the instrument shown in Fig. 5.1A. Roughly hundreds of 7 to 9 day-old blowflies *L. sericata* ((East Lansing, MI) were put into the clean plastic box without water or food. Agar plates with 24 h-old *P. mirabilis* cultures (10^7 bacteria were plated initially and incubated at 37°C for 24 h) were put on each side of the plastic box and were connected to the box by a white tunnel (Charlotte Pipe, Charlotte, NC). There was a plastic screen in the middle part of the tunnel to prevent flies from flying into the agar plates. Two pieces of sticky traps (Bell Laboratories Inc., Chicago, IL) were put on the tunnel wall to catch the attracted flies. After 24 h, female and male flies on the sticky traps were counted separately. Female flies were dissected to check the gravid condition.

The oviposition assay was performed using the system shown in Fig. 5.1B. Hundreds of 7 to 12 days old blowflies were put in the cage with water and sugar (Wal-Mart, Bentonville, AR) supplied. Fresh agar plates with 10^7 bacteria plated and incubated for 30 min at 37°C were put inside the cage to see whether flies had a preference for where they laid eggs. A steel screen was put on the top of each agar plate to prevent oviposition directly on the agar surface. Wet paper towels underneath each plate provided the surface for egg-laying since flies prefer to lay eggs on rough (Crombie, 1941), wet (Kamal, 1958) surfaces. The paper towel was taken out after 6 h and the egg number was counted. The temperature was set to be 21°C for both assays.
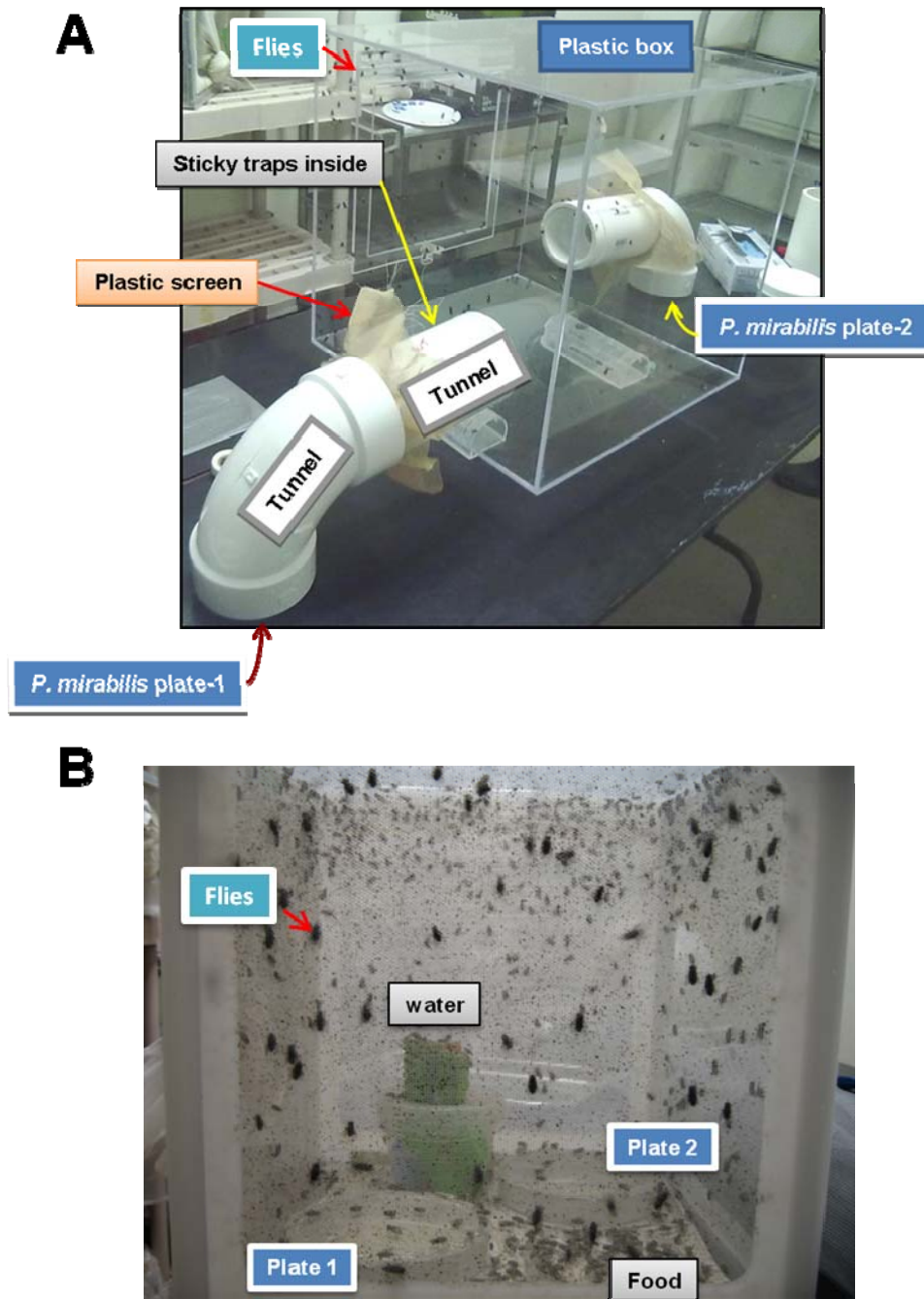
Figure 5.1 Instrument for fly attraction assay (A) and fly oviposition assay (B).

CHAPTER VI

PROTEIN ACETYLATION IN *ESCHERICHIA COLI* INCREASES STRESS RESISTANCE

6.1 Overview

Acetylation of lysine residues is conserved in all three kingdoms; however, its role in prokaryotes is unknown. Here we demonstrate that acetylation enables the reference bacterium *Escherichia coli* to withstand environmental stress. Specifically, the bacterium becomes more resistant to heat and oxidative stress when its proteins are acetylated as shown by deletion of the gene encoding acetyltransferase YfiQ and the gene encoding deacetylase CobB and by overproducing YfiQ and CobB. Furthermore, we show that the increase in oxidative stress resistance with acetylation is due to the induction of catalase activity through enhanced *katG* expression. This is the first demonstration of a specific environmental role of acetylation in prokaryotes.

6.2 Introduction

The post-translational modification of acetylation occurs for all three domains of life (Escalante-Semerena, 2010) and regulates diverse aspects of metabolism in that 2700 proteins in mammals are acetylated related to central metabolism, mRNA splicing, protein synthesis, cell morphology, and cell cycle (Linda I et al., 2010). Although identified in 1963 for eukaryotes (Linda I et al., 2010), in bacteria, the role of acetylation has not been well characterized even though this modification is relatively common in that at least 91 proteins are acetylated in the best-studied strain, *E. coli,* including the stress related heat shock proteins like DnaK and superoxide dismutase (Yu, 2008; Zhang et al., 2009).

In *Salmonella enterica*, there is only one major bacterial protein acetyltransferase, Pat, and one nicotinamide adenine dinucleotide-dependent deacetylase, CobB. These two enzymes

control the status of lysine acetylation for acetyl-CoA synthetase as well as the acetylation of a number of central metabolic enzymes in *S. enterica* (Wang et al., 2010). In *E. coli*, there are 23 putative lysine acetyltransferases that add acetyl groups to the epsilon amine of lysine using acetyl-coenzyme A as a substrate (Escalante-Semerena, 2010). Ten Gcn-5 acetyltransferases in *E. coli* are confirmed for their function while the other thirteen remain enigmatic, including YfiQ which is the homolog of the single acetyltransferase in *S. enteric* (Escalante-Semerena, 2010). Hence we chose to study YfiQ as the acetyltransferase because we expect that it also plays an important role in *E. coli* similar to Pat in *S. enteric* (Escalante-Semerena, 2010), and chose to study CobB as the deacetylase since it is the only confirmed deacetylase activity in *E. coli* (Li et al., 2010), and studied the bacterial physiology by changing the acetylation status controlled by these two genes in *E. coli*.

Bacteria respond to various stresses by producing global regulators (Farr and Kogoma, 1991). The universal stress proteins UspA and UspD are required for the resistance to superoxide-generating agents (Nachin et al., 2005). Catalases KatG and KatE break down the H_2O_2 into H_2O and O_2 (Robbe-Saule et al., 2001). OxyR regulates the peroxide-mediated stress response in which at least 30 proteins are elevated over the basal levels upon the addition of peroxide stress (Farr and Kogoma, 1991). In addition, the sigma factor RpoS is regulates *katG* in an OxyR-dependent way (Ivanova et al., 1994). The RpoS regulator is also required for acid, heat, and salt resistance in *E. coli* O157:H7 (Cheville et al., 1996).

Since the ability of bacteria to respond rapidly to stress is a hallmark of their success and since protein modifications allow the most rapid response, we hypothesized that conserved protein acetylation may be related to the ability of the cell to withstand stress. Here we demonstrate that cells with decreased acetylation, through enhanced deacetylase CobB activity, are less resistant to heat and oxidative stress. DNA microarrays and quantitative, reverse-

transcription polymerase chain reaction (qRT-PCR) both showed induction of *katG* under oxidative stress conditions. Hence we propose that the activity of some regulator that controls stress gene expression especially the *katG* expression is altered by acetylation.

6.3 Results

6.3.1 YfiQ increases stress resistance and CobB decreases stress resistance

To test our hypothesis that lysine acetylation is related to stress resistance, we subjected *E. coli yfiQ* and *cobB* mutants to heat and oxidative stress (Fig. 6.1). Decreasing acetylation by deleting *yfiQ* decreased heat and oxidative stress by 10 fold and 4 fold, respectively, while increasing acetylation by deleting *cobB* increased heat and oxidative stress resistance by 3 fold and 100 fold, respectively. These results were complemented by increasing acetylation by producing YfiQ via plasmid pCA24N_*yfiQ* (370-fold increase in heat resistance and 110-fold increase in oxidative stress resistance) and by decreasing acetylation by producing CobB via plasmid pCA24N_*cobB* (27-fold reduction in heat resistance and 10-fold reduction in oxidative stress resistance). Therefore, acetylation by YfiQ increases resistance to heat and oxidative stress while deacetylation by CobB decreases it.

6.3.2 CobB decreases catalase activity

Since producing CobB decreased resistance to hydrogen peroxide (Fig. 6.1A), we investigated whether this phenotype was related to RpoS since RpoS is a positive regulator of catalase activity via *katG* and *katE* (Lacour and Landini, 2004). Catalase deactivates H_2O_2 by converting it to H_2O and O_2 (Robbe-Saule et al., 2001). Using two independent assays, we found that removing acetylation by producing CobB abolished catalase activity and increasing acetylation by deleting *cobB* increased catalase activity by 4.4 fold (Fig. 6.2). Therefore, acetylation increases catalase activity. However, the catalase activity was not changed much by YfiQ (Fig. 6.2). This is probably because of the contribution of other nine functional
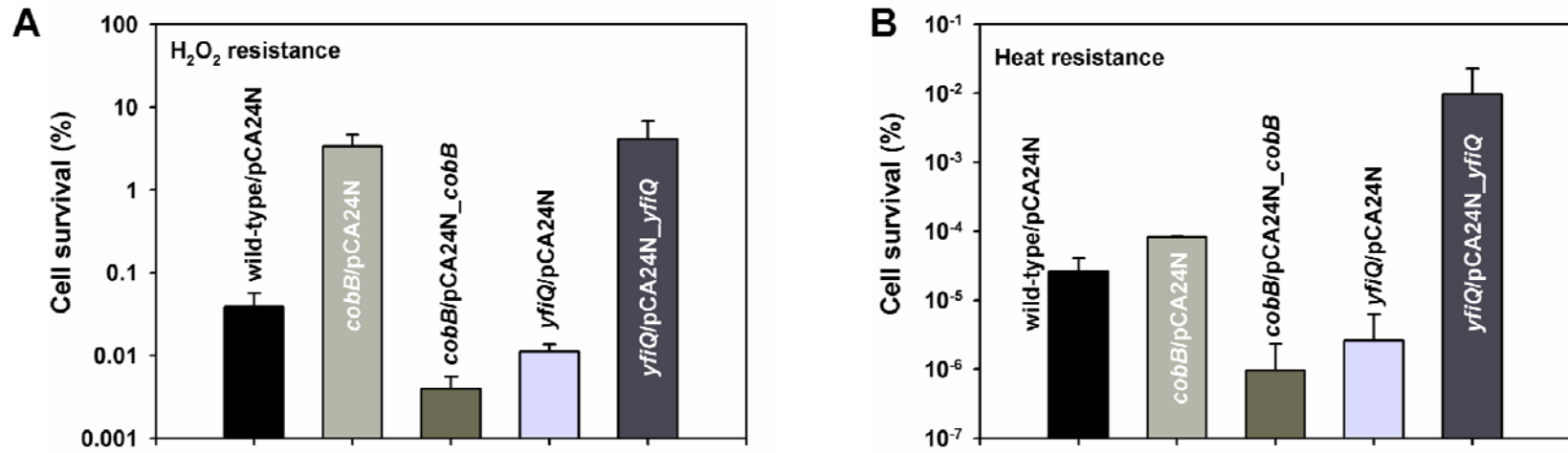
Figure 6.1 Resistance to oxidative and heat stress. *E. coli* BW25113 wild-type/pCA24N, *cobB*/pCA24N, *cobB*/pCA24N_*cobB*, *yfiQ*/pCA24N, and *yfiQ*/pCA24N_*yfiQ* were tested for H_2O_2 resistance ability (A) and heat resistance ability (B) in Luria-Bertani medium (LB) medium at 37°C.
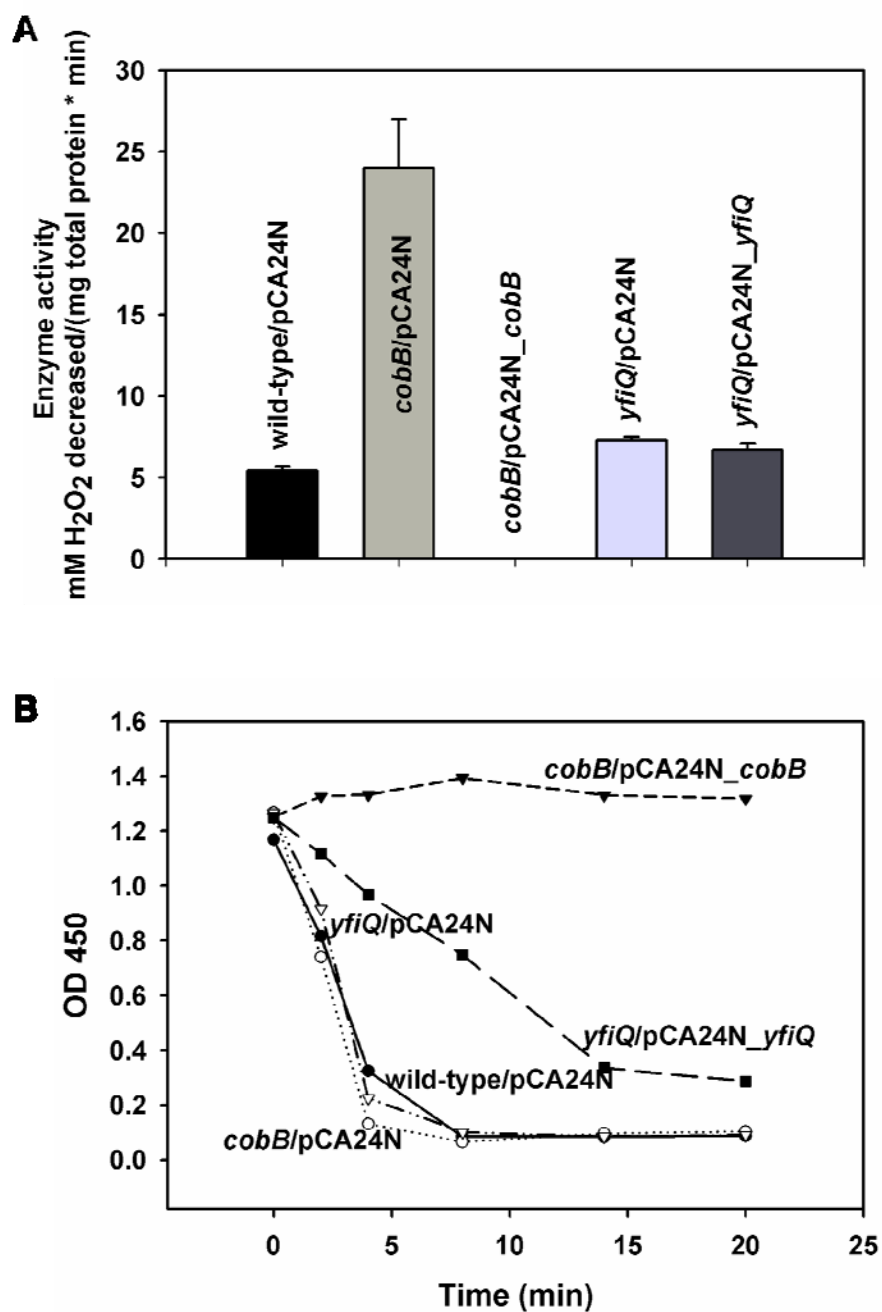
Figure 6.2 Catalase activity. The *E. coli* BW25113 wild-type/pCA24N, *cobB*/pCA24N, *cobB*/pCA24N_*cobB*, *yfiQ*/pCA24N, and *yfiQ*/pCA24N_*yfiQ* were compared for their catalase activity using the spectrophotometric method (A) and colorimetric method using dicarboxidine/lactoperoxidase (B).

acetyltransferases in *E. coli* (Escalante-Semerena, 2010).

6.3.3 Catalase related proteins KatG, KatE, and RpoS are not acetylated

Since catalase activity was affected by acetylation (Fig. 6.2), we investigated whether catalases KatG and KatE, as well as the regulator that controls catalase gene expression, RpoS, are acetylated. After analyzing around 100 peptide sequences, the mass spectrometry (MS) results indicated that none of these proteins are directly acetylated on lysine residues. Hence, the KatG, KatE, and RpoS are all not acetylated and the increased catalase activity by acetylation is not because of direct modification of these three proteins.

6.3.4 Catalase genes are induced by acetylation

To check if there are any differences in transcription of the catalase genes caused by acetylation, we measured gene expression via qRT-PCR for *rpoS*, *katG*, and *katE* (Table 6.1). *katG* was repressed 3.8 ± 0.3 fold in the *cobB*/pCA24N_*cobB* strain compared to the *cobB*/pCA24N strain without H_2O_2 addition. With the addition of 10 mM H_2O_2 for 10 min, *katG* was repressed even more (25 ± 2 fold) for *cobB*/pCA24N_*cobB* vs. *cobB*/pCA24N. Hence, catalase genes are induced due to acetylation of some unknown cellular proteins. Probably stress activates some regulator via post-translational modification which leads to induction of *katG*.

Table 6.1   qRT-PCR results for catalase-related genes *rpoS*, *katG*, and *katE*. ΔCt is the threshold difference between each gene and the housekeeping gene *rrsG*. Fold change indicates the gene transcription difference between the *cobB*/pCA24N_*cobB* strain vs. the *cobB*/pCA24N strain in LB medium at 37°C with 20 mM H_2O_2 for 10 min. Fold changes are relative to the *cobB*/pCA24N sample.

Strain name	*rpoS*		*katG*		*katE*	
	ΔCt	Fold change	ΔCt	Fold change	ΔCt	Fold change
No stress						
cobB/pCA24N	12.36 ± 0.07	1.00	8.96 ± 0.07	1.00	11.8 ± 0.1	1.00
cobB/pCA24N_*cobB*	11.8 ± 0.1	1.47	10.90 ± 0.07	-3.84	12.48 ± 0.04	-1.60
1 min H_2O_2 treatment						
cobB/pCA24N	11.0 ± 0.3	1.00	7.7 ± 0.3	1.00	10.1 ± 0.3	1.00
cobB/pCA24N_*cobB*	13.5 ± 0.1	-5.66	11.87 ± 0.07	-18.00	13.03 ± 0.08	-7.62
10 min H_2O_2 treatment						
cobB/pCA24N	11.7 ± 0.1	1.00	7.4 ± 0.3	1.00	10.9 ± 0.3	1.00
cobB/pCA24N_*cobB*	13.2 ± 0.2	-2.83	12.05 ± 0.09	-25.11	13.1 ± 0.1	-4.59

6.3.5 Acetylation induces the transcription of genes involved for various stresses

To analyze the global effect of acetylation on gene transcription, a whole-transcriptome analysis was performed with the *cobB*/pCA24N_*cobB* strain vs. the *cobB*/pCA24N strain with the rationale that production of CobB should remove the acetyl groups on all the cell proteins. We found that in addition to *katG* and *katE,* various stress-related genes are repressed by deacetylation, including the heat shock genes *dnaK* (Seyer et al., 2003), osmotic stress genes *osmB* (Jung et al., 1990) and *osmY* (Hengge-Aronis et al., 1993), acid resistance genes *gadABCE* and *hdeABD* (Lee et al., 2007c), cold shock genes *cspAB* (Ulusu and Tezcan, 2001), carbon starvation gene *csiD* and *slp* (Alexander and St John, 1994), and general stress gene *yhbO* (Abdallah et al., 2006) (Table 6.2). Hence, protein acetylation is involved in various bacterial stress response systems.

6.3.6 YfiQ increases growth yield and CobB decreases it

We found that cells with acetylation from producing YfiQ had a dramatically increased growth yield in rich medium while cells that lacked acetylation had reduced yield (Fig. 6.3). Therefore, acetylation helps cells cope with the stress associated with stationary phase growth.

6.4 Discussion and future work

Previously, the stress proteins heat shock protein DnaK (Yu et al., 2008), heat shock chaperone HtpG, superoxide dismutase SodA (Yu et al., 2008), SodB (Zhang et al., 2009), alkylhydroperoxide reductase AhpC (Zhang et al., 2009), and thioredoxin TrxA (Zhang et al., 2009) were acetylated in *E. coli*. However, there has been no prior report connecting the post-translational modification of acetylation and resistance to any environmental stress, and there has been no connection made between acetylation and a specific stress pathway. We discovered here that acetylation plays a significant role in the resistance to both oxidative stress and heat resistance. We also found using DNA microarrays that acetylation controls an even broader range of stresses by altering expression of genes related to stress resistance (including osmotic, acid, cold, and carbon starvation); this is the first whole-transcriptome study for acetylation. Bacteria sense stresses via some two-component systems and then regulate various genes transcription. Since these stress resistance genes are activated less in the CobB overproduction strain (due to deacetylation), we predict that one or more proteins (a sensor or regulator) in the signal transduction pathway of a two-component system, or the essential genes that the regulator directly controls, need the acetylation step to be activated. Thus, the acetylation state of all two-component systems in *E. coli* should be investigated. Here we connected protein acetylation to the resistance to specific stresses (oxidative and heat) and showed that for oxidative stress, the resistance stems from changes in transcription of the *katG* gene which encodes catalase.

Table 6.2 **Summary of the DNA microarray results showing the stress genes that are repressed by production of CobB.** Fold change indicates the gene transcription difference between the *cobB*/pCA24N_*cobB* strain vs. the *cobB*/pCA24N strain when cultured in LB medium at 37°C with 20 mM H_2O_2 for 10 min and with 0.1 mM IPTG to induce production of CobB.

Gene	Fold change	Gene function
dnaK	-4.0	chaperone Hsp70; DNA biosynthesis; autoregulated heat shock proteins
osmB	-3.3	osmotically inducible lipoprotein
osmY	-3.0	hyperosmotically inducible periplasmic protein
gadC	-12.1	predicted glutamate-GABA antiporter; glutamate-dependent enzyme, may function in protection against cytoplasmic acidification
gadB	-18.4	glutamate decarboxylase isozyme
gadE	-6.5	transcriptional regulator of the *gadABC* operon
gadA	-14.9	glutamate decarboxylase A; RpoS regulon. EvgAS regulon. H-NS repressed. Induced by acid shock and salt stress.
cspB	-3.2	cold shock protein
cspA	-3.0	cold shock protein
katE	-3.7	catalase; hydroperoxidase HPII(III)
katG	-4.9	catalase; hydroperoxidase HPI(I)
csiD	-3.2	carbon starvation induced gene
yhbO	-3.5	stress-resistance protein, protease homolog
slp	-11.3	outer membrane protein induced after carbon starvation
hdeB	-16.0	periplasmic chaperone of acid-denatured proteins; H-NS repressed
hdeA	-14.9	periplasmic chaperone of acid-denatured proteins; H-NS repressed
hdeD	-7.5	putative membrane transporter, H-NS repressed
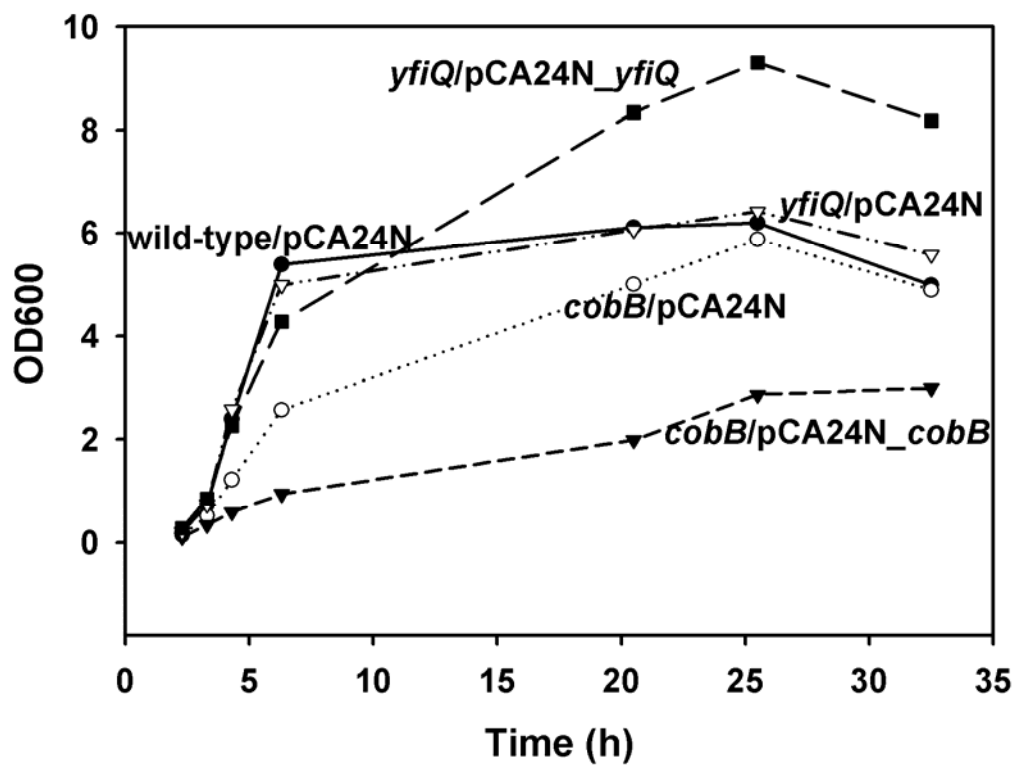
Figure 6.3 Growth curves. The strains were grown in LB medium with 30 μg/mL chloramphenicol to retain the plasmids at 37°C, and 0.1 mM IPTG was added to induce *cobB* and *yfiQ* expression after 2 h.

6.5 Experimental procedures

6.5.1 Bacterial strains, plasmids, and growth conditions

The bacterial strains and plasmids used in this study are listed in Table 6.3. *E. coli* K-12 BW25113 and its isogenic mutants (Baba et al., 2006) were obtained from the Genome Analysis Project in Japan. Plasmids pCA24N_*cobB* and pCA24N_*yfiQ*, carrying *cobB* and *yfiQ* under control of the P_{T5-lac} promoter with tight regulation via the *lacI*^{q} repressor, and the empty plasmid pCA24N were also obtained from the Genomic Analysis Project in Japan (Kitagawa et al., 2005). Expression of *cobB* and *yfiQ* was induced by 0.1 mM isopropyl-β-*D*-thiogalactopyranoside (IPTG) (Sigma, St. Louis, MO). All experiments were conducted in LB medium (Sambrook et al., 1989) at 37°C. Kanamycin (50 μg/mL) was used for pre-culturing the isogenic knock-outs. Chloramphenicol (30 μg/mL) was used for maintaining the pCA24N-based plasmids.

For the growth tests, overnight cultures for wild-type/pCA24N, *cobB*/pCA24N, *cobB*/pCA24N_*cobB*, *yfiQ*/pCA24N, and *yfiQ*/pCA24N_*yfiQ* were diluted to a turbidity of 0.05 at 600 nm and grown in LB with 30 μg/mL chloramphenicol for 2 h at 37°C. Then 0.1 mM IPTG was used to induce *cobB* and *yfiQ* expression. One mL culture was taken out at each time point and cell turbidity at 600 nm was measured.

6.5.2 Stress assays

Overnight cultures for wild-type/pCA24N, *cobB*/pCA24N, *cobB*/pCA24N_*cobB*, *yfiQ*/pCA24N, and *yfiQ*/pCA24N_*yfiQ* were diluted to a turbidity of 0.05 at 600 nm and grown in LB with 30 μg/mL chloramphenicol for 2 h at 37°C. Then 0.1 mM IPTG was used to induce *cobB* and *yfiQ* expression for 10 to 12 h. Cells were centrifuged and resuspended in phosphate buffered saline (PBS) to a turbidity of 1.0. For heat resistance assay, samples were treated at

65°C for 20 min at 37°C (Zhang et al., 2007). For the H_2O_2 resistance assay, samples were

mixed with 20 mM H_2O_2 for 20 min at 37°C (Wang et al., 2011).

Table 6.3 *E. coli* **strains and plasmids used in this study.** Km^r and Cm^r denote kanamycin and chloramphenicol resistance, respectively.

Strain/Plasmid	Genotype	Source
Strain		
BW25113	*lacI*^{q} *rrnB*$_{T14}$ *ΔlacZ*$_{WJ16}$ *hsdR514 ΔaraBAD*$_{AH33}$ *ΔrhaBAD*$_{LD78}$	(Datsenko and Wanner, 2000)
BW25113 *cobB*	BW25113 Δ*cobB* Ω Km^r	(Baba et al., 2006)
BW25113 *yfiQ*	BW25113 Δ*yfiQ* Ω Km^r	(Baba et al., 2006)
Plasmid		
pCA24N	Cm^r; *lacI*^{q}, pCA24N	(Kitagawa et al., 2005)
pCA24N_*cobB*	Cm^r; *lacI*^{q}, pCA24N p$_{T5-lac}$::*cobB*	(Kitagawa et al., 2005)
pCA24N_*yfiQ*	Cm^r; *lacI*^{q}, pCA24N p$_{T5-lac}$::*yfiQ*	(Kitagawa et al., 2005)
pCA24N_*tnaA*	Cm^r; *lacI*^{q}, pCA24N p$_{T5-lac}$::*tnaA*	(Kitagawa et al., 2005)
pCA24N_*rpoS*	Cm^r; *lacI*^{q}, pCA24N p$_{T5-lac}$::*rpoS*	(Kitagawa et al., 2005)
pCA24N_*katG*	Cm^r; *lacI*^{q}, pCA24N p$_{T5-lac}$::*katG*	(Kitagawa et al., 2005)
pCA24N_*katE*	Cm^r; *lacI*^{q}, pCA24N p$_{T5-lac}$::*katE*	(Kitagawa et al., 2005)

6.5.3 Catalase assays

Overnight cultures for wild-type/pCA24N, *cobB*/pCA24N, *cobB*/pCA24N_*cobB*, *yfiQ*/pCA24N, and *yfiQ*/pCA24N_*yfiQ* were diluted to a turbidity of 0.05 at 600 nm and grown

for 2 h in LB with 30 μg/mL chloramphenicol at 37°C. 0.1 mM IPTG was added and the cultures

were grown for another 4 h. Catalase activity was then measured in two different ways in this

study. For the spectrophotometric assay (Gusarov and Nudler, 2005), one mL culture for each

sample was washed and resuspended into PBS buffer for a turbidity at 600 nm of 0.5. For each sample, catalase activity was measured by checking the rate of H_2O_2 decrease which is reflected by the rate of change of absorbance at 240 nm value at 37°C. Two tubes were used for each sample, and 5 mM H_2O_2 was added for one while the other one was used as a control. The conversion between H_2O_2 concentration and absorbance was that 10 mM H_2O_2 is equal to 0.36 at OD 240 nm (Gusarov and Nudler, 2005).

The second method for catalase activity check used a colorimetric assay with dicarboxidine/lactoperoxidase (Macvanin and Hughes, 2010). The cultures were washed and resuspended in M9 glucose medium with 30 μg/mL chloramphenicol for a turbidity of 1.0 at 600 nm. IPTG (0.1 mM) was added to each sample to induce the expression of *cobB* and *yfiQ*. The cultures were then incubated at 37°C for 4 h. Before the test, a solution of 50 μg/mL of lactoperoxidase was mixed with an equal volume of 1 mM dicarboxidine solution in water (dicarboxidine is converted into a yellow product in a reaction catalyzed by the activity of lactoperoxidase, and the amount of color developed is directly proportional to the amount of H_2O_2 present in the medium). To start the reaction, 10 mM H_2O_2 was added to the culture, and. samples (10 μL) were taken after every 2 minutes at the beginning and 5 to 10 minutes later. The samples were added to a 200 μL reaction mixture. The absorbance (OD 450 nm) was measured immediately. Higher catalase activity causes faster decrease of OD 450 nm.

6.5.4 qRT-PCR

qRT-PCR was performed using the StepOne™ Real-Time PCR System (Applied Biosystems, Foster City, CA). After isolating RNA (Ren et al., 2004a) using RNA*later*™ (Ambion, Austin, TX), 50 ng of total RNA was used for the qRT-PCR reaction using the *Power* SYBR® Green RNA-to-C_T™ *1-Step* Kit (Applied Biosystems). The primers are listed in Table 6.4. The housekeeping gene *rrsG* was used to normalize gene expression data (Lee et al., 2009a).

The annealing temperature was 60°C for all the genes in this study. To investigate the transcription level of *rpoS*, *katG*, and *katE* under oxidative stress conditions, overnight cultures of BW25113 wild-type/pCA24N, *cobB*/pCA24N, *cobB*/pCA24N_*cobB*, *yfiQ*/pCA24N, and *yfiQ*/pCA24N_*yfiQ* were cultured to a turbidity of 0.05 at 600 nm, grown 2 h, then 0.1 mM IPTG was added for another 4 h to induce *cobB* and *yfiQ* expression, and then the cells were exposed to 20 mM H_2O_2 for 10 min.

Table 6.4   Primers used for qRT-PCR in this study.

Primer name	Sequence
rpoS-f	5'-AGAGTAACTTGCGTCTGGTGGTAAA-3'
rpoS-r	5'-ATAGTACGGGTTTGGTTCATAATCG-3'
katG-f	5'-CTGGTGTGGTTGGTGTTGAG-3'
katG-r	5'-AGTGACTCGGTGGTGGAAAC-3'
katE-f	5'- GATCTTCTCGATCCAACCAAAC-3'
katE-r	5'-CACCAAGACGACTGATTTGTGT-3'
rrsG-f	5'-TATTGCACAATGGGCGCAAG-3'
rrsG-r	5'-ACTTAACAAACCGCTGCGT-3'

6.5.5 Whole-transcriptome analysis

Overnight cultures of BW25113 *cobB*/pCA24N and *cobB*/pCA24N_*cobB* were cultured to a turbidity of 0.05 at 600 nm, grown 2 h, then 0.1 mM IPTG was added for another 4 h to induce *cobB* expression, and then the cells were exposed to 20 mM H_2O_2 for 10 min. Cell pellets

were collected and resuspended in RNA*later* (Ambion Inc., Austin, TX), and total RNA was isolated using the RNeasy Mini Kit (Qiagen Inc., Valencia, CA) (Ren et al., 2004a). The *E. coli* GeneChip Genome 2.0 array (Affymetrix, P/N 900551) was used, and cDNA synthesis, fragmentation, and hybridizations were performed as described previously (González Barrios et al., 2006b). If the gene with the larger transcription rate did not have a consistent transcription rate based on the 11-15 probe pairs (*P*-value less than 0.05), these genes were discarded. A gene was considered differentially expressed when the *P*-value for comparing two chips was lower than 0.05 (to assure that the change in gene expression was statistically significant and that false positives arise less than 5%) and if their fold change is higher than standard deviation for the whole genome (Ren et al., 2004b).

6.5.6 MS

His-tagged RpoS, KatG, and KatE were purified from pCA24N-based plasmids in the *cobB* mutant (to purify potential acetylated proteins) and in the *yfiQ* mutant (to purify the potential unacetylated proteins). Overnight cultures were diluted in 1 L LB medium to a turbidity as 0.05 at 600 nm. Each sample was grown at 37°C until the cell turbidity at 600 nm reaches 0.6 to 1.0. Cultures were kept at 4°C for 45 min and then induced with 0.1 mM IPTG overnight at room temperature. Cell pellets were collected and lysed with a French Press. Supernatants were treated with 1 mL Ni-NTA agarose resin for 2 h. Purified His-tag proteins were digested with trypsin and cleaned with a zip-tip cleaning method. Samples were eluted with 4 μL 0.1% formic acid plus 25% and 50% acetonitrile. The MS results were obtained using 4800 MALDI TOF/TOF Analyzer (Applied Biosystems/MDS Sciex, Carlsbad, CA) (Sherrod et al., 2008).

CHAPTER VII

CONCLUSIONS AND RECOMMENDATIONS

7.1 Conclusions

We show OmpA influences the biofilm formation of *E. coli* differently on hydrophobic and hydrophilic surfaces since we found that it represses cellulose production which is hydrophilic in *Escherichia coli*. Production of OmpA increased biofilm formation on polystyrene, polypropylene, and polyvinyl surfaces while it decreased biofilm formation on glass surfaces. Sand column assays corroborated that OmpA decreases attachment to hydrophilic surfaces. The *ompA* mutant formed sticky colonies, and the extracellular polysaccharide that caused stickiness was identified as cellulose. A whole-transcriptome study revealed that OmpA induces the CpxRA two-component signal transduction pathway that responds to membrane stress. CpxA phosphorylates CpxR and results in reduced *csgD* expression. Reduced CsgD production represses *adrA* expression and results in reduced cellulose production since CsgD and AdrA are responsible for 3,5-cyclic diguanylic acid (c-di-GMP) synthesis and cellulose production. Real-time polymerase chain reaction confirmed *csgD* and *adrA* are repressed by OmpA. Biofilm and cellulose assays with double deletion mutants *adrA ompA*, *csgB ompA*, and *cpxR ompA* confirmed OmpA decreased cellulose production and increased biofilm formation on polystyrene surfaces through CpxR and AdrA. Further evidence of the link between OmpA and the CpxRA system was that overproduction of OmpA disrupted the membrane and led to cell lysis. Therefore, OmpA inhibits cellulose production through the CpxRA stress response system, and this reduction in cellulose increases biofilm formation on hydrophobic surfaces.

We also report simultaneously the discovery and protein engineering of BdcA (formerly YjgI) for biofilm dispersal using the universal signal c-di-GMP in *E. coli*. The *bdcA* deletion reduced biofilm dispersal, and production of BdcA increased biofilm dispersal to wild-type

levels. Since BdcA increases motility and extracellular DNA production while decreasing exopolysaccharide, cell length, and aggregation, we reasoned that BdcA decreases the concentration of c-di-GMP, the intracellular messenger that controls cell motility through flagellar rotation and biofilm formation through synthesis of curli and cellulose. Consistently, c-di-GMP levels increase upon deleting *bdcA,* and purified BdcA binds c-di-GMP but does not act as a phosphodiesterase. Additionally, BdcR (formerly YjgJ) is a negative regulator of *bdcA*. To increase biofilm dispersal, we used protein engineering to evolve BdcA for greater c-di-GMP binding and found that the single amino acid change E50Q causes nearly complete removal of biofilms via dispersal without affecting initial biofilm formation.

We identify two kinds of bacteria in the salivary gland extracts of the blowfly *Lucilia sericata*: *Proteus mirabilis* and *Providencia stuartii*. We focus on *P. mirabilis* since it aggressively out-competed both *Pseudomonas aeruginosa* and *E. coli* during biofilm formation, since it swarmed significantly, and since it is expected that the swarming phenotype depends on quorum sensing. In addition, *P. mirabilis* produces a strong smell during its growth, which probably attracts blowflies. We performed transposon mutagenesis with the *P. mirabilis* strain isolated from the *L. sericata* salivary gland and screened ~3000 swarming-deficient mutants to identify 60 mutants with at least a 3-fold decrease in swarming motility (23 were sequenced). Furthermore, swarming was tested with these 23 mutants in the presence of eight chemicals (at 10 μM and 250 μM) which were previously identified as attractants for blowflies (benzoic acid, butyric acid, indole, lactic acid, *p*-cresol, phenol, KOH, and NaOH), and two other chemicals important in *P. mirabilis* metabolism (putrescine and ammonia). We found lactic acid, phenol, NaOH, KOH, putrescine, and ammonia have the ability to restore the swarming motility of seven different mutants to 25 to 100% of the wild-type level. Hence, these compounds are necessary

for swarming (5 of these compounds have never been associated with swarming previously with this strain) and they have been linked to specific genes in *P. mirabilis*.

We also demonstrate that acetylation enables the reference bacterium *E. coli* to withstand environmental stress. Specifically, the bacterium becomes more resistant to heat and oxidative stress when proteins are acetylated. Furthermore, we show that the increase in oxidative stress via acetylation is due to the induction of catalase genes especially *katG*. A whole-transcriptome profile shows that the acetylation changes transcription of genes involved in various stresses including heat, cold, starvation, osmotic, acid, and oxidative stresses. Hence acetylation is proved to be an important post-translational modification that is required for bacterial stress resistance. This is the first demonstration of a specific environmental role of acetylation in prokaryotes.

7.2 Recommendations

By testing biofilm formation with mutants of important genes from the TqsA microarray list (Herzberg et al., 2006), we identified BdcA as an important biofilm dispersal protein, as well as identified some other proteins that obviously changed biofilm formation (Table 4.1). YecT is repressed -4.6 fold with the expression of *tqsA*. An initial biofilm test showed that the *yecT* mutant has over 8-fold decreased biofilm formation at 15 h in LB medium at 37°C. This phenotype is complemented using YecT overproduced from the pCA24N plasmid. Bioinformatics search showed that YecT is located on the membrane and has one transmembrane helix. In addition, the YecT protein is predicted to be a DNA-binding protein. It has signal peptide sequence which may direct the transport of protein. YecT did not change cell aggregation, swimming motility, pH, or the concentration of the cell signaling molecules indole and AI-2. DNA microarrays showed in the *yecT* knockout mutant that the envelope stress response system genes *rseA*, *rpoESHL*, *cpxP* were repressed 2.3 to 2.6 fold, and DLP12

prophage genes were induced 2.1 to 2.3 fold. Hence the mechanism about how YecT works for controlling biofilm formation is promising.

By performing a whole-genome transcriptome temporal study, we identified that cold shock proteins were induced 2 to 23 fold in the biofilm cells relative to the suspension cells after 4 to 7 h incubation at 37°C in *E. coli* (Domka et al., 2007). Additionally, in our other biofilm DNA microarray studies involving biofilm stress protein BhsA (Zhang et al., 2007), AI-2 transporter TqsA (Herzberg et al., 2006), *E. coli* O157:H7 biofilms treated with epinephrine, norepinephrine, and indole (Bansal et al., 2007), and cell signal 7-hydroxyindole (Lee et al., 2007b), cold shock proteins were also differentially expressed. Therefore, we investigated their role in biofilm formation for *E. coli* BW25113. Static biofilm assay showed that among *cspABFGI*, deletion of *cspG* caused some of the most significant biofilm increases in glucose-containing medium, so we focused on CspG. Flow cell experiments and COMSTAT analysis in M9C glucose medium corroborated that CspG decreases biofilm formation. Since there were no significant changes in specific growth rates for the *cspABFGI* mutations, the phenotypic changes are not due to growth defects. To determine the genetic basis of CspG-based reduction of biofilms, a whole transcriptome analysis was performed using biofilm cells at both 30°C and 37°C. Both 30°C and 37°C microarray analyses showed that CspG represses expression of acid resistance genes (e.g., *gadABCE* and *hdeABD*) and fatty acid genes (e.g., *prpBCD*). CspG also influenced expression of genes for outer membrane proteins (e.g., CspG induced *nmpC* and *ompW* at 37°C and CspG repressed *ompACX* at 30°C). Similarly, CspG induced genes related to sulfur metabolism (e.g, *cysDNPUW*) at 37°C and repressed these genes at 30°C. Furthermore, more cold shock proteins were expressed at the lower temperature. Overexpressing *cspG* in 29 isogenic mutants revealed that 15 genes (*astC*, *cysKP*, *dctA*, *gatBCD*, *nmpC*, *prpBD*, *putP*, *rbsC*, *tnaA*, *ybiM* and *yfiD*) may be necessary for CspG to control biofilm formation; normally

overproduction of CspG reduces biofilm yet in these 15 mutants, biofilm formation was unchanged or increased. Expression of CspG had a negligible effect on extracellular indole, cell growth rate, pH, cell aggregation, hydrophobicity, and curli formation; however, inactivation of *cspG* increased motility 4-fold. Moreover, we identified that CspG is a RNA-binding protein. Hence it is possible that the RNA is critical for CspG function. Further study should focus on identifying the sequence and role of the CspG-binding RNA. We can first isolate His-tagged CspG which comes out together with the RNA pieces. The next step is to use protease to remove CspG and get purified RNA. Reverse transcription should be performed then to convert RNA into single-strand cDNA (with reverse transcriptase), and then double-strand DNA (with DNA polymerase). Finally we can use blunt-end cloning to insert this piece of DNA into a vector and do a sequencing to see what this RNA is. We can remove the corresponding gene from the *cspG* mutant then to see if CspG still can change biofilm formation and swimming motility without the RNA-binding. If CspG cannot work on controlling phenotypes without this RNA, then it will be clear that this cold shock protein needs a nucleotide chaperone to work.

Although we successfully identified BdcA as a c-di-GMP-binding protein and engineered it for better binding, the binding motif on this protein remains to be elucidated. A straight-forward method would be to perform random mutagenesis with this protein and screen for mutations that abolish BdcA function as evidenced as by reduced swimming motility and dispersal due to reduced binding of c-di-GMP. The nucleotide sequences for c-di-GMP binding by BdcA are critical and their identification may allow further improvements in BdcA function. It would also be beneficial to get the crystal structure of this protein to model its binding to c-di-GMP.

To make BdcA a general and useful tool for removing biofilm rather than a mere lab toy, we need to prove that BdcA will work for removing biofilms in other bacteria. A broad host

plasmid such as pMMB206 should be used to express *bdcA* instead of the pCA24N plasmid which is limited to use with *E. coli*. Our initial results show that BdcA can cause biofilm dispersal in *P. aeruginosa*. More tests on different strains should be performed (*Pseudomonas putida*, *Pseudomonas fluorescens*, *Rhizobium meliloti*, and *Proteus mirabilis*), and BdcA is expected to work for biofilm dispersal in any organism as where c-di-GMP is utilized an internal signal for biofilm formation (which may be all bacteria as none are known to date that do not use c-di-GMP this way).

To practically control biofilm dispersal, conjugation may be combined with BdcA biofilm dispersal to treat multi-species biofilms. By using an *E. coli* host with both the biofilm dispersal plasmid pMMB206_BdcAE50Q and the conjugation helper plasmid pRK2013, the pMMB206_BdcAE50Q plasmid may be mobilized via conjugation into target bacteria which are desired to be removed. After the target bacteria receive the gene for the BdcAE50Q, we can induce the production of BdcAE50Q with IPTG and remove the biofilms of both the donor *E. coli* and the recipient bacteria.

We have already identified several putative interkingdom signals that work for complementing *P. mirabilis* swarming. To test if they can also affect fly behavior, the fly attraction and oviposition assay should be applied for all the swarming-deficient mutants. For the mutants that are unable to attract flies as well as the wild-type strain, it is desirable to add back the chemical which can complement mutant swarming motility and test if this chemical can complement mutants for fly attraction and oviposition ability. In addition, the concentration of these chemicals that the *P. mirabilis* wild-type normally produces should also be checked. In this way, we will be able to confirm that these effective chemicals can be called as interkingdom signals that not only change the *P. mirabilis* swarming motility, but also attract flies for oviposition.

We discovered that acetylation plays a significant role in the resistance to both oxidative stress and heat resistance. We also found that acetylation controls an even broader range of stresses by altering expression of genes related to stress resistance (osmotic, acid, cold, and carbon starvation) using DNA microarrays which is the first whole transcriptome study for acetylation. Bacteria sense stresses via some two-component systems and then regulate various genes transcription. Since these stress resistance genes are activated less in the CobB overproduction strain (due to deacetylation), we predict that one or more proteins (a sensor or regulator) in the signal transduction pathway of a two-component system, or the essential genes that the regulator directly controls, need the acetylation step to be activated. Thus, the acetylation state of all two-component systems in *E. coli* should be investigated.

REFERENCES

Abdallah, J., Kern, R., Malki, A., Eckey, V., and Richarme, G. (2006) Cloning, expression, and purification of the general stress protein YhbO from *Escherichia coli*. *Protein Expr Purif* **47**: 455-460.

Abeyrathne, P.D., and Lam, J.S. (2007) WaaL of *Pseudomonas aeruginosa* utilizes ATP in in vitro ligation of O antigen onto lipid A-core. *Mol Microbiol* **65**: 1345-1359.

Ahmad, A., Broce, A., and Zurek, L. (2006) Evaluation of significance of bacteria in larval development of *Cochliomyia macellaria* (Diptera: Calliphoridae). *J Med Entomol* **43**: 1129-1133.

Albert Siryaporn, and Goulian, M. (2008) Cross-talk suppression between the CpxA–CpxR and EnvZ–OmpR two-component systems in *E. coli*. *Mol Microbiol* **70**: 494-506.

Alexander, D.M., and St John, A.C. (1994) Characterization of the carbon starvation-inducible and stationary phase-inducible gene *slp* encoding an outer membrane lipoprotein in *Escherichia coli*. *Mol Microbiol* **11**: 1059-1071.

Arnold, K., Bordoli, L., Kopp, J., and Schwede, T. (2006) The SWISS-MODEL workspace: a web-based environment for protein structure homology modelling. *Bioinformatics* **22**: 195-201.

Atlas, R.M. (2004) *Handbook of Microbiological Media*. London: CRC Press.

Baba, T., Ara, T., Hasegawa, M., Takai, Y., Okumura, Y., Baba, M. et al. (2006) Construction of *Escherichia coli* K-12 in-frame, single-gene knockout mutants: the Keio collection. *Mol Syst Biol* **2**: 2006 0008.

Bansal, T., Alaniz, R.C., Wood, T.K., and Jayaraman, A. (2010) The bacterial signal indole increases epithelial-cell tight-junction resistance and attenuates indicators of inflammation. *Proc Natl Acad Sci U S A* **107**: 228-233.

Bansal, T., Englert, D., Lee, J., Hegde, M., Wood, T.K., and Jayaraman, A. (2007) Differential effects of epinephrine, norepinephrine, and indole on *Escherichia coli* O157:H7 chemotaxis, colonization, and gene expression. *Infect Immun* **75**: 4597-4607.

Barken, K.B., Pamp, S.J., Yang, L., Gjermansen, M., Bertrand, J.J., Klausen, M. et al. (2008) Roles of type IV pili, flagellum-mediated motility and extracellular DNA in the formation of mature multicellular structures in *Pseudomonas aeruginosa* biofilms. *Environ Microbiol* **10**: 2331-2343.

Barraud, N., Hassett, D.J., Hwang, S.H., Rice, S.A., Kjelleberg, S., and Webb, J.S. (2006) Involvement of nitric oxide in biofilm dispersal of *Pseudomonas aeruginosa*. *J Bacteriol* **188**: 7344-7353.

Barraud, N., Storey, M.V., Moore, Z.P., Webb, J.S., Rice, S.A., and Kjelleberg, S. (2009) Nitric oxide-mediated dispersal in single- and multi-species biofilms of clinically and industrially relevant microorganisms. *Microb Biotechnol* **2**: 370-378.

Belas, R., Goldman, M., and Ashliman, K. (1995) Genetic analysis of *Proteus mirabilis* mutants defective in swarmer cell elongation. *J Bacteriol* **177**: 823-828.

Beloin, C., Valle, J., Latour-Lambert, P., Faure, P., Kzreminski, M., Balestrino, D. et al. (2004) Global impact of mature biofilm lifestyle on *Escherichia coli* K-12 gene expression. *Mol Microbiol* **51**: 659-674.

Bendouah, Z., Barbeau, J., Hamad, W.A., and Desrosiers, M. (2006) Biofilm formation by *Staphylococcus aureus* and *Pseudomonas aeruginosa* is associated with an unfavorable evolution after surgery for chronic sinusitis and nasal polyposis. *Otolaryngol Head Neck Surg* **134**: 991-996.

Blattner, F.R., Plunkett, 3rd, G., Bloch, C.A., Perna, N.T., Burland, V., Riley, M. et al. (1997) The complete genome sequence of *Escherichia coli* K-12. *Science* **277**: 1453-1474.

Boehm, A., Kaiser, M., Li, H., Spangler, C., Kasper, C.A., Ackermann, M. et al. (2010) Second messenger-mediated adjustment of bacterial swimming velocity. *Cell* **141**: 107-116.

Broce, A.B. (1980) Sexual behavior of screwworm flies stimulated by swormlure-2. *Ann Entomol Soc Amer* **73**: 386-389.

Brown, B.L., Grigoriu, S., Kim, Y., Arruda, J.M., Davenport, A., Wood, T.K. et al. (2009) Three dimensional structure of the MqsR:MqsA complex: a novel TA pair comprised of a toxin homologous to RelE and an antitoxin with unique properties. *PLoS Pathog* **5**: e1000706.

Cazander, G., van Veen, K.E.B., Bouwman, L.H., Bernards, A.T., and Jukema, G.N. (2009) The influence of maggot excretions on PAO1 biofilm formation on different biomaterials. *Clin Orthop Relat Res* **467**: 536-545.

Chai, T.J., and Foulds, J. (1977) Purification of protein A, an outer membrane component missing in *Escherichia coli* K-12 *ompA* mutants. *Biochim Biophys Acta* **493**: 210-215.

Characklis, W.G., Nevimons, M.J., and Picologlou, B.F. (1981) Influence of fouling biofilms on heat transfer. *Heat Transfer Eng* **3**: 23-27.

Cherepanov, P.P., and Wackernagel, W. (1995) Gene disruption in *Escherichia coli*: Tc^R and Km^R cassettes with the option of Flp-catalyzed excision of the antibiotic-resistance determinant. *Gene* **158**: 9-14.

Cheville, A.M., Arnold, K.W., Buchrieser, C., Cheng, C.M., and Kaspar, C.W. (1996) *rpoS* regulation of acid, heat, and salt tolerance in *Escherichia coli* O157:H7. *Appl Environ Microbiol* **62**: 1822-1824.

Clark, K., Evans, L., and Wall, R. (2006) Growth rates of the blowfly, *Lucilia sericata*, on different body tissues. *Forensic Sci Int* **156**: 145-149.

Clemmer, K.M., and Rather, P.N. (2007) Regulation of flhDC expression in *Proteus mirabilis*. *Res Microbiol* **158**: 295-302.

Cozzone, A.J. (1988) Protein phosphorylation in prokaryotes. *Annu Rev Microbiol* **42**: 97-125.

Crombie, A.C. (1941) On oviposition, olfactory conditioning and host selection in *Rhizopertha Dominica* fab. (Insecta, Coleoptera) *J Exp Biol* **18**: 62-78.

D'Argenio, D.A., and Miller, S.I. (2004) Cyclic di-GMP as a bacterial second messenger. *Microbiology* **150**: 2497-2502.

Da Re, S., and Ghigo, J.M. (2006) A CsgD-independent pathway for cellulose production and biofilm formation in *Escherichia coli*. *J Bacteriol* **188**: 3073-3087.

Danese, P.N., and Silhavy, T.J. (1998) CpxP, a stress-combative member of the Cpx regulon. *J Bacteriol* **180**: 831-839.

Danese, P.N., Pratt, L.A., and Kolter, R. (2000a) Exopolysaccharide production is required for development of *Escherichia coli* K-12 biofilm architecture. *J Bacteriol* **182**: 3593-3596.

Danese, P.N., Pratt, L.A., Dove, S.L., and Kolter, R. (2000b) The outer membrane protein, antigen 43, mediates cell-to-cell interactions within *Escherichia coli* biofilms. *Mol Microbiol* **37**: 424-432.

Daniels, R., Vanderleyden, J., and Michiels, J. (2004) Quorum sensing and swarming migration in bacteria. *FEMS Microbiol Rev* **28**: 261-289.

Datsenko, K.A., and Wanner, B.L. (2000) One-step inactivation of chromosomal genes in *Escherichia coli* K-12 using PCR products. *Proc Natl Acad Sci U S A* **97**: 6640-6645.

Davies, D.G., Parsek, M.R., Pearson, J.P., Iglewski, B.H., Costerton, J.W., and Greenberg, E.P. (1998) The involvement of cell-to-cell signals in the development of a bacterial biofilm. *Science* **280**: 295-298.

De Jesus, A.J., Olsen, A.R., Bryce, J.R., and Whiting, R.C. (2004) Quantitative contamination and transfer of *Escherichia coli* from foods by houseflies, *Musca domestica* L. (Diptera: Muscidae). *Int J Food Microbiol* **93**: 259-262.

Dethier, V.G. (1947) *Chemical Insect Attractants and Repellents*. Philadelphia: Blakiston Press.

Di Martino, P., Fursy, R., Bret, L., Sundararaju, B., and Phillips, R.S. (2003) Indole can act as an extracellular signal to regulate biofilm formation of *Escherichia coli* and other indole-producing bacteria. *Can J Microbiol* **49**: 443-449.

DiGiuseppe, P.A., and Silhavy, T.J. (2003) Signal detection and target gene induction by the CpxRA two-component system. *J Bacteriol* **185**: 2432-2440.

Domka, J., Lee, J., and Wood, T.K. (2006) YliH (BssR) and YceP (BssS) regulate *Escherichia coli* K-12 biofilm formation by influencing cell signaling. *Appl Environ Microbiol* **72**: 2449-2459.

Domka, J., Lee, J., Bansal, T., and Wood, T.K. (2007) Temporal gene-expression in *Escherichia coli* K-12 biofilms. *Environ Microbiol* **9**: 332-346.

Dorel, C., Lejeune, P., and Rodrigue, A. (2006) The Cpx system of *Escherichia coli*, a strategic signaling pathway for confronting adverse conditions and for settling biofilm communities? *Res Microbiol* **157**: 306-314.

Dorel, C., Vidal, O., Prigent-Combaret, C., Vallet, I., and Lejeune, P. (1999) Involvement of the Cpx signal transduction pathway of *E. coli* in biofilm formation. *FEMS Microbiol Lett* **178**: 169-175.

Dow, J.M., Fouhy, Y., Lucey, J.F., and Ryan, R.P. (2006) The HD-GYP domain, cyclic di-GMP signaling, and bacterial virulence to plants. *Mol Plant Microbe Interact* **19**: 1378-1384.

Dowd, S.E., Sun, Y., Wolcott, R.D., Domingo, A., and Carroll, J.A. (2008a) Bacterial tag-encoded FLX amplicon pyrosequencing (bTEFAP) for microbiome studies: bacterial diversity in the ileum of newly weaned *Salmonella*-infected pigs. *Foodborne Pathog Dis* **5**: 459-472.

Dowd, S.E., Wolcott, R.D., Sun, Y., McKeehan, T., Smith, E., and Rhoads, D. (2008b) Polymicrobial nature of chronic diabetic foot ulcer biofilm infections determined using bacterial tag encoded FLX amplicon pyrosequencing (bTEFAP). *PLoS ONE* **3**: e3326.

Dowd, S.E., Callaway, T.R., Wolcott, R.D., Sun, Y., McKeehan, T., Hagevoort, R.G., and Edrington, T.S. (2008c) Evaluation of the bacterial diversity in the feces of cattle using 16S rDNA bacterial tag-encoded FLX amplicon pyrosequencing (bTEFAP). *BMC Microbiol* **8**: 125.

Duan, J., Wu, S., Zhang, X., Huang, G., Du, M., and Hou, B. (2008) Corrosion of carbon steel influenced by anaeroic biofilm in natural seawater. *Electrochim acta* **54**: 22-28.

Dürr, S., and Thomason, J.C. (2009) *Biofouling*. Oxford, UK: Blackwell publishing Ltd.

Emmens, R.L., and Murray, M.D. (1982) The role of bacterial odours in oviposition by *Lucilia cuprina* (Wiedemann) (Diptera: Calliphoridae), the Australian sheep blowfly. *Bull Ent Res* **72**: 367-375.

Erdmann, G.R. (1987) Antibacterial action of myiasis-causing flies. *Parasitol Today* **3**: 214-216.

Escalante-Semerena, J.C. (2010) N^{ε}-lysine acetylation control conserved in all three life domains. *Microbe* **5**: 340-344.

Farr, S.B., and Kogoma, T. (1991) Oxidative stress responses in *Escherichia coli* and *Salmonella typhimurium*. *Microbiol Rev* **55**: 561-585.

Flemming, H.C., Schaule, G., and Mc Donogh, R. (1992) Biofouling - a biofilm problem. *Recents Progres en Genie des Procedes* **6**: 209-213.

Fletcher, M. (1977) The effects of culture concentration and age, time, and temperature on bacterial attachment to polystyrene. *Can. J. Microbiol.* **23**: 1-6.

FoodNet (June 2006). CDC FoodNet Surveillance Report for 2004. URL <http://www.cdc.gov/foodnet/annual/2004/report.pdf>

Fraser, G.M., Bennett, J.C., and Hughes, C. (1999) Substrate-specific binding of hook-associated proteins by FlgN and FliT, putative chaperones for flagellum assembly. *Mol Microbiol* **32**: 569-580.

Frenzen, P.D., Drake, A., and Angulo, F.J. (2005) Economic cost of illness due to *Escherichia coli* O157 infections in the United States. *J Food Prot* **68**: 2623-2630.

Gaddy, J.A., Tomaras, A.P., and Actis, L.A. (2009) The *Acinetobacter baumannii* 19606 OmpA protein plays a role in biofilm formation on abiotic surfaces and the interaction of this pathogen with eukaryotic cells. *Infect Immun* on-line: doi:10.1128/IAI.00096-00009.

García-Contreras, R., Zhang, X.S., Kim, Y., and Wood, T.K. (2008) Protein translation and cell death: the role of rare tRNAs in biofilm formation and in activating dormant phage killer genes. *PLoS ONE* **3**: e2394.

García, B., Latasa, C., Solano, C., Garcia-del Portillo, F., Gamazo, C., and Lasa, I. (2004) Role of the GGDEF protein family in *Salmonella* cellulose biosynthesis and biofilm formation. *Mol Microbiol* **54**: 264-277.

Gerstel, U., and Römling, U. (2003) The *csgD* promoter, a control unit for biofilm formation in *Salmonella typhimurium*. *Res Microbiol* **154**: 659-667.

Gherardini, P.F., Ausiello, G., Russell, R.B., and Helmer-Citterich, M. (2010) Modular architecture of nucleotide-binding pockets. *Nucleic Acids Res* **38**: 3809-3816.

Gjermansen, M., Nilsson, M., Yang, L., and Tolker-Nielsen, T. (2010) Characterization of starvation-induced dispersion in *Pseudomonas putida* biofilms: genetic elements and molecular mechanisms. *Mol Microbiol* **75**: 815-826.

González Barrios, A.F., Zuo, R., Ren, D., and Wood, T.K. (2006a) Hha, YbaJ, and OmpA regulate *Escherichia coli* K12 biofilm formation and conjugation plasmids abolish motility. *Biotechnol Bioeng* **93**: 188-200.

González Barrios, A.F., Zuo, R., Hashimoto, Y., Yang, L., Bentley, W.E., and Wood, T.K. (2006b) Autoinducer 2 controls biofilm formation in *Escherichia coli* through a novel motility quorum-sensing regulator (MqsR, B3022). *J Bacteriol* **188**: 305-316.

Greenberg, B. (1973) *Biology and Disease Transmission*. Princeton, NJ: Princeton University Press.

Grossman, T.H., and Silverman, P.M. (1989) Structure and function of conjugative pili: inducible synthesis of functional F pili by *Escherichia coli* K-12 containing a *lac-tra* operon fusion. *J Bacteriol* **171**: 650-656.

Gualdi, L., Tagliabue, L., Bertagnoli, S., Ierano, T., De Castro, C., and Landini, P. (2008) Cellulose modulates biofilm formation by counteracting curli-mediated colonization of solid surfaces in *Escherichia coli*. *Microbiology* **154**: 2017-2024.

Gusarov, I., and Nudler, E. (2005) NO-mediated cytoprotection: instant adaptation to oxidative stress in bacteria. *Proc Natl Acad Sci U S A* **102**: 13855-13860.

Han, T.H., Lee, J.H., Cho, M.H., Wood, T.K., and Lee, J. (2010) Environmental factors affecting indole production in *Escherichia coli*. *Res Microbiol* **162**: 108-116.

Hancock, V., and Klemm, P. (2007) Global gene expression profiling of asymptomatic bacteriuria *Escherichia coli* during biofilm growth in human urine. *Infect Immun* **75**: 966-976.

Hansen, M.C., Palmer, R.J., Jr., Udsen, C., White, D.C., and Molin, S. (2001) Assessment of GFP fluorescence in cells of *Streptococcus gordonii* under conditions of low pH and low oxygen concentration. *Microbiology* **147**: 1383-1391.

Hengge-Aronis, R., Lange, R., Henneberg, N., and Fischer, D. (1993) Osmotic regulation of rpoS-dependent genes in *Escherichia coli*. *J Bacteriol* **175**: 259-265.

Herzberg, M., Kaye, I.K., Peti, W., and Wood, T.K. (2006) YdgG (TqsA) controls biofilm formation in *Escherichia coli* K-12 through autoinducer 2 transport. *J Bacteriol* **188**: 587-598.

Hong, S.H., Wang, X., and Wood, T.K. (2010a) Controlling biofilm formation, prophage excision and cell death by rewiring global regulator H-NS of *Escherichia coli*. *Microb Biotechnol* **3**: 344-356.

Hong, S.H., Lee, J., and Wood, T.K. (2010b) Engineering global regulator Hha of *Escherichia coli* to control biofilm dispersal. *Microb Biotechnol* **3**: 717-728.

Hu, L.I., Lima, B.P., and Wolfe, A.J. (2010) Bacterial protein acetylation: the dawning of a new age. *Mol Microbiol* **77**: 15-21.

Hughes, D.T., and Sperandio, V. (2008) Inter-kingdom signalling: communication between bacteria and their hosts. *Nat Rev Microbiol* **6**: 111-120.

Hunt, S.M., Werner, E.M., Huang, B., Hamilton, M.A., and Stewart, P.S. (2004) Hypothesis for the role of nutrient starvation in biofilm detachment. *Appl Environ Microbiol* **70**: 7418-7425.

Inoue, T., Shingaki, R., Hirose, S., Waki, K., Mori, H., and Fukui, K. (2007) Genome-wide screening of genes required for swarming motility in *Escherichia coli* K-12. *J Bacteriol* **189**: 950-957.

Ivanova, A., Miller, C., Glinsky, G., and Eisenstark, A. (1994) Role of *rpoS* (*katF*) in *oxyR*-independent regulation of hydroperoxidase I in *Escherichia coli*. *Mol Microbiol* **12**: 571-578.

Izard, D., Husson, M.O., Vincent, P., Leclerc, H., Monget, D., and Boeufgras, J.M. (1984) Evaluation of the four-hour rapid 20E system for identification of members of the family *Enterobacteriaceae*. *J Clin Microbiol* **20**: 51-54.

Jackson, D.W., Suzuki, K., Oakford, L., Simecka, J.W., Hart, M.E., and Romeo, T. (2002) Biofilm formation and dispersal under the influence of the global regulator CsrA of *Escherichia coli*. *J Bacteriol* **184**: 290-301.

Jaenike, J., Unckless, R., Cockburn, S.N., Boelio, L.M., and Perlman, S.J. (2010) Adaptation via symbiosis: recent spread of a *Drosophila* defensive symbiont. *Science* **329**: 212-215.

Jaklič, D., Lapanje, A., Zupančič, K., Smrke, D., and Gunde-Cimerman, N. (2008) Selective antimicrobial activity of maggots against pathogenic bacteria. *J Med Microbiol* **57**: 617-625.

Janda, J.M., and Abbott, S.L. (2005) *The enterobacteria*. Washington, DC: ASM press.

Jayaraman, A., and Wood, T.K. (2008) Bacterial quorum sensing: signals, circuits, and implications for biofilms and disease. *Annu Rev Biomed Eng* **10**: 145-167.

Jayaraman, A., Mansfeld, F.B., and Wood, T.K. (1999a) Inhibiting sulfate-reducing bacteria in biofilms by expressing the antimicrobial peptides indolicidin and bactenecin. *J Ind Microbiol Biotechnol* **22**: 167-175.

Jayaraman, A., Ornek, D., Duarte, D.A., Lee, C.-C., Mansfeld, F.B., and Wood, T.K. (1999b) Axenic aerobic biofilms inhibit corrosion of copper and aluminum. *Appl Microbiol Biotechnol* **52**: 787-790.

Jayaraman, A., Hallock, P.J., Carson, R.M., Lee, C.-C., Mansfeld, F.B., and Wood, T.K. (1999c) Inhibiting sulfate-reducing bacteria in biofilms on steel with antimicrobial peptides generated in situ. *Appl Microbiol Biotechnol* **52**: 267-275.

Johansen, J., Eriksen, M., Kallipolitis, B., and Valentin-Hansen, P. (2008) Down-regulation of outer membrane proteins by noncoding RNAs: unraveling the cAMP-CRP- and σ^E-dependent CyaR-*ompX* regulatory case. *J Mol Biol* **383**: 1-9.

Johnsen, G., Wasteson, Y., Heir, E., Berget, O.I., and Herikstad, H. (2001) *Escherichia coli* O157:H7 in faeces from cattle, sheep and pigs in the southwest part of Norway during 1998 and 1999. *Int J Food Microbiol* **65**: 193-200.

Jubelin, G., Vianney, A., Beloin, C., Ghigo, J.M., Lazzaroni, J.C., Lejeune, P., and Dorel, C. (2005) CpxR/OmpR interplay regulates curli gene expression in response to osmolarity in *Escherichia coli*. *J Bacteriol* **187**: 2038-2049.

Jung, J.U., Gutierrez, C., Martin, F., Ardourel, M., and Villarejo, M. (1990) Transcription of *osmB*, a gene encoding an *Escherichia coli* lipoprotein, is regulated by dual signals. Osmotic stress and stationary phase. *J Biol Chem* **265**: 10574-10581.

Kamal, A.S. (1958) Comparative study of thirteen species of sarcosaprophagous calliphoridae and sarcophagidae (diptera) I. Bionomics. *Ann Entomol Soc Am* **51**: 261-271.

Kaplan, J.B. (2010) Biofilm dispersal: mechanisms, clinical implications, and potential therapeutic uses. *J Dent Res* **89**: 205-218.

Kaplan, J.B., Ragunath, C., Ramasubbu, N., and Fine, D.H. (2003) Detachment of *Actinobacillus actinomycetemcomitans* biofilm cells by an endogenous β-hexosaminidase activity. *J Bacteriol* **185**: 4693-4698.

Karatan, E., and Watnick, P. (2009) Signals, regulatory networks, and materials that build and break bacterial biofilms. *Microbiol Mol Biol Rev* **73**: 310-347.

Kelly, S.M., Pitcher, M.C.L., Farmery, S.M., and Gibson, G.R. (1994) Isolation of *Helicobacter pylori* from feces of patients with dyspepsia in the United Kingdom. *Gastroenterology* **107**: 1671-1674.

Kiefer, F., Arnold, K., Künzli, M., Bordoli, L., and Schwede, T. (2009) The SWISS-MODEL Repository and associated resources. *Nucleic Acids Res* **37**: D387-392.

Kim, Y., and Wood, T.K. (2010) Toxins Hha and CspD and small RNA regulator Hfq are involved in persister cell formation through MqsR in *Escherichia coli*. *Biochemical and Biophysical Research Communications* **391**: 209-213.

Kim, Y., Wang, X., Ma, Q., Zhang, X.S., and Wood, T.K. (2009) Toxin-antitoxin systems in *Escherichia coli* influence biofilm formation through YjgK (TabA) and fimbriae. *J Bacteriol* **191**: 1258-1267.

Kim, Y., Wang, X., Zhang, X.S., Grigoriu, S., Page, R., Peti, W., and Wood, T.K. (2010) *Escherichia coli* toxin/antitoxin pair MqsR/MqsA regulate toxin CspD. *Environ Microbiol* **12**: 1105-1121.

Kitagawa, M., Ara, T., Arifuzzaman, M., Ioka-Nakamichi, T., Inamoto, E., Toyonaga, H., and Mori, H. (2005) Complete set of ORF clones of *Escherichia coli* ASKA library (a complete set of *E. coli* K-12 ORF archive): unique resources for biological research. *DNA Res* **12**: 291-299.

Kjelleberg, S., and Givskov, M. (2007) *The biofilm mode of life: mechanisms and adaptations*. Norfolk, VA: Horizon Bioscience.

Kleinschmidt, J.H. (2003) Membrane protein folding on the example of outer membrane protein A of *Escherichia coli*. *Cell Mol Life Sci* **60**: 1547-1558.

Kobayashi, H., Kærn, M., Araki, M., Chung, K., Gardner, T.S., Cantor, C.R., and Collins, J.J. (2004) Programmable cells: interfacing natural and engineered gene networks. *Proc Natl Acad Sci U S A* **101**: 8414-8419.

Korea, C.G., Badouraly, R., Prevost, M.C., Ghigo, J.M., and Beloin, C. (2010) *Escherichia coli* K-12 possesses multiple cryptic but functional chaperone-usher fimbriae with distinct surface specificities. *Environ Microbiol* **12**: 1957-1977.

Krasteva, P.V., Fong, J.C., Shikuma, N.J., Beyhan, S., Navarro, M.V.A.S., Yildiz, F.H., and Sondermann, H. (2010) *Vibrio cholerae* VpsT regulates matrix production and motility by directly sensing cyclic di-GMP. *Science* **327**: 866-868.

Krishna, R.G., and Wold, F. (1993) Post-translational modification of proteins. *Adv Enzymol Relat Areas Mol Biol* **67**: 265-298.

Kubota, H., Senda, S., Nomura, N., Tokuda, H., and Uchiyama, H. (2008) Biofilm formation by lactic acid bacteria and resistance to environmental stress. *J Biosci Bioeng* **106**: 381-386.

Kulshina, N., Baird, N.J., and Ferré-D'Amaré, A.R. (2009) Recognition of the bacterial second messenger cyclic diguanylate by its cognate riboswitch. *Nat Struct Mol Biol* **16**: 1212-1217.

Lacour, S., and Landini, P. (2004) SigmaS-dependent gene expression at the onset of stationary phase in *Escherichia coli*: function of SigmaS-dependent genes and identification of their promoter sequences. *J Bacteriol* **186**: 7186-7195.

Landini, P., and Zehnder, A.J.B. (2002) The global regulatory *hns* gene negatively affects adhesion to solid surfaces by anaerobically grown *Escherichia coli* by modulating expression of flagellar genes and lipopolysaccharide production. *J Bacteriol* **184**: 1522-1529.

Lee, J., Jayaraman, A., and Wood, T.K. (2007a) Indole is an inter-species biofilm signal mediated by SdiA. *BMC Microbiol* **7**: 42.

Lee, J., Maeda, T., Hong, S.H., and Wood, T.K. (2009a) Reconfiguring the quorum-sensing regulator SdiA of *Escherichia coli* to control biofilm formation via indole and N-acylhomoserine lactones. *Appl Environ Microbiol* **75**: 1703-1716.

Lee, J., Bansal, T., Jayaraman, A., Bentley, W.E., and Wood, T.K. (2007b) Enterohemorrhagic *Escherichia coli* biofilms are inhibited by 7-hydroxyindole and stimulated by isatin. *Appl Environ Microbiol* **73**: 4100-4109.

Lee, J., Attila, C., Cirillo, S.L., Cirillo, J.D., and Wood, T.K. (2009b) Indole and 7-hydroxyindole diminish *Pseudomonas aeruginosa* virulence. *Microb Biotechnol* **2**: 75-90.

Lee, J., Zhang, X.S., Hegde, M., Bentley, W.E., Jayaraman, A., and Wood, T.K. (2008) Indole cell signaling occurs primarily at low temperatures in *Escherichia coli*. *ISME J* **2**: 1007-1023.

Lee, J., Page, R., Garcia-Contreras, R., Palermino, J.M., Zhang, X.S., Doshi, O. et al. (2007c) Structure and function of the *Escherichia coli* protein YmgB: a protein critical for biofilm formation and acid-resistance. *J Mol Biol* **373**: 11-26.

Lee, V.T., Matewish, J.M., Kessler, J.L., Hyodo, M., Hayakawa, Y., and Lory, S. (2007d) A cyclic-di-GMP receptor required for bacterial exopolysaccharide production. *Mol Microbiol* **65**: 1474-1484.

Li, R., Gu, J., Chen, Y.Y., Xiao, C.L., Wang, L.W., Zhang, Z.P. et al. (2010) CobB regulates *Escherichia coli* chemotaxis by deacetylating the response regulator CheY. *Mol Microbiol* **76**: 1162-1174.

Liaw, S.J., Lai, H.C., Ho, S.W., Luh, K.T., and Wang, W.B. (2001) Characterisation of *p*-nitrophenylglycerol-resistant *Proteus mirabilis* super-swarming mutants. *J Med Microbiol* **50**: 1039-1048.

Linda I, H., Bruno P, L., and Alan J, W. (2010) Bacterial protein acetylation: the dawning of a new age. *Molecular Microbiology* **77**: 15-21.

Liu, D. (2010) *Molecular detection of foodborne pathogens*. Boca Raton, FL: CRC Press.

Lower, B.H., Yongsunthon, R., F. P. Vellano III, and Lower, S.K. (2005) Simultaneous force and fluorescence measurements of a protein that forms a bond between a living bacterium and a solid surface. *J Bacteriol* **187**: 2127-2137.

Lu, T.K., and Collins, J.J. (2007) Dispersing biofilms with engineered enzymatic bacteriophage. *Proc Natl Acad Sci U S A* **104**: 11197-11202.

Ma, Q., and Wood, T.K. (2009) OmpA influences *Escherichia coli* biofilm formation by repressing cellulose production through the CpxRA two-component system. *Environ Microbiol* **11**: 2735-2746.

Macvanin, M., and Hughes, D. (2010) Assays of sensitivity of antibiotic-resistant bacteria to hydrogen peroxide and measurement of catalase activity. *Methods Mol Biol* **642**: 95-103.

Maeda, T., V. Sanchez-Torres, and T. K. Wood (2008) Metabolic engineering to enhance bacterial hydrogen production. *Microb Biotechnol* **1**: 30-39.

Mah, T.F., Pitts, B., Pellock, B., Walker, G.C., Stewart, P.S., and O'Toole, G.A. (2003) A genetic basis for *Pseudomonas aeruginosa* biofilm antibiotic resistance. *Nature* **426**: 306-310.

Mai-Prochnow, A., Lucas-Elio, P., Egan, S., Thomas, T., Webb, J.S., Sanchez-Amat, A., and Kjelleberg, S. (2008) Hydrogen peroxide linked to lysine oxidase activity facilitates biofilm differentiation and dispersal in several gram-negative bacteria. *J Bacteriol* **190**: 5493-5501.

Méndez-Ortiz, M.M., Hyodo, M., Hayakawa, Y., and Membrillo-Hernández, J. (2006) Genome-wide transcriptional profile of *Escherichia coli* in response to high levels of the second messenger 3',5'-cyclic diguanylic acid. *J Biol Chem* **281**: 8090-8099.

Miller, M.B., and Bassler, B.L. (2001) Quorum sensing in bacteria. *Annu Rev Microbiol* **55**: 165-199.

Mobley, H.L., and Belas, R. (1995) Swarming and pathogenicity of *Proteus mirabilis* in the urinary tract. *Trends Microbiol* **3**: 280-284.

Monika Hilker, T.M. (2002) *Chemoecology of insect eggs and egg decomposition*. Hoboken, NJ: Blackwell Publishing.

Monteiro, C., Saxena, I., Wang, X., Kader, A., Bokranz, W., Simm, R. et al. (2009) Characterization of cellulose production in *Escherichia coli* Nissle 1917 and its biological consequences. *Environ Microbiol* **11**: 1105-1116.

Morgan, R., Kohn, S., Hwang, S.H., Hassett, D.J., and Sauer, K. (2006) BdlA, a chemotaxis regulator essential for biofilm dispersion in *Pseudomonas aeruginosa*. *J Bacteriol* **188**: 7335-7343.

Morgenstein, R.M., Clemmer, K.M., and Rather, P.N. (2010) Loss of the waaL O-antigen ligase prevents surface activation of the flagellar gene cascade in *Proteus mirabilis*. *J Bacteriol* **192**: 3213-3221.

Mori, H., Isono, K., Horiuchi, T., and Miki, T. (2000) Functional genomics of *Escherichia coli* in Japan. *Res Microbiol* **151**: 121-128.

Morikawa, M. (2006) Beneficial biofilm formation by industrial bacteria *Bacillus subtilis* and related species. *J Biosci Bioeng* **101**: 1-8.

Nachin, L., Nannmark, U., and NystrÖm, T. (2005) Differential roles of the universal stress proteins of *Escherichia coli* in oxidative stress resistance, adhesion, and motility. *J Bacteriol* **187**: 6265-6272.

Nakao, R., Tashiro, Y., Nomura, N., Kosono, S., Ochiai, K., Yonezawa, H. et al. (2008) Glycosylation of the OMP85 homolog of *Porphyromonas gingivalis* and its involvement in biofilm formation. *Biochem Biophys Res Commun* **365**: 784-789.

Nakhamchik, A., Wilde, C., and Rowe-Magnus, D.A. (2008) Cyclic-di-GMP regulates extracellular polysaccharide production, biofilm formation, and rugose colony development by *Vibrio vulnificus*. *Appl Environ Microbiol* **74**: 4199-4209.

Nazni, W.A., Seleena, B., Lee, H.L., Jeffery, J., T.A.R., T.R., and Sofian, M.A. (2005) Bacteria fauna from the house fly, Musca domestica (L.). *Trop Biomed* **22**: 225-231.

Newell, P.D., Monds, R.D., and O'Toole, G.A. (2009) LapD is a bis-(3',5')-cyclic dimeric GMP-binding protein that regulates surface attachment by *Pseudomonas fluorescens* Pf0-1. *Proc Natl Acad Sci U S A* **106**: 3461-3466.

Nicholson, E.B., Concaugh, E.A., Foxall, P.A., Island, M.D., and Mobley, H.L. (1993) *Proteus mirabilis* urease: transcriptional regulation by UreR. *J Bacteriol* **175**: 465-473.

Orme, R., lan Douglas, C.W., Rimmer, S., and Webb, M. (2006) Proteomic analysis of *Escherichia coli* biofilms reveals the overexpression of the outer membrane protein OmpA. *Proteomics* **6**: 4269-4277.

Örnek, D., Jayaraman, A., Syrett, B.C., Hsu, C.-H., Mansfeld, F.B., and Wood, T.K. (2002) Pitting corrosion inhibition of aluminum 2024 by *Bacillus* biofilms secreting polyaspartate or γ-polyglutamate. *Appl Microbiol Biotechnol* **58**: 651-657.

Otto, K., and Silhavy, T.J. (2002) Surface sensing and adhesion of *Escherichia coli* controlled by the Cpx-signaling pathway. *Proc Natl Acad Sci U S A* **99**: 2287-2292.

Patel, N.J., Zaborina, O., Wu, L., Wang, Y., Wolfgeher, D.J., Valuckaite, V. et al. (2007) Recognition of intestinal epithelial HIF-1α activation by *Pseudomonas aeruginosa*. *Am J Physiol Gastrointest Liver Physiol* **292**: G134-142.

Paul, K., Nieto, V., Carlquist, W.C., Blair, D.F., and Harshey, R.M. (2010) The c-di-GMP binding protein YcgR controls flagellar motor direction and speed to affect chemotaxis by a "backstop brake" mechanism. *Mol Cell* **38**: 128-139.

Peitsch, M.C. (1995) Protein Modeling by E-mail. *Nature Biotechnol* **13**: 658-660.

Pratt, L.A., and Kolter, R. (1998) Genetic analysis of *Escherichia coli* biofilm formation: roles of flagella, motility, chemotaxis and type I pili. *Mol Microbiol* **30**: 285-293.

Prigent-Combaret, C., Prensier, G., Le Thi, T.T., Vidal, O., Lejeune, P., and Dorel, C. (2000) Developmental pathway for biofilm formation in curli-producing *Escherichia coli* strains: role of flagella, curli and colanic acid. *Environ Microbiol* **2**: 450-464.

Prigent-Combaret, C., Brombacher, E., Vidal, O., Ambert, A., Lejeune, P., Landini, P., and Dorel, C. (2001) Complex regulatory network controls initial adhesion and biofilm formation in *Escherichia coli* via regulation of the *csgD* gene. *J Bacteriol* **183**: 7213-7223.

Raivio, T.L., and Silhavy, T.J. (1999) The σ^E and Cpx regulatory pathways: overlapping but distinct envelope stress responses. *Curr Opin Microbiol* **2**: 159-165.

Ramos, J.L., Martínez-Bueno, M., Molina-Henares, A.J., Terán, W., Watanabe, K., Zhang, X. et al. (2005) The TetR family of transcriptional repressors. *Microbiol Mol Biol Rev* **69**: 326-356.

Rao, F., See, R.Y., Zhang, D., Toh, D.C., Ji, Q., and Liang, Z.X. (2010) YybT is a signaling protein that contains a cyclic dinucleotide phosphodiesterase domain and a GGDEF domain with ATPase activity. *J Biol Chem* **285**: 473-482.

Reisner, A., Haagensen, J.A.J., Schembri, M.A., Zechner, E.L., and Molin, S. (2003) Development and maturation of *Escherichia coli* K-12 biofilms. *Mol Microbiol* **48**: 933-946.

Ren, D., Sims, J.J., and Wood, T.K. (2001) Inhibition of biofilm formation and swarming of *Escherichia coli* by (*5Z*)-4-bromo-5-(bromomethylene)-3-butyl-2(*5H*)-furanone. *Environ Microbiol* **3**: 731-736.

Ren, D., Bedzyk, L.A., Thomas, S.M., Ye, R.W., and Wood, T.K. (2004a) Gene expression in *Escherichia coli* biofilms. *Appl Microbiol Biotechnol* **64**: 515-524.

Ren, D., Bedzyk, L.A., Ye, R.W., Thomas, S.M., and Wood, T.K. (2004b) Differential gene expression shows natural brominated furanones interfere with the autoinducer-2 bacterial signaling system of *Escherichia coli*. *Biotechnol Bioeng* **88**: 630-642.

Rice, K.C., Mann, E.E., Endres, J.L., Weiss, E.C., Cassat, J.E., Smeltzer, M.S., and Bayles, K.W. (2007) The *cidA* murein hydrolase regulator contributes to DNA release and biofilm development in *Staphylococcus aureus*. *Proc Natl Acad Sci U S A* **104**: 8113-8118.

Rice, S.A., Koh, K.S., Queck, S.Y., Labbate, M., Lam, K.W., and Kjelleberg, S. (2005) Biofilm formation and sloughing in *Serratia marcescens* are controlled by quorum sensing and nutrient cues. *J Bacteriol* **187**: 3477-3485.

Richardson, O.H. (1916) A chemotropic response of the house fly (Musca Domestica L.). *Science* **43**: 613-616.

Robacker, D.C. (2001) Roles of putrescine and 1-pyrroline in attractiveness of technical-grade putrescine to the mexican fruit fly (Diptera: Tephritidae). *The Florida entomologist* **84**: 679-685.

Robbe-Saule, V., Coynault, C., Ibanez-Ruiz, M., Hermant, D., and Norel, F. (2001) Identification of a non-haem catalase in *Salmonella* and its regulation by RpoS (σ^S). *Mol Microbiol* **39**: 1533-1545.

Romero, R., Schaudinn, C., Kusanovic, J.P., Gorur, A., Gotsch, F., Webster, P. et al. (2008) Detection of a microbial biofilm in intraamniotic infection. *Am J Obstet Gynecol* **198**: 135.e131-135.e135.

Römling, U., Rohde, M., Olsén, A., Normark, S., and Reinköster, J. (2000) *AgfD*, the checkpoint of multicellular and aggregative behaviour in *Salmonella typhimurium* regulates at least two independent pathways. *Mol Microbiol* **36**: 10-23.

Rosche, B., Li, X.Z., Hauer, B., Schmid, A., and Buehler, K. (2009) Microbial biofilms: a concept for industrial catalysis? *Trends Biotechnol* **27**: 636-643.

Roux, A., Beloin, C., and Ghigo, J.M. (2005) Combined inactivation and expression strategy to study gene function under physiological conditions: application to identification of new *Escherichia coli* adhesins. *J Bacteriol* **187**: 1001-1013.

Rui, L., Kwon, Y.M., Fishman, A., Reardon, K.F., and Wood, T.K. (2004) Saturation mutagenesis of toluene *ortho*-monooxygenase of *Burkholderia cepacia* G4 for Enhanced 1-naphthol synthesis and chloroform degradation. *Appl Environ Microbiol* **70**: 3246-3252.

Sambrook, J., Fritsch, E.F., and Maniatis, T. (1989) *Molecular Cloning, A Laboratory Manual*. Cold Spring Harbor, NY: Cold Spring Harbor Laboratory Press.

Sanderson, M.W., Sargeant, J.M., Shi, X., Nagaraja, T.G., Zurek, L., and Alam, M.J. (2006) Longitudinal emergence and distribution of *Escherichia coli* O157 genotypes in a beef feedlot. *Appl Environ Microbiol* **72**: 7614-7619.

Sauer, K., Cullen, M.C., Rickard, A.H., Zeef, L.A., Davies, D.G., and Gilbert, P. (2004) Characterization of nutrient-induced dispersion in *Pseudomonas aeruginosa* PAO1 biofilm. *J Bacteriol* **186**: 7312-7326.

Savageau, M.A. (1983) *Escherichia coli* habitats, cell types, and molecular mechanisms of gene control. *Am Nat* **122**: 732-744.

Schembri, M.A., Kjaergaard, K., and Klemm, P. (2003) Global gene expression in *Escherichia coli* biofilms. *Mol Microbiol* **48**: 253-267.

Schmidt, A.J., Ryjenkov, D.A., and Gomelsky, M. (2005) The ubiquitous protein domain EAL is a cyclic diguanylate-specific phosphodiesterase: enzymatically active and inactive EAL domains. *J Bacteriol* **187**: 4774-4781.

Schmidtchen, A., Wolff, H., Rydengard, V., and Hansson, C. (2003) Detection of serine proteases secreted by *Lucilia sericata* in vitro and during treatment of a chronic leg ulcer. *Acta Derm Venereol* **83**: 310-311.

Seyer, K., Lessard, M., Piette, G., Lacroix, M., and Saucier, L. (2003) *Escherichia coli* heat shock protein DnaK: production and consequences in terms of monitoring cooking. *Appl Environ Microbiol* **69**: 3231-3237.

Sherlock, O., Dobrindt, U., Jensen, J.B., Munk Vejborg, R., and Klemm, P. (2006) Glycosylation of the self-recognizing *Escherichia coli* Ag43 autotransporter protein. *J Bacteriol* **188**: 1798-1807.

Sherrod, S.D., Diaz, A.J., Russell, W.K., Cremer, P.S., and Russell, D.H. (2008) Silver nanoparticles as selective ionization probes for analysis of olefins by mass spectrometry. *Anal Chem* **80**: 6796-6799.

Smith, S.G.J., Mahon, V., Lambert, M.A., and Fagan, R.P. (2007) A molecular Swiss army knife: OmpA structure, function and expression. *FEMS Microbiol Lett* **273**: 1-11.

Solano, C., García, B., Valle, J., Berasain, C., Ghigo, J.M., Gamazo, C., and Lasa, I. (2002) Genetic analysis of *Salmonella enteritidis* biofilm formation: critical role of cellulose. *Mol Microbiol* **43**: 793-808.

Sommerfeldt, N., Possling, A., Becker, G., Pesavento, C., Tschowri, N., and Hengge, R. (2009) Gene expression patterns and differential input into curli fimbriae regulation of all GGDEF/EAL domain proteins in *Escherichia coli*. *Microbiology* **155**: 1318-1331.

Sperandio, V., Torres, A.G., and Kaper, J.B. (2002) Quorum sensing *Escherichia coli* regulators B and C (QseBC): a novel two-component regulatory system involved in the regulation of flagella and motility by quorum sensing in *E. coli*. *Mol Microbiol* **43**: 809-821.

Steinberger, R.E., Allen, A.R., Hansma, H.G., and Holden, P.A. (2002) Elongation correlates with nutrient deprivation in *Pseudomonas aeruginosa*-unsaturates biofilms. *Microb Ecol* **43**: 416-423.

Stevenson, L.G., and Rather, P.N. (2006) A novel gene involved in regulating the flagellar gene cascade in *Proteus mirabilis*. *J Bacteriol* **188**: 7830-7839.

Sturgill, G., and Rather, P.N. (2004) Evidence that putrescine acts as an extracellular signal required for swarming in *Proteus mirabilis*. *Mol Microbiol* **51**: 437-446.

Sutherland, I. (2001) Biofilm exopolysaccharides: a strong and sticky framework. *Microbiology* **147**: 3-9.

Tan, S.W., Yap, K.L., and Lee, H.L. (1997) Mechanical transport of rotavirus by the legs and wings of *Musca domestica* (Diptera: Muscidae). *J Med Entomol* **34**: 527-531.

Thomas, J.E., Gibson, G.R., Darboe, M.K., Dale, A., and Weaver, L.T. (1992) Isolation of *Helicobacter pylori* from human faeces. *Lancet* **340**: 1194-1195.

Typas, A., Nichols, R.J., Siegele, D.A., Shales, M., Collins, S.R., Lim, B. et al. (2008) High-throughput, quantitative analyses of genetic interactions in *E. coli*. *Nat Meth* **5**: 781-787.

Ueda, A., and Wood, T.K. (2009) Connecting quorum sensing, c-di-GMP, pel polysaccharide, and biofilm formation in *Pseudomonas aeruginosa* through tyrosine phosphatase TpbA (PA3885). *PLoS Pathog* **5**: e1000483.

Ueda, A., and Wood, T.K. (2010) Tyrosine phosphatase TpbA of *Pseudomonas aeruginosa* controls extracellular DNA via cyclic diguanylic acid concentrations. *Environ Microbiol Reports* **2**: 449-455.

Ulusu, N.N., and Tezcan, E.F. (2001) Cold shock proteins. *Turk J Med Sci* **31**: 283-290.

Van Houdt, R., and Michiels, C.W. (2005) Role of bacterial cell surface structures in *Escherichia coli* biofilm formation. *Res Microbiol* **156**: 626-633.

Van Houdt, R., Aertsen, A., Moons, P., Vanoirbeek, K., and Michiels, C.W. (2006) *N*-acyl-L-homoserine lactone signal interception by *Escherichia coli*. *FEMS Microbiol Lett* **256**: 83-89.

Vidal, O., Longin, R., Prigent-Combaret, C., Dorel, C., Hooreman, M., and Lejeune, P. (1998) Isolation of an *Escherichia coli* K-12 mutant strain able to form biofilms on inert surfaces: involvement of a new *ompR* allele that increases curli expression. *J Bacteriol* **180**: 2442-2449.

Walker, K.E., Moghaddame-Jafari, S., Lockatell, C.V., Johnson, D., and Belas, R. (1999) ZapA, the IgA-degrading metalloprotease of *Proteus mirabilis*, is a virulence factor expressed specifically in swarmer cells. *Mol Microbiol* **32**: 825-836.

Wang, Q., Zhang, Y., Yang, C., Xiong, H., Lin, Y., Yao, J. et al. (2010) Acetylation of metabolic enzymes coordinates carbon source utilization and metabolic flux. *Science* **327**: 1004-1007.

Wang, X., Dubey, A.K., Suzukl, K., Baker, C.S., Babltzke, P., and Romeo, T. (2005) CsrA post-transcriptionally represses *pgaABCD*, responsible for synthesis of a biofilm polysaccharide adhesin of *Escherichia coli*. *Mol Microbiol* **56**: 1648-1663.

Wang, X., Rochon, M., Lamprokostopoulou, A., Lünsdorf, H., Nimtz, M., and Römling, U. (2006) Impact of biofilm matrix components on interaction of commensal *Escherichia coli* with the gastrointestinal cell line HT-29. *Cell Mol Life Sci* **63**: 2352-2363.

Wang, X., Kim, Y., S. H. Hong, Ma, Q., B. L. Brown, M. Pu et al. (2011) Antitoxin MqsA helps mediate the bacterial general stress response. *Nat Chem Biol* **In press**.

Waters, C.M., and Bassler, B.L. (2005) Quorum sensing: cell-to-cell communication in bacteria. *Annu Rev Cell Dev Biol* **21**: 319-346.

Whitaker, I.S., Twine, C., Whitaker, M.J., Welck, M., Brown, C.S., and Shandall, A. (2007) Larval therapy from antiquity to the present day: mechanisms of action, clinical applications and future potential. *Postgrad Med J* **83**: 409-413.

Wold, F. (1981) In vivo chemical modification of proteins (post-translational modification). *Annu Rev Biochem* **50**: 783-814.

Wolfe, A.J., Parikh, N., Lima, B.P., and Zemaitaitis, B. (2008) Signal integration by the two-component signal transduction response regulator CpxR. *J Bacteriol* **190**: 2314-2322.

Wood, T.K. (2009) Insights on *Escherichia coli* biofilm formation and inhibition from whole-transcriptome profiling. *Environ Microbiol* **11**: 1-15.

Wood, T.K., and Peretti, S.W. (1991) Effect of chemically-induced, cloned-gene expression on protein synthesis in *E. coli*. *Biotechnol Bioeng* **38**: 397-412.

Wood, T.K., Hong, S.H., and Ma, Q. (2011) Engineering biofilm formation and dispersal. *Trends Biotechnol* **29**: 87-94.

Wood, T.K., González Barrios, A.F., Herzberg, M., and Lee, J. (2006) Motility influences biofilm architecture in *Escherichia coli*. *Appl Microbiol Biotechnol* **72**: 361-367.

Wu, L., Estrada, O., Zaborina, O., Bains, M., Shen, L., Kohler, J.E. et al. (2005) Recognition of host immune activation by *Pseudomonas aeruginosa*. *Science* **309**: 774-777.

Yang, X., Ma, Q., and Wood, T.K. (2008) The R1 conjugative plasmid increases *Escherichia coli* biofilm formation through an envelope stress response. *Appl Environ Microbiol* **74**: 2690-2699.

Yu, B.J., Kim, J.A., Moon, J.H., Ryu, S.E., and Pan, J.G. (2008) The diversity of lysine-acetylated proteins in *Escherichia coli*. *J Microbiol Biotechnol* **18**: 1529-1536.

Zhang, J., Sprung, R., Pei, J., Tan, X., Kim, S., Zhu, H. et al. (2009) Lysine acetylation is a highly abundant and evolutionarily conserved modification in *Escherichia coli*. *Mol Cell Proteomics* **8**: 215-225.

Zhang, X.S., García-Contreras, R., and Wood, T.K. (2007) YcfR (BhsA) influences *Escherichia coli* biofilm formation through stress response and surface hydrophobicity. *J Bacteriol* **189**: 3051-3062.

Zhang, X.S., García-Contreras, R., and Wood, T.K. (2008) *Escherichia coli* transcription factor YncC (McbR) regulates colanic acid and biofilm formation by repressing expression of periplasmic protein YbiM (McbA). *ISME J* **2**: 615-631.

Zogaj, X., Nimtz, M., Rohde, M., Bokranz, W., and Römling, U. (2001) The multicellular morphotypes of *Salmonella typhimurium* and *Escherichia coli* produce cellulose as the second component of the extracellular matrix. *Mol Microbiol* **39**: 1452-1463.

APPENDIX

THE R1 CONJUGATIVE PLASMID INCREASES *ESCHERICHIA COLI* BIOFILM

FORMATION THROUGH ENVELOPE STRESS RESPONSE

Abstract

Differential gene expression in biofilm cells suggests that adding the derepressed conjugation plasmid R1*drd*19 increases biofilm formation by affecting envelope stress (*rseA, cpxAR*), biofilm-related genes (*bssR*, *cstA*), energy production (*glpDFK*), acid resistance (*gadABCEX, hdeABD*), cell motility (*csgBEFG, yehCD, yadC, yfcV*), outer membrane proteins (*ompACF*), phage shock proteins (*pspABCDE*), cold shock proteins (*cspACDEG*), and phage-related genes. To investigate the link between the identified genes and biofilm formation upon adding R1*drd*19, 40 isogenic mutants were classified according to their different biofilm formation phenotypes. Cells with Class I mutations (*rseA, bssR, cpxA,* and *ompA*) exhibited no difference in biofilm formation compared to the wild-type strain and no increase upon adding R1*drd*19. Class II mutations (*gatC, yagI, ompC, cspA, pspD, pspB, ymgB, gadC, pspC, ymgA, slp, cpxP, cpxR, cstA, rseC, ompF,* and *yqjD*) increased biofilm formation compared to the wild-type strain but decreased biofilm formation upon adding R1*drd*19. Class III mutations increased biofilm formation compared to the wild-type strain and increased biofilm upon adding R1*drd*19. Class IV mutations increased biofilm formation compared to the wild-type strain but had little difference upon adding R1*drd*19, and Class V mutations had no difference compared to the wild-type strain but increased upon adding R1*drd*19. Therefore, proteins encoded by the

_____

genes of Class I are involved in R1*drd*19-promoted biofilm formation, primarily through their impact on cell motility. We hypothesize that the pili formed upon adding the conjugation plasmid disrupt the membrane (induce *ompA*) and activate the two-component system CpxAR as well as the other envelope stress response system, RseA-σ^E, both of which, along with BssR, play a key role in bacterial biofilm formation.

Introduction

Conjugation transfers genetic material between bacteria through cell-to-cell contact (59); hence, it spreads virulence factors (20) and influences bacterial resistance to antibiotics (38). Conjugation is affected by growth conditions and biofilm structure (26), and biofilms promote conjugation (41). The reverse is also true as conjugative plasmids promote biofilm formation (20, 47), and Ghigo has proposed that conjugative pili act as adhesion factors. In addition, thicker biofilms were observed in mature biofilms harboring conjugation plasmids (46).

Plasmid R1, originally from the host *Salmonella enterica* ser. *paratyphi* (20), is a F-like conjugative plasmid of the IncFII incompatibility group (13). The transfer region of R1 consists of four DNA transfer genes (*traYALE*), a large *tra* operon constituting at least 34 genes that have high homology with the F plasmid (35), *finP* and *finO* which encode the fertility inhibition complex FinPO (66), *traM* and *traJ* which lie outside of the *tra* operon (4), as well as the conjugative transfer origin locus *oriT* (4). TraM is a positive regulator of the *tra* genes (43), and TraJ disrupts the host nucleoid-associated protein, a repressor of the *tra* operon (62). The *tra* promoter is repressed by FinO and FinP (36); therefore, disruption of *finO* in R1*drd*19 promotes conjugation constitutively (46). Plasmid RI represses conjugal pili synthesis, but R1*drd*19 synthesizes these pili constitutively (20). Since, the genetic mechanism by which conjugation plasmids control biofilm formation has not been elucidated (we found previously addition of R1*drd*19 increases biofilm formation by increasing aggregation and decreasing cell motility

(21)), our goal here was to use DNA microarrays and isogenic mutants to investigate this mechanism.

Single time point DNA microarrays have been used to explore the genetic basis of *E. coli* K-12 biofilm formation (5, 24, 32, 49, 54) and one temporal study has been completed (14); one common trend is that stress genes are induced. With DNA microarrays, we identified five induced stress response genes (*hslST, hha, soxS,* and *ycfR*) in 7 h *E. coli* biofilm cells harboring a conjugative plasmid compared to suspension cells with a conjugative plasmid (49), and recently we showed how YcfR mediates this stress response in *E. coli* and how stress increases *E. coli* biofilm formation (67). In addition, the envelope stress response genes, such as *pspABCDE*, *cpxAR*, *rpoE*, and *rseA*, were induced in *E. coli* 8-day-old biofilms cells compared to exponentially-growing planktonic cells regardless of the presence of a conjugation plasmid (5). *rpoS* plays a key role during biofilm formation because it encodes the sigma S factor which regulates a number of stress-related genes (54). *yeaGH* were also identified as putative stress response genes (54) since they are regulated by RpoS in *Salmonella enterica*. In addition, cold-shock protein regulators *cspABFGI* and the heat-shock protein regulator *htgA* were induced in a temporal fashion during biofilm formation (14). In human urine, stress genes were also induced in asymptomatic bacteriuria *E. coli* during biofilm formation (e.g., *cspAGH*, *ibpAB*, *pphA*, *soxS*, *yfiD*) (24).

CpxAR is a two component system for response to cell envelope stress (10). CpxAR also controls the synthesis of adhesive organelles (45) and appears to help cells respond to adverse conditions (16). CpxA is a histidine kinase that functions in the inner membrane (12) as the sensor to envelope stress (e.g., cell invasion, high pH (40), and unassembled P-pilus subunits (11)). CpxR is the response regulator which resides in the cytoplasm (12); it is phosphorylated by CpxA which auto-phosphorylates and then transfers the phosphate to CpxR (CpxR~P).

Accumulation of surface adherence factors such as pili subunits in the cytoplasm or in the outer membrane leads to activation of the Cpx system (16). The outer membrane protein NlpE activates the Cpx system when NlpE is overproduced, but the Cpx pathway is activated in an NlpE-independent manner in the presence of envelope stress (12). CpxR~P positively regulates virulence (39) and the porin OmpC (3), but negatively regulates both genes which encode adherence factors (e.g., *csgBD*) (31) and motility genes (e.g., *motAB, cheAW*) (10). At the post-transcription level, CpxR-P controls pili monomer secretion (16).

Sigma E (σ^E) specifically responds to cell envelope stress (1), and it is required in the expression of periplasmic folding catalysts, proteases, and other outer membrane components of the envelope (19). RseA is a 216 aa, trans-membrane, anti-sigma factor that can form an inhibitory complex that blocks σ^E from binding to RNA polymerase (7); hence, this anti-sigma factor can control envelope stress (9). The stability of RseA (and therefore its effect on σ^E) is based on outer membrane protein OmpC which activates the protease DegS which cleaves RseA (1). In the presence of envelope stress, the two-component system CpxAR is the dominant regulator over RseA-σ^E (16). Another outer membrane protein, OmpA, is linked to σ^E through the small RNA MicA (60); MicA is a negative antisense regulator of OmpA synthesis, and this sRNA is induced by overexpression of σ^E (60).

Recently, we found BssR (YliH) is a biofilm repressor because it repressed motility of *E. coli* in LB, induced indole which is an inhibitor of biofilm formation, and repressed autoinducer-2 (AI-2) induced genes (15). DNA microarray analysis reveals that 13 stress response genes (e.g., *sdiA, ydaD, ydaK*) are induced and that 51 stress response genes (e.g., *yodC, yjbJ, rpoS*) are repressed by deletion of *bssR* in *E. coli* K-12 wild-type (15).

Here, five pairs of DNA microarrays (*E. coli* BW25113 with and without R1*drd*19 at 7 h, 15 h, and 24 h in complex medium, *E. coli* ATCC25404 with and without R1*drd*19 at 24 h in

complex medium, and *E. coli* MG1655 with and without R1*drd*19 at 24 h in minimal medium) were used to identify genes related to enhanced biofilm formation upon adding a conjugative plasmid. Based on the identified genes, forty isogenic knockout mutations were investigated and classified. It was determined that R1*drd*19 mediates an increase in biofilm formation through its interaction with CpxAR, RseA, BssR, and OmpA.

Materials and methods

Bacterial strains, plasmids, and growth conditions.

The *E. coli* strains and plasmids used are listed in Table 1. The three *E. coli* strains were chosen since their biofilm formation has been studied in our lab: BW25113 (14), MG1655 (22), ATCC25404 (63). pCM18 (25) constitutively expresses the green fluorescence protein (GFP), so it was used to visualize the biofilms; this plasmid was maintained by the addition of 300 μg/mL erythromycin. Luria-Bertani (LB) (52) was used for overnight cultures. LB and M9 minimal medium with 0.4% casamino acids and 0.4% glucose (M9C glu) (50) were used to form biofilms. To maintain R1*drd*19 (20), 30 μg/mL chloramphenicol was added to the overnight cultures, and 50 μg/mL of kanamycin was added to the overnight cultures for growing the isogenic knock-out strains (2). After the overnight cultures, antibiotics were omitted in the crystal-violet biofilm assay, the aggregation assay, and the motility assay. *Vibrio harveyi* was cultured in Autoinducer Bioassay (AB) medium for the AI-2 assay (58).

The knockout deletions of all the strains were confirmed by Baba et al. (2) using the polymerase chain reaction (PCR) by amplifying the regions flanking the deleted gene using two specific primers in the kanamycin gene (K1: 5'-CAGTCATAGCCGAATAGCCT and K2: 5'-CGGTGCCCTGAATGAACTGC). For example, to confirm the *cpxA* deletion, forward primer 5'-GCCAATAAAATCCTGTTAGTTGA was used with K1 and reverse primer 5'-GCCCGATATCCGGTTGATGTATA was used with K2. For *rseA*, forward primer 5'-

GCCAGCGAGCAGTTAACGGACCA and reverse primer 5'-CCTTGCGCTGCCCCGAACTTAAT were used. For *ompA*, forward primer 5'-GCCTACACTTCAGGCTATGCACA and reverse primer was 5'-GCCAAATATCAACAACTTGAAAA were used. For *bssR*, forward primer 5'-CCAACCCGGCTACCCCACAAATC and reverse primer 5'-CCATTGCGTGGGCTAACTTTAAG were used.

Conjugation.

Plasmid R1*drd*19 was conjugated (65) into the 40 isogenic mutants using donor strain *E. coli* BW25113 *cysB*/R1*drd*19. The recipient colonies were selected on M9C glu plates containing 30 μg/mL of chloramphenicol, and the presence of R1*drd*19 was confirmed using four antibiotics (100 μg/mL of ampicillin, 50 μg/mL of kanamycin, 30 μg/mL of chloramphenicol, and 100 μg/mL of streptomycin) (20).

Crystal violet biofilm assay.

This assay was based on that of Pratt and Kolter (44) but was modified to achieve consistent biofilm formation upon addition of the conjugation plasmid. *E. coli* strains were grown in LB medium for 16 h then the overnight cultures were inoculated into fresh LB; when the turbidity reached 1.5 at 600 nm, these cultures were diluted to a turbidity of 0.05 at 600 nm in LB and added to polystyrene 96-well plates and incubated at 37°C for 7 h without shaking. Each biofilm assay data point was the average from 10 wells for each of 3 to 20 independent cultures.

Flow cell biofilm experiment and image analysis.

Strains were cultured overnight in LB medium with erythromycin to maintain pCM18 and chloramphenicol to maintain R1*drd*19. All the flow cells (14) were inoculated at a turbidity of 0.05 at 600 nm at 37°C for two hours at a flow rate of 13 mL/h, then fresh LB medium with

300 μg/mL erythromycin was added at 13 mL/h. After 24 h, a TCS SP5 confocal microscope (Leica Microsystems GmbH, Wetzlar) was used to view the flow cell biofilms by imaging approximately eight random positions; for each position, 25 images were taken. IMARIS confocal software (BITplane, Zurich, Switzerland) was applied to process the images. Those 200 color confocal flow chamber images were converted to gray scale by using Image Converter (Neomesh Microsystems, Wainuiomata, Wellington, New Zealand). COMSTAT confocal software (27) was used to determine the biofilm parameters.

Growth rate measurement.

Strains and the mutants carrying the conjugation plasmid R1*drd*19 were grown in LB medium with appropriate antibiotics, and the turbidity at 600 nm was measured from 0.08 to 0.6 as function of time. Two independent cultures were used for each growth rate.

RNA isolation and DNA microarrays.

To study the impact of R1*drd*19 on *E. coli* wild-type biofilm formation, *E. coli* BW25113 biofilms with and without R1*drd*19 were developed on glass wool (Corning Glass Works, Corning, NY) for 7 h, 15 h, and 24 h in LB. Similarly, *E. coli* ATCC25404 biofilms with and without R1*drd*19 were developed on glass wool for 24 h in LB, and *E. coli* MG1655 biofilms with and without R1*drd*19 were developed on glass wool for 24 h in M9C glu. Different media were chosen for the different strains because they are the media in which R1*drd*19 influenced biofilm formation to the largest extent (data not shown). Biofilm cells were removed by sonicating the glass wool in 200 mL of sterile 0.85% NaCl solution at 0°C, then the total RNA was isolated as described previously (49). The *E. coli* Genechip antisense genome array (Affymetrix, P/N 900381) was used to analyze the complete *E. coli* transcriptome as described previously (22). Based on the manufacturer's guidelines, each array contains probes for more than 4200 open reading frames (ORFs). Each ORF is covered by 15 probe pairs

consisting of a perfect match and a mismatch pair. Expression of each gene is evaluated by comparing intensity of the perfect match probe and the mismatch probe in each of the 15 probe pairs, leading to reliable gene expression profiles (http://www.affymetrix.com/products/arrays/specific/ecoli_antisense.affx). Total signal intensity was scaled automatically in the software to an average value of 500. Genes were identified as differentially expressed if the P value was less than 0.05 and if the expression ratio was greater than 2 to 2.5-fold for all genes since the standard deviation for the expression ratio for the genes in the data was 1.3 to 3.3 (48). The gene functions were obtained from the National Center for Biotechnology Information database (http://www.ncbi.nlm.nih.gov/) (18) the Institute for Genomic Research, University of California at San Diego, and the UNAM database (http://ecocyc.org/) (34).

Motility assay.

Cell motility (56) was examined by inoculating 16 h overnight cultures into fresh LB, by growing until the turbidity at 600 nm reached around 1, and by inoculating motility agar plates (1% tryptone, 0.25 % NaCl, and 0.3 % agar) with these exponentially-growing cells using a toothpick. Motility halos were quantified using at least three plates for each culture, and two independent cultures for each strain.

Aggregation assay.

This assay was modified slightly (51); *E. coli* strains were cultured for 16 h overnight in LB, and these overnight cultures were inoculated into fresh LB to create exponentially-growing cells at a turbidity 1.5 at 600 nm. The cells were washed with LB medium to remove antibiotics, and diluted in 3 mL of LB to a turbidity at 600 nm of 2.5. The cultures were placed in 14 mL sterile tubes, and incubated quiescently at 37°C for 7 h. The turbidity was measured 5 mm underneath the surface to determine the cell concentration which is an indirect determination of

cell aggregation. Each data point was the average of two tubes for each independent culture, and two independent cultures were conducted for each strain.

AI-2 assay.

V. harveyi BB170 was inoculated in AB medium and cultured at 30°C at 250 rpm for 16 hours. *E. coli* LB overnight cultures with antibiotics (16 h, 30°C) were inoculated into fresh LB medium without antibiotics, and 1.5 mL of the cell culture was taken at intervals and quickly centrifuged at 16,000 g for 5 min. The samples were filter sterilized and stored at 0°C. Overnight cultures of *V. harveyi* BB170 were diluted 5000-fold in 50 mL of AB medium. The diluted *V. harveyi* BB170 culture (1.8 mL) and 0.2 ml of *E. coli* supernatants were mixed together and incubated at 30°C at 250 rpm for four hours as at that time *V. harveyi* BB170 has the lowest bioluminescence. Luminescence of cultures (0.1 mL) was measured with a luminometer (Turner Design 20/20 luminometer) after the mixture was preheated at 37°C for 2 min. Two independent cultures were performed, and the average was used to conclude.

Microarray data accession numbers.

The expression data have been deposited in the NCBI Gene Expression Omnibus (GEO, http://www.ncbi.nlm.nih.gov/geo/) and are accessible through GEO Series Accession Number (GSM147162 ~ 147165 and GSM153383 ~ 153388) (18).

Results

Conjugation plasmid R1drd19 promotes E. coli biofilm formation.

Addition of R1*drd*19 had no affect on the growth rate of *E. coli* BW25113 wild-type strain in LB medium (1.53 ± 0.00 h^{-1} for the wild-type vs. 1.56 ± 0.05 h^{-1} with R1*drd*19) (Table 2). However, in 96-well plates, adding R1*drd*19 increased BW25113 biofilm formation 1.9 ± 0.6-fold in LB at 7 h and increased ATCC25404 biofilm formation 3.5 ± 0.5 fold in LB at 24 h.

To corroborate the 96-well biofilm assay, continuous flow cells were used to study the *E. coli* BW25113 biofilm architecture with and without R1*drd*19 in LB at 37°C after 24 h. COMSTAT analysis (Table 2) indicated that upon adding R1*drd*19, the biofilm biomass of BW25113 increased 3.7-fold and the mean thickness of BW25113 increased 3.5-fold. Hence, R1*drd*19 increases biofilm formation considerably without affecting planktonic growth.

Gene expression profiles upon adding R1drd19.

To gain insight into the genetic basis of the increased biofilm formation upon adding conjugation plasmid R1*drd*19, gene expression profiles of the biofilm cells were determined at 7 h, 15 h, and 24 h for BW25113 in LB, at 24 h for MG1655 in M9C glu, and at 24 h for ATCC25404 in LB. The specific media were chosen to maximize the effect of R1*drd*19 on biofilm formation of each strain as well as to see the effect of the conjugation plasmid in both minimal and rich media. Multiple strains were used so that a general effect of R1*drd*19 on biofilm formation could be discerned, and the microarrays were conducted at multiple times with BW25113 to get a temporal response. The most induced and repressed genes for the five sets of microarray data are summarized in Table 3. The genes differently expressed upon adding R1*drd*19 involved amino acid transport and metabolism, carbohydrate transport and metabolism, cell motility, cell wall/membrane biogenesis, defense mechanisms, energy production and conversion, inorganic ion transport and metabolism, lipid transport and metabolism, posttranslational modification, protein turnover, chaperones, replication, recombination and repair, secondary metabolites biosynthesis, transport and catabolism, signal transduction mechanisms, transcription, phage and phage related genes, and genes with unknown functions.

The gene expression profile varies in different strains and medium backgrounds. At 7 h with BW25113, adding R1*drd*19 induced 451 genes (10% of the genome) more than 2.0 fold and repressed 291 genes (7% of the genome) more than 2.0 fold. At 15 h with BW25113, adding

R1*drd*19 induced 112 genes (2.5% of the genome), and repressed 10 genes more than 2.0 fold (0.2% of the genome). At 24 h with BW25113, adding R1*drd*19 induced 30 genes more than 2.0 fold (0.7% of the genome), and repressed 275 genes more than 2.0 fold (6% of the genome). At 24 h with MG1655, adding R1*drd*19 induced 39 genes more than 2.5 fold (0.9% of the genome), and repressed 50 genes more than 2.5 fold (1.1% of the genome). At 24 h with ATCC25404, adding R1*drd*19 induced 53 genes more than 2.0 fold (1.2% of the genome), and repressed 9 genes (0.2% of the genome) more than 2.0 fold. The only set of genes consistently induced among the five microarray data sets including both strains and growth conditions is the replication, recombination and repair genes *insA_1*, *insA_2*, and *insA_5*. The genes encoding oligopeptide ABC transporters *oppABCDF* were induced up to 4-fold in the BW25113 7 h and 15 h microarrays. Also, energy production and conversion genes (*sdhABCD*, *sucABCD*, *nuoABCEFGHIJKLM*, and *atpEFH*) were induced 2 to 7-fold, in the BW25113 7 h and 15 h microarrays. Within the same set of microarray data, the most consistent group of genes with differential expression upon adding R1*drd*19 is the 23 e14 phage genes in MG1655 at 24 h in M9C glu which were induced 3- to 104-fold. The *psp* operon was also induced consistently in BW25113 at 15 h in LB. The genes that were chosen for further study (40 isogenic mutants) are based primarily on two criteria: (i) they were significantly induced or repressed upon adding R1*drd*19 to BW25113 (hence their study was facilitated using the Keio collection of single gene knock-outs for this strain) or (ii) they were located just upstream or downstream of those with marked differential expression.

Biofilm formation of isogenic mutants.

Based on the microarray results, biofilm formation was tested with R1*drd*19 for 40 related isogenic knockout mutants of BW25113 at 7 h in LB using the crystal violet assay (Fig. 1). To aid in their analysis, the isogenic mutants were categorized into five classes: cells with

Class I mutations (*rseA, bssR, cpxA,* and *ompA*) exhibited no difference in biofilm formation compared to the wild-type strain and no increase upon adding R1*drd*19 (Fig. 1A); Class II mutations (*gatC, yagI, ompC, cspA, pspD, pspB, ymgB, gadC, pspC, ymgA, slp, cpxP, cpxR, cstA, rseC, ompF* and *yqjD*) increased biofilm formation compared to the wild-type strain and the addition of R1*drd*19 decreased biofilm formation relative to that formed by the mutant (Fig. 1B); Class III mutations (*gadA*) increased biofilm formation compared to the wild-type strain and increased biofilm upon adding R1*drd*19 (Fig. 1C); Class IV mutations (*aceB, glgS, glpD, csgG, hdeD, pspA, gadB, tnaA,* and *crl)* increased biofilm formation compared to the wild-type strain but had little change in biofilm upon adding R1*drd*19 (Fig. 1D); and Class V mutations (*flhC, nmpC, flhD, pspE, icdA, atpF, atpH, rseB,* and *sodB*) had no difference compared to the wild-type strain but increased biofilm upon adding R1*drd*19 (Fig. 1E). It appears that the deletion of Class I or II genes blocked the effects of R1*drd*19 on BW25113, which indicates that these genes are key genes involved in R1*drd*19-related induction of biofilm formation.

To corroborate the 96-well biofilm results for the Class I mutants, we also conducted flow cell experiments in the presence and absence of R1*drd*19 (*rseA*/R1*drd*19, *bssR*/R1*drd*19, *cpxA*/R1*drd*19, and *ompA*/R1*drd*19) in LB at 37°C after 24 h (Fig. 2C/2D/2E/2F). Flow cells experiments were also conducted with *rseA, bssR, cpxA,* and *ompA* as negative controls. COMSTAT analysis (Table 2) indicated there is no increase in biomass or mean thickness by adding R1*drd*19 to cells with the *rseA, bssR, cpxA,* and *ompA* mutations compared to the wild-type strain. Hence, the biofilm biomass of *rseA*/R1*drd*19, *bssR*/R1*drd*19, *cpxA*/R1*drd*19, and *ompA*/R1*drd*19 decreased dramatically compared to BW25113/R1*drd*19 (4.1-fold, 3.7-fold, 2.2-fold, and 3.5-fold, respectively), as did the biofilm mean thickness (2.8-fold, 2.8-fold, 2.3-fold, and 13-fold, respectively) (Table 2). In contrast to the wild-type strain, adding R1*drd*19 decreased or did not alter biomass, substratum coverage, and mean thickness of the four Class I

mutants (Table 2). Therefore, the Class I mutations (*rseA*, *bssR, cpxA,* and *ompA*) prevent R1*drd*19 from increasing biofilm formation as it does with the wild-type strain, and there was good agreement between the 96-well and the flow cells biofilm experiments. Furthermore, normalization of biofilm formation by cell growth does not affect the classification of the Class I genes (data not shown).

R1drd19 increases aggregation through Class I genes.

To study the role of aggregation in biofilm formation of *E. coli* with R1*drd*19, we tested the aggregation of the four *E. coli* BW25113 Class I mutants and the 17 Class II mutants that we identified as related to R1*drd*19 and biofilms. For the wild-type strain, addition of R1*drd*19 increases aggregation 3 ± 1-fold in LB. Except for *cstA*, Class II mutations have an apparent inverse effect of these mutations on biofilm enhancement by R1*drd*19 and aggregation stimulated by the presence of the plasmid in that the mutations alone have no significant effect on aggregation of the wild-type strain, but they increased aggregation 4- to 47-fold upon adding R1*drd*19 relative to the wild-type strain (except *cpxR* which is the partner of class I gene *cpxA* and is part of the same two-component system) (Table 4). However, for Class I, the mutations again have no effect on aggregation compared to the wild-type strain, but addition of R1*drd*19 did not increase aggregation except for *rseA* where there was an extraordinary increase in aggregation (267-fold) upon adding R1*drd*19 (Table 4). Since the addition of R1*drd*19 increased the aggregation of the wild-type strain, but not aggregation for 3 of the 4 Class one mutants, R1*drd*19 enhanced aggregation of the wild-type strain requires Class I genes *bssR, cpxA,* and *ompA*. In contrast, the Class II proteins repress aggregation since their inactivation results in increased aggregation. Also, this increase in aggregation is inversely proportional to biofilm formation as shown in Fig. 1B. Therefore, R1*drd*19 increases aggregation using Class I proteins, and Class II proteins repress aggregation.

R1drd19 increases biofilm formation by decreasing motility through Class I and Class II genes.

Addition of R1*drd*19 decreased BW25113 wild-type motility 24 ± 7%. The motility of wild-type BW25113 was not substantial, forming only a diameter of 0.6 ± 0.1 cm after 8 h. Similar to the aggregation results, we conducted motility assays for the Class I and II mutants (Table 4). 88% of the 17 Class II mutants increased wild-type motility from 1.6- to 7.0-fold, and except for *slp,* all of them were more motile upon adding R1*drd*19 compared to the wild-type strain although for 88% of them, the relative increase was less than without R1*drd*19 (Table 4). Hence, one of the reasons for the failure of the conjugation plasmid to increase biofilm formation appears to be the enhanced motility that occurs with the Class II mutants.

Supporting this idea, deletion of the Class I genes prevented R1*drd*19 from decreasing motility as it did for the wild-type strain (Table 4), and motility was increased for *rseA*, *bssR,* and *ompA*. One of the Class I genes, *cpxA*, encodes the upstream protein CpxA in the CpxR-P regulation pathway that down-regulates motility genes (10) (Fig. 4). *cpxA*, *cpxR,* and *cpxP* were induced by adding R1*drd*19 1.3-fold, 2.5-fold, and 6.1-fold at 7 h in LB respectively (Table 3), which indicates activation of the two-component system that led to 16 motility genes being repressed by adding R1*drd*19 upon addition to the wild-type strain (Table 3). Therefore, it appears that R1*drd*19 increases wild-type biofilm because it initiates the pathway which represses cell motility through the Class I genes.

R1drd19 increases biofilm formation by increasing the quorum sensing signal AI-2.

In the microarray data of ATCC25404 in LB at 24 hours (Table 3), adding R1*drd*19 repressed *glpDKF* 3.0- to 5.7-fold; the *glpD* mutation represses *lsr* transcription, which results in accumulation of extracellular AI-2 (64). Therefore, we studied the effect of R1*drd*19 on extracellular AI-2 concentrations. As expected, extracellular AI-2 concentrations in both the

wild-type strain BW25113 and BW25113/R1*drd*19 accumulated in the stationary phase (61) and

decreased at the end of the stationary phase (Fig. 3). However, the addition of R1*drd*19 increased

extracellular AI-2 3.4-fold at a turbidity of 3.5 (Fig. 3).   As a positive control, AI-2

concentrations for the *glpD* mutant were assayed and this mutation increased AI-2 7.1-fold as

expected (64). Therefore, adding R1*drd*19 increases the cell quorum sensing signal AI-2

probably by repressing *glpD* which leads to an increase of biofilm formation in *E. coli* as has

been seen with direct addition of AI-2 (22).

Discussion

In this study, we show clearly that *E. coli* biofilm formation is induced by adding

R1*drd*19 in different strains (*E. coli* BW25113, MG1655, and ATCC25404) and in different rich

and minimal media. Using a whole-transcriptome approach, we discovered the addition of this

conjugation plasmid affects consistently Class I gene expression (*rseA*, *bssR*, *cpx* operon, and

ompA) in different *E. coli* strains. We discovered that mutations in these genes prevent the

addition of R1*drd*19 from increasing biofilm formation as it does in the wild-type strain.

We hypothesize that the pili formed by the conjugation plasmid lead to unassembled or

misfolded proteins in the membrane that increase *E. coli* K-12 biofilm formation through the

associated stress response (Fig. 4) much like acid, heat, hydrogen peroxide, and cadmium stress

have been shown by us to increase *E. coli* biofilm formation (67). The envelope stress response

system responds to pili (11), and regulates genes involved in biofilm formation. RseA and CpxA

are the sensors in the two different envelope stress response systems respectively, the RseA-σ^E

envelope stress response system and the CpxAR two component system.   Although highly

speculative, the Class I protein OmpA may also sense the signal from pili in the outer membrane,

and act as the activator of CpxAR two-component system. Therefore, three of the four Class I

genes are involved in early regulation of the biofilm pathway by sensing the signal from

conjugative pili which initiates the envelope stress response system and regulates biofilm-related genes, including adherence genes and motility genes. Upon deletion of *rseA*, *cpxA*, and *ompA*, *E. coli* is not able to sense the signal upon adding R1*drd*19, and thus this conjugation plasmid fails to increase biofilm formation.

The envelope stress gene *rseA* was induced 2.3-fold in the 7 h microarray data with BW25113, and this gene was differentially expressed in other microarray studies (repressed 2.5-fold in BW25113 at 24 h in LB and repressed 2.3 fold in MG1655 at 24 h in M9C glu) (Table 3). RseA, the anti-sigma E factor (1), is induced by adding R1*drd*19 in *E. coli* strains. It appears conjugation promotes RseA binding to σ^E, and σ^E is blocked from binding RNA polymerase, and thus possibly represses certain biofilm-related genes. Furthermore, *rseA* is induced by cold-shock (42), and is down-regulated by OmpC, which is up-regulated in biofilm cells compared to stationary cultures (54). Here, cold-shock genes *cspACDG* were induced 2.5 to 3.5-fold by R1*drd*19 in the BW25113 strains (Table 3). Hence, we also speculate that cold shock proteins are possibly involved in the mechanism of biofilm increase upon adding R1*drd*19 through the RseA system.

The relationship between Cpx, stress, and biofilm is more clear. Cpx expression in relation to envelope stress is derived from the expression of protein folding catalysts (DsbA, PpiA, and PpiD) and degrading factors like DegP, which cleaves RseA and releases σ^E (17). At the transcriptional level, Cpx represses genes for adherence, taxis, and motility, whereas it activates genes involved in folding factor/protein degradation, outer membrane proteins, and multidrug resistance (16). *cpxAR* and *cpxP* were induced in BW25113 upon R1*drd*19 addition at 7 h in LB (1.3-, 2.5- and 6.1-fold respectively), and *cpxR* and *cpxP* were induced 3.5-fold in BW25113 at 15 h in LB. Possibly associated with *cpxAR* and *cpxP* induction, 16 cell motility genes were repressed 1.7 to 4.9-fold upon adding R1*drd*19 in BW25113 at 7 h in LB. Curli

genes, *csgBEFG*, were also repressed 2.8-, 3.7-, 2.3-, and 6.5-fold, respectively. Hence, our DNA microarray data showed that at the transcriptional level, the genes related to motility were repressed by adding R1*drd*19, and CpxR is the potential regulator involved in this mechanism (Table 3).

The function of OmpA upon R1*drd*19 addition is less clear even though we found it is necessary for R1*drd*19 to increase *E. coli* biofilm formation. *ompACF*, the genes encoding outer membrane proteins, were induced 3.0-, 2.8-, and 2.5-fold respectively, upon R1*drd*19 addition in BW25113 at 7 h in LB. *ompA* was also induced 2.8- and 3.0-fold respectively, upon R1*drd*19 addition in BW25113 at 15 h in LB and in ATCC25404 at 24 h in LB. We predict that OmpA, similar with another outer membrane protein, NlpE, is positioned early in the stress response system. Adding R1*drd*19 induces *ompA* gene expression; consequently, overproduced OmpA activates the two-component system CpxAR to mediate biofilm formation. In addition, OmpA enhances *E. coli* swarming without significantly affecting swimming (30); usually swarming and biofilm formation are correlated (55), so addition of R1*drd*19 increase OmpA which may then facilitate biofilm formation through its link to swarming.

bssR was repressed in two out of five sets of microarray data (Table 3). In LB medium, the deletion of *bssR* repressed *mtr*, which encodes the protein importing indole and induced *acrEF* that encode proteins involved in the export of indole (15). DNA microarrays indicated that BssR regulates genes involved in biofilm formation (15), and 130 genes out of them were affected by quorum sensing via AI-2. However, how R1*drd*19 interacts with BssR is not clear. It is possible that R1*drd*19 increases biofilm formation through indole regulated by BssR. As the deletion of *bssR* decreased indole concentration in BW25113 in LB glu and BssR decreased biofilm formation in LB glu, adding indole to *bssR* mutant with R1*drd*19 would possibly recover

the biofilm formation back to the same level as the wild-type strain with R1*drd*19. Class II mutations also prevent R1*drd*19 from increasing biofilm formation.

Supporting the hypothesis of the link between the cell envelope stress response system and R1*drd*19 addition, we found that the genes that encode murein were induced upon adding R1*drd*19 to the *E. coli* strains: *murE*, *glmS*, and *yeaF* were induced 2.5- to 3.3-fold in BW25113 in LB at 7 h (Table 3). Murein contributes to the mechanical stability of the *E. coli* cell wall (29). We postulate that the murein genes were induced due to the response to the cell envelope stress upon adding R1*drd*19. *lpp*, the gene encoding murein lipoprotein, was also induced 2.8 and 2.1-fold upon adding R1*drd*19 in LB for BW25113 at 7 hours and 15 hours, and for ATCC25404 at 24 hours (Table 3). *bolA*, a possible regulator of murein genes (53), was also induced 2.0 -fold in BW25113 in LB at 15 hours, but repressed 2.0-fold in ATCC25404 in LB at 24 hours upon adding R1*drd*19. In addition, the operon encoding oligopeptide permeases, *oppABCDF* (28), were induced 2.8 to 4.0-fold upon adding R1*drd*19 in BW25113 in LB at 7 hours; these permeases assist murein recycling (23). Hence, induction of the murein genes upon R1*drd*19 addition corroborates that the cell experienced envelope stress.

The conjugation plasmid may also increase cell persistence by inducing persistence genes in *E. coli*. Persisters are responsible for high resistance in biofilm due to various antimicrobials (57). Our microarray data indicated the conjugation plasmid has a significant effect on persistence gene transcription. In MG1655, 23 e-14 prophage genes (b1137 ~ 1159) were induced 3- to 104-fold by adding R1*drd*19; we also identified CP 4-6 prophage genes were induced (b0275 in all the BW25113 microarrays and *yafXZ* in BW25113 15 h microarray data). Both e-14 prophage and CP 4-6 prophage genes were reported as induced in persister cells (37). Another operon associated with cell persistence, *pspABCDE* (33), was also induced upon R1*drd*19 addition (Table 3). The *psp* genes in this operon were induced 3.5- to 6.5-fold in

BW25113 at 15 hours in LB, 1.6- to 2.5-fold in ATCC25404 at 24 hours in LB, and repressed

3.5- to 4.3-fold in MG1655 at 24 hours in M9C glu upon adding R1*drd*19. Therefore, the

addition of the conjugation plasmid may influence cell persistence.

By investigating the differentially expressed genes of the host rather than the R1 plasmid

itself, it was discovered here that cell envelope stress is one of the key reasons for the increase in

biofilm formation upon addition of a conjugation plasmid. Understanding how biofilms form

when they are influenced by a conjugation plasmid is important since these plasmids enhance

biofilm formation while overriding the importance of flagella, type I fimbriae, Ag43, and curli

(46).

Reference

1. **Alba, B. M., and C. A. Gross.** 2004. Regulation of the *Escherichia coli* sigma E-dependent envelope stress response. Mol. Microbiol. **52:**613-619.
2. **Baba, T., T. Ara, M. Hasegawa, Y. Takai, Y. Okumura, M. Baba, K. A. Datsenko, M. Tomita, B. L. Wanner, and H. Mori.** 2006. Construction of *Escherichia coli* K-12 in-frame, single-gene knockout mutants: the Keio collection. Mol. Syst. Biol.**:**online.
3. **Batchelor, E., D. Walthers, L. J. Kenney, and M. Goulian.** 2005. The *Escherichia coli* CpxA-CpxR envelope stress response system regulates expression of the porins OmpF and OmpC. J. Bacteriol. **187:**5723-5731.
4. **Bayer, M., R. Eferl, G. Zellnig, K. Teferle, A. Dijkstra, G. Koraimann, and G. Högenauer.** 1995. Gene *19* of plasmid R1 is required for both efficient conjugative DNA transfer and bacteriophage R17 infection. J. Bacteriol. **177:**4279-4288.
5. **Beloin, C., J. Valle, P. Latour-Lambert, P. Faure, M. Kzreminski, D. Balestrino, J. A. J. Haagensen, S. Molin, G. Prensier, B. Arbeille, and J.-M. Ghigo.** 2004. Global impact of mature biofilm lifestyle on *Escherichia coli* K-12 gene expression. Mol. Microbiol. **51:**659-674.
6. **Blattner, F. R., G. Plunkett, 3rd, C. A. Bloch, N. T. Perna, V. Burland, M. Riley, J. Collado-Vides, J. D. Glasner, C. K. Rode, G. F. Mayhew, J. Gregor, N. W. Davis, H. A. Kirkpatrick, M. A. Goeden, D. J. Rose, B. Mau, and Y. Shao.** 1997. The complete genome sequence of *Escherichia coli* K-12. Science **277:**1453-1474.
7. **Campbell, E. A., J. L. Tupy, T. M. Gruber, S. Wang, M. M. Sharp, C. A. Gross, and S. A. Darst.** 2003. Crystal structure of *Escherichia coli* sigmaE with the cytoplasmic domain of its anti-sigma RseA. Mol. Cell. **11:**1067-1078.
8. **Datsenko, K. A., and B. L. Wanner.** 2000. One-step inactivation of chromosomal genes in *Escherichia coli* K-12 using PCR products. PNAS **97:**6640-6645.
9. **De Las Peñas, A., L. Connolly, and C. A. Gross.** 1997. The sigmaE-mediated response to extracytoplasmic stress in *Escherichia coli* is transduced by RseA and RseB, two negative regulators of sigmaE. Mol. Microbiol. **24:**373-385.

10. **De Wulf, P., O. Kwon, and E. C. C. Lin.** 1999. The CpxRA signal transduction system of *Escherichia coli*: growth-related autoactivation and control of unanticipated target operons. J. Bacteriol. **181:**6772-6278.

11. **De Wulf, P., A. M. McGuire, X. Liu, and E. C. C. Lin.** 2002. Genome-wide profiling of promoter recognition by the two-component response regulator CpxR-P in *Escherichia coli*. J. Biol. Chem. **277:**26652-26661.

12. **DiGiuseppe, P. A., and T. J. Silhavy.** 2003. Signal detection and target gene induction by the CpxRA two-component system. J. Bacteriol. **185:**2432-2440.

13. **Dionisio, F., I. C. Conceição, A. C. R. Marques, L. Fernandes, and I. Gordo.** 2005. The evolution of a conjugative plasmid and its ability to increase bacterial fitness. Biol. Lett. **1:**250-252.

14. **Domka, J., J. Lee, T. Bansal, and T. K. Wood.** 2007. Temporal gene-expression in *Escherichia coli* K-12 biofilms. Environ. Microbiol. **9:**332-346.

15. **Domka, J., J. Lee, and T. K. Wood.** 2006. YliH (BssR) and YceP (BssS) regulate *Escherichia coli* K-12 biofilm formation by influencing cell signaling. Appl. Environ. Microbiol. **72:**2449-2459.

16. **Dorel, C., P. Lejeune, and A. Rodrigue.** 2006. The Cpx system of *Escherichia coli*, a strategic signaling pathway for confronting adverse conditions and for settling biofilm communities? Res. Microbiol. **157:**306-314.

17. **Duguay, A. R., and T. J. Silhavy.** 2004. Quality control in the bacterial periplasm. Biochim. Biophys. Acta. **1694:**121-134.

18. **Edgar, R., M. Domrachev, and A. E. Lash.** 2002. Gene Expression Omnibus: NCBI gene expression and hybridization array data repository. Nucleic Acids Res. **30:**207-210.

19. **Egler, M., C. Grosse, G. Grass, and D. H. Nies.** 2005. Role of the extracytoplasmic function protein family sigma factor RpoE in metal resistance of *Escherichia coli*. J. Bacteriol. **187:**2297-2307.

20. **Ghigo, J. M.** 2001. Natural conjugative plasmids induce bacterial biofilm development. Nature **412:**442-445.

21. **González Barrios, A. F., R. Zuo, D. Ren, and T. K. Wood.** 2006. Hha, YbaJ, and OmpA regulate *Escherichia coli* K12 biofilm formation and conjugation plasmids abolish motility. Biotechnol. Bioeng. **93:**188-200.

22. **González Barrios, A. F., R. Zuo, Y. Hashimoto, L. Yang, W. E. Bentley, and T. K. Wood.** 2006. Autoinducer 2 controls biofilm formation in *Escherichia coli* through a novel motility quorum sensing regulator (MqsR, B3022). J. Bacteriol. **188:**305-306.

23. **Goodell, E. W.** 1985. Recycling of murein by *Escherichia coli*. J. Bacteriol. **163:**305-310.

24. **Hancock, V., and P. Klemm.** 2007. Global gene expression profiling of asymptomatic bacteriuria *Escherichia coli* during biofilm growth in human urine. Infect. Immun. **75:**966-976.

25. **Hansen, M. C., R. J. Palmer, Jr, C. Udsen, D. C. White, and S. Molin.** 2001. Assessment of GFP fluorescence in cells of *Streptococcus gordonii* under conditions of low pH and low oxygen concentration. Microbiology **147:**1383-1391.

26. **Hausner, M., and S. Wuertz.** 1999. High rates of conjugation in bacterial biofilms as determined by quantitative in situ analysis. Appl. Environ. Microbiol. **65:**3710-3713.

27. **Heydorn, A., A. T. Nielsen, M. Hentzer, C. Sternberg, M. Givskov, B. K. Ersbøll, and S. Molin.** 2000. Quantification of biofilm structures by the novel computer program COMSTAT. Microbiology **146:**2395-2407.

28. **Higgins, C. F., and M. M. Hardie.** 1983. Periplasmic protein associated with the oligopeptide permeases of *Salmonella typhimurium* and *Escherichia coli*. J. Bacteriol. **155:**1434-1438.

29. **Höltje, J. V.** 1998. Growth of the stress-bearing and shape-maintaining murein sacculus of *Escherichia coli*. Microbiol. Mol. Biol. Rev. **62:**181-203.

30. **Inoue, T., R. Shingaki, S. Hirose, K. Waki, H. Mori, and K. Fukui.** 2007. Genome-wide screening of genes required for swarming motility in *Escherichia coli* K-12. J. Bacteriol. **189:**950-957.

31. **Jubelin, G., A. Vianney, C. Beloin, J. M. Ghigo, J. C. Lazzaroni, P. Lejeune, and C. Dorel.** 2005. CpxR/OmpR interplay regulates curli gene expression in response to osmolarity in *Escherichia coli*. J. Bacteriol. **187:**2038-2049.

32. **Junker, L. M., J. E. Peters, and A. G. Hay.** 2006. Global analysis of candidate genes important for fitness in a competitive biofilm using DNA-array-based transposon mapping. Microbiology **152:**2233 - 2245.

33. **Kaldalu, N., R. Mei, and K. Lewis.** 2004. Killing by ampicillin and ofloxacin induces overlapping changes in *Escherichia coli* transcription profile. Antimicrob. Agents Chemother. **48:**890-896.

34. **Keseler, I. M., J. Collado-Vides, S. Gama-Castro, J. Ingraham, S. Paley, I. T. Paulsen, M. Peralta-Gil, and P. D. Karp.** 2005. EcoCyc: a comprehensive database resource for *Escherichia coli*. Nucleic Acids Res. **33:**D334-D337.

35. **Koraimann, G., and G. Högenauer.** 1989. A stable core region of the *tra* operon mRNA of plasmid R1-19. Nucleic Acids Res. **17:**1283-1298.

36. **Koraimann, G., C. Koraimann, V. Koronakis, S. Schlager, and G. Högenauer.** 1991. Repression and derepression of conjugation of plasmid R1 by wild-type and mutated *finP* antisense RNA. Mol. Microbiol. **5:**77-87.

37. **Lindsay, S., M. Tasab, A. Rickard, M. Kertesz, P. Gilbert.** 2007. Persister cells: mechanisms towards biofilm recalcitrance. Quebec, Canada, Fourth ASM conference on Biofilms.

38. **Mazel, D., and J. Davies.** 1999. Antibiotic resistance in microbes. Cell. Mol. Life Sci. **56:**742-754.

39. **Nakayama, S., and H. Watanabe.** 1998. Identification of *cpxR* as a positive regulator essential for expression of the *Shigella sonnei virF* gene. J. Bacteriol. **180:**3522-3528.

40. **Nakayama, S., and H. Watanabe.** 1995. Involvement of *cpxA*, a sensor of a two-component regulatory system, in the pH-dependent regulation of expression of *Shigella sonnei virF* gene. J. Bacteriol. **177:**5062-5069.

41. **Nancharaiah, Y. V., P. Wattiau, S. Wuertz, S. Bathe, S. V. Mohan, P. A. Wilderer, and M. Hausner.** 2003. Dual labeling of *Pseudomonas putida* with fluorescent proteins for in situ monitoring of conjugal transfer of the TOL plasmid. Appl. Environ. Microbiol. **69:**4846-4852.

42. **Polissi, A., W. De Laurentis, S. Zangrossi, F. Briani, V. Longhi, G. Pesole, and G. Dehò** 2003. Changes in *Escherichia coli* transcriptome during acclimatization at low temperature. Res. Microbiol. **154:**573-580.

43. **Pölzleitner, E., E. L. Zechner, W. Renner, R. Fratte, B. Jauk, G. Högenauer, and G. Koraimann.** 1997. TraM of plasmid R1 controls transfer gene expression as an integrated control element in a complex regulatory network. Mol. Microbiol. **25:**495-507.

44. **Pratt, L. A., and R. Kolter.** 1998. Genetic analysis of *Escherichia coli* biofilm formation: roles of flagella, motility, chemotaxis and type I pili. Mol. Microbiol. **30:**285-293.

45. **Raivio, T. L., and T. J. Silhavy.** 1999. The sigmaE and Cpx regulatory pathways: overlapping but distinct envelope stress responses. Curr. Opin. Microbiol. **2:**159-165.

46. **Reisner, A., J. A. J. Haagensen, M. A. Schembri, E. L. Zechner, and S. Molin.** 2003. Development and maturation of *Escherichia coli* K-12 biofilms. Mol. Microbiol. **48:**933-946.

47. **Reisner, A., B. M. Höller, S. Molin, and E. L. Zechner.** 2006. Synergistic effects in mixed *Escherichia coli* biofilms: conjugative plasmid transfer drives biofilm expansion. J. Bacteriol. **188:**3582-3588.

48. **Ren, D., L. A. Bedzyk, S. M. Thomas, R. W. Ye, and T. K. Wood.** 2004. Differential gene expression shows natural brominated furanones interfere with the autoinducer-2 bacterial signaling system of *Escherichia coli*. Biotechnol. Bioengr. **88:**630-642.

49. **Ren, D., L. A. Bedzyk, S. M. Thomas, R. W. Ye, and T. K. Wood.** 2004. Gene expression in *Escherichia coli* biofilms. Appl. Microbiol. Biotechnol. **64:**515-524.

50. **Rodriguez, R. L., and R. C. Tait.** 1983. Recombinant DNA Techniques: An Introduction. Benjamin/Cummings Publishing, Menlo Park, CA.

51. **Roux, A., C. Beloin, and J. M. Ghigo.** 2005. Combined inactivation and expression strategy to study gene function under physiological conditions: application to identification of new *Escherichia coli* adhesins. J. Bacteriol. **187:**1001-1013.

52. **Sambrook, J., E. F. Fritsch, and T. Maniatis.** 1989. Molecular Cloning, A Laboratory Manual. Cold Spring Harbor Laboratory Press, Cold Spring Harbor, NY.

53. **Santos, J. M., M. Lobo, A. P. A. Matos, M. A. De Pedro, and C. M. Arraiano.** 2002. The gene *bolA* regulates *dacA* (PBP5), *dacC* (PBP6) and *ampC* (AmpC), promoting normal morphology in *Escherichia coli*. Mol. Microbiol. **45:**1729-1740.

54. **Schembri, M. A., K. Kjærgaard, and P. Klemm.** 2003. Global gene expression in *Escherichia coli* biofilms. Mol. Microbiol. **48:**253-267.

55. **Shrout, J. D., D. L. Chopp, C. L. Just, M. Hentzer, M. Givskov, and M. R. Parsek.** 2006. The impact of quorum sensing and swarming motility on *Pseudomonas aeruginosa* biofilm formation is nutritionally conditional. Mol. Microbiol. **62:**1264-1277.

56. **Sperandio, V., A. G. Torres, and J. B. Kaper.** 2002. Quorum-sensing *Escherichia coli* regulators B and C (QseBC): a novel two-component regulatory system involved in the regulation of flagella and motility by quorum sensing in *E. coli*. Mol. Microbiol. **43:**809-821.

57. **Spoering, A. L., and K. Lewis.** 2001. Biofilms and planktonic cells of *Pseudomonas aeruginosa* have similar resistance to killing by antimicrobials. J. Bacteriol. **183:**6746-6751.

58. **Surette, M. G., and B. L. Bassler.** 1998. Quorum sensing in *Escherichia coli* and *Salmonella typhimurium*. Proc. Natl. Acad. Sci. U S A **95:**7046-7050.

59. **Tatum, E. L., and J. Lederberg.** 1947. Gene recombination in the bacterium *Escherichia coli*. J. Bacteriol. **53:**673-684.

60. **Udekwu, K. I., and E. G. H. Wagner.** 2007. Sigma E controls biogenesis of the antisense RNA MicA. Nucleic Acids Res. **in press**.

61. **Wang, L., Y. Hashimoto, C. Tsao, J. Valdes, and W. Bentley.** 2005. Cyclic AMP (cAMP) and cAMP receptor protein influence both synthesis and uptake of extracellular Autoinducer 2 in *Escherichia coli*. J. Bacteriol. **187:**2066-2076.

62. **Will, W. R., and L. S. Frost.** 2006. Characterization of the opposing roles of H-NS and TraJ in transcriptional regulation of the F-plasmid *tra* operon. J. Bacteriol. **188:**507-514.

63. **Wood, T. K., A. F. G. Barrios, M. Herzberg, and J. Lee.** 2006. Motility influences biofilm architecture in *Escherichia coli*. Appl. Microbiol. Biotechnol. **72:**361-367.

64. **Xavier, K. B., and B. L. Bassler.** 2005. Regulation of uptake and processing of the quorum-sensing autoinducer AI-2 in *Escherichia coli*. J. Bacteriol. **187:**238-248.

65. **Yee, D. C., J. A. Maynard, and T. K. Wood.** 1998. Rhizoremediation of trichloroethylene by a recombinant, root-colonizing *Pseudomonas fluorescens* strain expressing toluene *ortho*-Monooxygenase constitutively. Appl. Environ. Microbiol. **64:**112-118.

66. **Yoshioka, Y., H. Ohtsubo, and E. Ohtsubo.** 1987. Repressor gene *finO* in plasmids R100 and F: constitutive transfer of plasmid F is caused by insertion of IS3 into F *finO*. J. Bacteriol. **169:**619-623.

67. **Zhang, X., R. García Contreras, and T. K. Wood.** 2007. YcfR (BhsA) influences *Escherichia coli* biofilm formation through stress response and surface hydrophobicity. J. Bacteriol. **189:**3051-3062.

Table 1. Bacterial strains and plasmids used in this study.

E. coli strain/plasmid	Genotype	Reference
Strains		
K-12 BW25113	*lacI*^{q} *rrnB*$_{T14}$ Δ*lacZ*$_{WJ16}$ hsdR514 Δ*araB*AD$_{AH33}$ Δ*rhaB*AD$_{LD78}$	(8)
K-12 BW25113 mutants (all)	BW25113 Δgene Ω Km^R	(2)
K-12 ATCC25404	Wild-type *E. coli*	ATCC
K-12 MG1655	F$^-$ lambda$^-$ *ilvG*- *rfb*-50 *rph*-1	(6)
Vibrio harveyi BB170	BB120 *luxN* :: Tn5 (AI-1 sensor$^-$, AI-2 sensor$^+$)	(58)
Plasmids		
R1*drd*19	Amp^r Km^r Cm^r Sm^r; IncFII *finO*	(20)
pCM18	Em^r; pTRKL2-P$_{CP25}$RBSII-*gfp*3*-To-T1	(25)

^{a} Amp^r, Km^r, Cm^r, Sm^r, and Em^r denote ampicillin, kanamycin, chloramphenicol, streptomycin, and erythromycin resistance, respectively.

Table 2. **Specific growth rates of *E. coli* strains in LB medium and flow cell COMSTAT analysis of biofilms formed in LB medium at 37°C after 24 h.** One standard deviation is shown.

Strain	Growth Rate, h^{-1}	Biomass, $\mu m^3/\mu m^2$	Substratum Coverage, %	Mean Thickness, μm	Roughness Coefficient
BW25113 WT	1.53 ± 0.00	3 ± 3	3 ± 2	4 ± 4	1.7 ± 0.2
BW25113/R1*drd*19	1.56 ± 0.05	11 ± 4	39 ± 16	14 ± 6	0.7 ± 0.3
rseA/R1*drd*19	1.22 ± 0.02	2.7 ± 0.5	4 ± 3	5 ± 1	1.4 ± 0.1
bssR/R1*drd*19	1.36 ± 0.00	3 ± 3	4 ± 5	5 ± 4	1.4 ± 0.4
cpxA/R1*drd*19	1.24 ± 0.05	5 ± 2	22 ± 7	6 ± 2	1.3 ± 0.2
ompA/R1*drd*19	0.98 ± 0.03	3 ± 1	5± 5	4 ± 1	1.6 ± 0.2
rseA	1.6 ± 0.1	9 ± 8	29 ± 9	11 ± 7	1.1 ± 0.1
bssR	1.37 ± 0.04	12 ± 9	47 ± 26	15 ± 9	0.9 ± 0.4
cpxA	1.22 ± 0.02	2.5 ± 0.5	23 ± 6	5 ± 1	1.11 ± 0.09
ompA	1.15 ± 0.00	3 ± 3	18 ± 10	4 ± 3	1.4 ± 0.2

Table 3. Differential gene expression upon adding the conjugation plasmid R1 to BW25113 in LB (temporal arrays), upon adding R1 to MG1655 in minimal medium after 24 h, and for adding R1 to ATCC25404 in LB after 24 h. Columns 3 to 7: fold changes (p ≤ 0.05) between biofilm samples of BW25113/R1*drd*19 vs. BW25113 at 7 h in LB (B/7/LB), at 15 h in LB (B/15/LB), at 24 h in LB (B/24/LB), at 24 h for MG1655/R1*drd*19 vs. MG1655 in M9C glu (M/24/M9Cglu), and at 24 hr for ATCC25404/R1*drd*19 vs. ATCC25404 in LB (A/24/LB). Complete results available via GEO access numbers GSM147162 ~ 147165 and GSM153383 ~ 153388.

Gene	b #	B/7/LB	B/15/LB	B/24/LB	M/24/M9Cglu	A/24/LB	Description
Signal transduction mechanisms							
cstA	b0598	5.7	3.2	-1.9	2.8	1.6	peptide transporter induced by carbon starvation
rseA	b2572	2.3	1.4	-2.5	-2.3	-1.7	anti-sigma factor that inhibits sigmaE
csrA	b2696	1.1	1.6	-2.8	-2.3	-1.7	carbon storage regulator, activator of *flhDC*, regulates biofilm formation
bssR (*yliH*)	b0836	1.1	1.3	-3.5	-2.5	-1.3	biofilm signal
crp	b3357	2.5	1.5	-1.2	1.0	-1.1	CRP transcriptional dual regulator
***cpxAR* two component system**							
cpxA	b3911	1.3	-1.2	1.0	1.1	-1.2	membrane sensor kinase/phosphatase, periplasmic stress sensor
cpxR	b3912	2.5	3.5	1.2	-1.2	-1.1	response regulator, periplasmic stress response
cpxP	b3913	6.1	3.5	1.0	1.1	-1.5	inhibitor of the cpx response; periplasmic adaptor protein
b3914	b3914	3.0	2.8	-1.4	-1.4	-1.5	
Cell wall/membrane biogenesis							
nmpC	b0553	4.0	2.3	1.1	1.4	1.1	outer membrane porin protein; locus of qsr prophage
ompX	b0814	1.3	1.3	-2.0	-1.9	1.5	outer membrane protease, receptor for phage OX2
ompF	b0929	2.5	1.2	-1.2	1.0	1.1	Beta barrel porin (OMP Functional Superfamily)
ompA	b0957	3.0	2.8	-1.7	-1.3	3.0	outer membrane protein 3a (II*;G;d)
ompC	b2215	2.8	2.8	1.1	1.0	1.6	outer membrane porin OmpC
Amino acid transport, acid resistance, and metabolism							
tnaA	b3708	6.5	-1.2	-1.1	1.1	1.5	L-cysteine desulfhydrase / tryptophanase
ariR (*ymgB*)	b1166	-2.8	1.3	-2.1	-1.1	-1.1	Hha-like regulator of acid resistance and biofilm formation

Gene	ID						Description
gadA	b3517	-1.1	-1.9	-1.1	-1.4	4.0	glutamate decarboxylase A subunit
gadB	b1493	-3.7	-1.2	-1.3	-1.5	8.6	glutamate decarboxylase B subunit
gadC	b1492	-1.3	1.0	1.0	-1.1	2.3	XasA GABA APC transporter
yhiE	b3512	-3.7	1.0	-1.4	-1.3	7.5	GadE transcriptional activator
yhiX	b3516	-1.1	1.2	-1.6	-1.4	2.5	GadX transcriptional activator
hdeA	b3510	2.0	1.2	-1.4	-1.4	11.3	acid-resistance protein, possible chaperone
hdeB	b3509	-1.3	1.0	-1.1	-1.3	9.8	10K-L protein, related to acid resistance protein
hdeD	b3511	1.2	-1.4	1.2	1.0	3.0	protein involved in acid resistance
oppA	b1243	4.0	3.2	1.0	1.2	-1.2	OppA-oligopeptide ABC transporter substrate-binding
oppB	b1244	2.8	1.6	1.0	1.1	-1.3	oligopeptide ABC transporter
oppC	b1245	3.2	1.7	1.0	1.2	-1.3	oligopeptide ABC transporter
oppD	b1246	3.7	1.5	-1.3	1.1	-1.2	oligopeptide ABC transporter
oppF	b1247	2.8	1.2	1.1	1.2	-1.2	oligopeptide ABC transporter
gcvH	b2904	5.7	1.5	-1.1	-1.1	1.1	dihydrolipoyl-GcvH-protein
tdcR	b3119	-7.0	-1.4	1.5	1.1	-1.4	threonine dehydratase operon activator protein
rhsB	b3482	-10.6	-1.2	1.2	-1.1	-1.1	RhsB protein in RhsB element
Carbohydrate transport and metabolism							
gatD	b2091	4.3	1.1	2.3	1.1	1.2	galactitol-1-phosphate dehydrogenase
gatC	b2092	5.3	1.2	1.6	1.0	-1.2	phosphotransferase Systems (PEP-dependent PTS)
gatB	b2093	2.5	1.4	-1.2	-1.3	-1.2	phosphotransferase Systems (PEP-dependent PTS)
gatA	b2094	2.6	1.5	-1.1	-2.3	-1.1	phosphotransferase Systems (PEP-dependent PTS)
gatZ	b2095	4.3	1.6	-1.7	-3.0	1.5	tagatose-1,6-bisphosphate aldolase 2
gatY	b2096	4.9	1.6	-2.5	-2.0	1.2	tagatose-1,6-bisphosphate aldolase 2
mglB	b2150	5.3	1.4	-1.3	1.0	-1.1	galactose ABC transporter
Cell motility and curli							
yadC	b0135	-4.9	-1.4	1.2	1.1	-1.1	putative fimbrial-like protein, pilus
htrE	b0139	-2.0	-1.2	1.2	1.1	-1.7	putative outer membrane fimbrial subunit export usher protein

ecpD	b0140	-2.0	-1.3	1.2	1.1	-1.6	putative periplasmic pilus chaperone
sfmA	b0530	-2.3	1.0	1.2	1.3	-1.1	putative fimbrial-like protein, pilus
sfmC	b0531	-2.3	-1.1	-1.2	1.2	-1.2	chaperoning, repair (refolding)
ybgP	b0717	-2.0	-1.1	1.2	1.5	-1.3	chaperoning, repair (refolding)
csgG	b1037	-6.5	-1.2	1.1	1.1	-1.2	curli production assembly/transport component, 2nd curli operon
csgF	b1038	-2.3	-1.1	1.2	1.1	-1.4	curli production assembly/transport component, 2nd curli operon
csgE	b1039	-3.7	-1.1	1.3	1.4	-1.6	curli production assembly/transport component, 2nd curli operon
csgB	b1041	-2.8	-1.2	1.2	-1.3	-1.3	minor curlin subunit precursor, nucleator for adhesive surface organelles
flgN	b1070	-2.3	1.0	1.0	1.1	1.0	flagellar biosynthesis; believed to be export chaperone for FlgK and FlgL
ycgR	b1194	-2.1	-1.1	1.2	1.2	-1.4	motility, chemotaxis, energytaxis (aerotaxis, redoxtaxis etc)
flhC	b1891	-1.7	1.0	1.2	1.2	-1.3	transcriptional activator of flagellar Class II operons
flhD	b1892	1.2	1.0	1.2	1.3	1.0	transcriptional activator of flagellar Class II operons
yehC	b2110	-4.6	-1.2	1.2	1.3	-1.4	chaperoning, repair (refolding)
yehD	b2111	-3.0	-1.2	1.1	1.3	-1.6	putative fimbrial-like protein, pilus
b2339	b2339	-4.3	-1.1	1.2	1.2	-1.4	putative fimbrial-like protein
yhcA	b3215	-2.5	-1.4	1.2	1.3	-1.1	chaperoning, repair (refolding)
fimA	b4314	2.6	1.6	1.2	1.1	-1.3	major type 1 subunit fimbriae (pilin)
fimH	b4320	-2.0	-1.2	1.2	1.0	-1.1	minor fimbrial subunit
Murein related genes							
murE	b0085	3.3	1.1	-1.1	-1.1	1.1	murein
bola	b0435	1.0	2.0	-2.0	-1.1	-1.1	a possible regulator of murein genes
lpp	b1677	2.8	2.1	1.1	1.0	2.3	murein lipoprotein; Braun's lipoprotein
yeaF	b1782	2.5	1.2	-1.2	1.0	1.3	MltA-interacting protein; outer membrane
glmS	b3729	2.5	1.5	1.2	-1.2	-1.2	glucosamine
Defense mechanisms							

serT	b0971	-2.1	1.0	5.3	1.1	1.0	serine tRNA (UGA)
proL	b2189	2.5	-1.2	7.0	1.0	1.7	tRNA
glyU	b2864	-5.3	1.1	1.2	1.6	1.1	tRNA
glyY	b4165	4.0	-1.1	4.3	2.8	1.3	tRNA
mcrC	b4345	-5.3	-1.3	1.0	1.2	-1.7	component of 5-methylcytosine-specific restriction enzyme McrBC

Energy production and conversion

gltA	b0720	4.0	2.5	-1.3	-1.2	-1.1	citrate synthase monomer, anaerobic respiration
sdhC	b0721	3.2	2.1	1.2	-1.1	1.5	succinate dehydrogenase membrane protein
sdhD	b0722	3.2	2.1	-1.2	1.1	1.2	succinate dehydrogenase membrane protein
sdhA	b0723	4.6	3.0	-1.2	-1.1	1.4	succinate dehydrogenase flavoprotein
sdhB	b0724	2.1	2.1	1.2	1.1	1.1	succinate dehydrogenase iron-sulfur protein
sucA	b0726	2.5	2.6	-1.2	-1.1	1.5	subunit of E1(0) component of 2-oxoglutarate dehydrogenase
sucB	b0727	3.2	3.2	-1.2	1.0	1.7	2-oxoglutarate dehydrogenase
sucC	b0728	2.8	3.5	-1.6	-1.2	1.7	succinyl-CoA synthetase, beta subunit
sucD	b0729	2.1	2.6	-1.3	1.0	1.1	succinyl-CoA synthetase, alpha subunit
aldA	b1415	2.8	2.6	-2.1	1.3	1.2	putative succinate-semialdehyde dehydrogenase / aldehyde dehydrogenase
nuoN	b2276	2.3	-1.1	1.2	1.1	1.0	NADH dehydrogenase I
nuoM	b2277	2.3	1.3	1.1	1.1	1.1	NADH dehydrogenase I
nuoL	b2278	3.7	1.3	1.2	1.1	1.1	NADH dehydrogenase I
nuoK	b2279	3.5	1.2	-1.1	-1.3	1.1	NADH dehydrogenase I
nuoJ	b2280	4.0	1.2	-1.1	1.0	1.1	NADH dehydrogenase I
nuoI	b2281	4.3	1.2	1.2	1.1	1.2	NADH dehydrogenase I
nuoH	b2282	3.0	1.4	-1.3	1.0	1.5	NADH dehydrogenase I
nuoG	b2283	4.3	1.4	1.1	1.1	1.1	NADH dehydrogenase I
nuoF	b2284	3.2	1.5	-1.2	1.0	1.2	NADH dehydrogenase I
nuoE	b2285	4.9	1.6	-1.1	1.2	1.4	NADH dehydrogenase I
nuoC	b2286	4.9	1.5	-1.2	1.0	1.4	NADH dehydrogenase I

nuoB	b2287	3.0	1.9	-1.2	-1.1	1.4	NADH dehydrogenase I
nuoA	b2288	3.2	2.0	-1.9	1.1	1.5	NADH dehydrogenase I
gabD	b2661	1.9	2.6	-1.7	-1.2	2.3	succinate-semialdehyde dehydrogenase I, NADP-dependent
mdh	b3236	4.3	2.6	-2.0	-1.1	1.2	malate dehydrogenase
glpA	b2241	-1.2	-1.1	1.5	3.2	-1.2	sn-glycerol-3-phosphate dehydrogenase (anaerobic), large subunit
glpD	b3426	1.1	1.2	-1.2	5.3	-4.3	sn-glycerol-3-phosphate dehydrogenase (aerobic)
glpK	b3926	3.5	1.0	1.4	6.1	-3.0	glycerol kinase
glpF	b3927	1.2	1.2	1.4	7.0	-5.7	MIP channel, glycerol diffusion
atpH	b3735	5.7	1.7	-1.5	1.0	-1.1	ATP synthase, F1 complex, delta subunit
atpF	b3736	6.5	2.0	-1.5	1.0	1.0	ATP synthase, F0 complex, b subunit
atpE	b3737	4.3	2.1	-1.9	1.1	1.0	ATP synthase, F0 complex, c subunit
aceB	b4014	5.3	1.6	-2.4	2.0	1.7	malate synthase A
Inorganic ion transport and metabolism							
sodB	b1656	7.0	2.5	1.2	-1.3	1.3	superoxide dismutase (Fe)
Lipid transport and metabolism							
fabB	b2323	6.1	2.0	-2.1	-1.9	1.1	beta-ketoacyl-ACP synthase I / malonyl-ACP decarboxylase
Posttranslational modification, protein turnover, chaperones							
mopB	b4142	5.3	1.3	-1.7	-2.1	1.1	GroES, 10 Kd chaperone binds to Hsp60 in presence of Mg-ATP
Replication, recombination and repair							
insA_2	b0275	3.0	3.0	2.1	3.7	4.6	IS1 protein InsA, CP 4- 6 prophage
insA_1	b1894	3.2	3.2	2.6	3.7	4.0	IS1 protein InsA
insA_5	b1894	2.8	3.2	3.7	4.0	5.3	IS1 protein InsA
Secondary metabolites biosynthesis, transport and catabolism							
glgS	b3049	2.0	2.1	-2.1	-2.5	1.0	glycogen biosynthesis, rpoS dependent
Transcription							
crl	b0240	2.8	2.1	-1.6	-1.5	3.0	Crl transcriptional regulator

ybdO	b0603	-7.0	-1.4	1.2	1.0	-1.5	putative transcriptional regulator (LysR familiy)
cspD	b0880	1.5	2.5	-2.5	-1.2	1.5	DNA replication inhibitor, nucleic acid-binding domain
cspG	b0990	2.5	1.2	1.0	1.1	1.2	CspG transcriptional regulator, temperature extremes
cspC	b1823	2.8	3.5	-1.1	1.7	1.9	Cold shock protein
cspA	b3556	2.0	1.4	-1.6	-2.1	2.5	CspA transcriptional activator
pspA	b1304	1.7	6.5	1.3	-4.3	2.3	phage shock protein, inner membrane protein
pspB	b1305	1.7	6.1	1.2	-3.7	2.1	phage shock protein
pspC	b1306	-1.1	6.5	1.6	-4.0	2.5	phage shock protein: activates phage shock-protein expression
pspD	b1307	2.3	6.1	1.4	-4.0	2.5	phage shock protein
pspE	b1308	2.8	3.5	1.4	-3.5	1.6	phage shock protein
rpsK	b3297	5.7	1.5	-2.3	-2.0	1.6	30S ribosomal subunit protein S11
rpsJ	b3321	5.3	-1.2	-2.8	-1.5	-1.1	30S ribosomal subunit protein S10
rpmD	b3302	6.5	1.3	-1.5	-1.1	1.5	50S ribosomal subunit protein L30
rplV	b3315	5.7	1.1	-2.1	-1.2	-1.1	50S ribosomal subunit protein L22
rplW	b3318	5.7	1.1	-2.8	-1.3	1.0	50S ribosomal subunit protein L23

Phage and phage related genes

yafX	b0248	1.4	-1.6	2.0	1.1	1.5	CP 4- 6 prophage
yafZ	b0252	1.1	-1.5	2.1	1.3	1.1	CP 4- 6 prophage
yagI	b0272	1.4	1.1	1.2	-1.4	1.2	function unknown, CP4-6 putative prophage remnant
icdA	b1136	4.6	2.5	-1.5	1.0	1.1	isocitrate dehydrogenase, NADP+-specific
lit	b1139	-2.5	-1.2	1.0	45.3	1.0	cell death peptidase, expression of T4 late genes; e14 prophage
intE	b1140	-2.1	1.2	1.2	16.0	-1.7	e14 integrase, in defective prophage
b1141	b1141	-2.3	1.1	1.4	52.0	-1.1	e14 excisionase, in defective prophage
ymfD	b1137	-3.2	-1.7	1.2	104.0	2.0	putative SAM- methyltransferase, function unknown; e14 prophage
ymfE	b1138	-1.7	-1.2	-1.1	39.4	-4.3	predicted membrane protein, function unknown, e14 prophage
ymfH	b1142	-1.9	1.1	1.1	8.6	-1.2	spurious translation, e14 prophage

ymfI	b1143	-1.5	1.4	1.2	84.4	1.1	function unknown, e14 prophage
ymfJ	b1144	-1.7	-1.1	1.2	14.9	-3.5	function unknown, e14 prophage
ymfK	b1145	-1.7	1.1	-1.1	7.0	4.3	putative CI-like repressor, e14 prophage
ymfT	b1146	-2.0	1.2	-1.2	5.7	-1.1	putative Cro-like repressor, e14 prophage
ymfL	b1147	-1.6	-1.1	1.4	21.1	-1.1	function unknown, e14 prophage
ymfM	b1148	-1.2	-1.2	1.1	9.8	9.8	function unknown, e14 prophage
ymfN	b1149	-1.1	-1.2	1.2	18.4	3.2	function unknown, e14 prophage
ymfR	b1150	1.5	-1.2	-1.1	2.6	5.3	function unknown, e14 prophage
ymfO	b1151	1.7	-1.1	1.0	4.9	2.3	function unknown, e14 prophage
ymfP	b1152	1.3	-1.2	-1.1	3.5	-1.1	function unknown, e14 prophage
ymfQ	b1153	1.4	-1.3	-1.1	3.7	-1.5	function unknown, e14 prophage
ymfS	b1155	-1.9	-1.3	-1.2	9.8	1.6	function unknown, e14 prophage
ycfK	b1154	-1.2	-1.3	1.2	10.6	1.0	putative tail fiber protein, e14 prophage
ycfA	b1156	-1.9	-1.3	1.1	4.3	1.3	phage lambda tail fiber assembly gene homolog, e14 prophage
stfE	b1157	-1.7	-1.2	-1.1	8.6	1.5	side-tail fiber protein, e14 prophage
pin	b1158	1.1	-1.3	-1.2	4.0	1.0	DNA invertase, site-specific recombination, e14 prophage
mcrA	b1159	-2.0	-1.5	1.1	12.1	-1.1	5-methylcytosine-specific restriction endonuclease B, e14; prophage gene
b1364	b1364	-6.5	1.2	-1.2	1.1	-1.4	Rac prophage
ydfO	b1549	-6.1	-1.3	-1.1	1.0	-1.6	Qin prophage
yfjW	b2642	-7.5	-1.3	-1.1	1.0	-1.2	CP4-57 prophage
yjhB	b4279	-6.1	-1.2	1.2	1.4	-1.2	KpLE2 phage-like element; putative transport protein (MFS family)

Function unknown

ykgI	b0303	-6.1	-1.2	1.4	1.5	-1.2	hypothetical protein
ymgA	b1165	-1.2	1.3	-2.6	-1.3	1.1	hypothetical protein
b1471	b1471	-10.6	-1.2	1.4	1.1	-1.4	putative glycoprotein
b1720	b1720	-7.5	-1.5	-1.2	1.1	-1.3	

|						
b2649	b2649	-6.5	-1.3	1.2	1.4	-1.4	hypothetical protein
yqeJ	b2848	-9.2	-1.5	-1.2	1.3	-1.6	hypothetical protein
yqjD	b3098	5.3	2.1	-2.6	-1.1	1.6	conserved hypothetical protein
yhaC	b3121	-9.8	-1.5	1.1	1.1	1.1	hypothetical protein
slp	b3506	-1.2	1.3	-1.6	-1.7	3.0	outer membrane protein induced after carbon starvation
yjcF	b4066	-7.0	-1.6	1.3	1.3	1.0	hypothetical protein

Table 4 Motility and aggregation assay results for *E. coli* BW25113 Class I and Class II mutants. Motility was determined after 8 h at 37°C, and aggregation was determined after 7 hr in LB at 37°C. Results are expressed as the ratio of the measurement for the indicated mutant to the measurement of the wild-type. Data are the average of two independent cultures, and one standard deviation is shown.

| Mutant	Biofilm Classification	Change (*n*-fold) Relative to Wild-type (WT)			
		Motility, 8h		Aggregation, 7h, LB	
		Without R1*drd*19	With R1*drd*19	Without R1*drd*19	With R1*drd*19
cpxA	Class 1	0.4 ± 0.1	0.39 ± 0.09	1.04 ± 0.06	1.1 ± 0.1
rseA	Class 1	2.8 ± 0.6	2.2 ± 0.5	1.13 ± 0.05	267 ± 43
bssR	Class 1	1.6 ± 0.4	1.7 ± 0.4	1.04 ± 0.04	1.14 ± 0.06
ompA	Class 1	1.0 ± 0.1	1.1 ± 0.1	1.01 ± 0.05	1.3 ± 0.1
ymgA	Class 2	7 ± 1	2.0 ± 0.4	1.01 ± 0.03	47 ± 24
slp	Class 2	1.2 ± 0.1	0.59 ± 0.07	1.00 ± 0.03	37 ± 6
cstA	Class 2	4.4 ± 0.4	3.2 ± 0.3	3.3 ± 0.5	9 ± 3
gatC	Class 2	3.9 ± 0.8	3.6 ± 0.7	1.11 ± 0.02	8.5 ± 0.8
yqjD	Class 2	2.2 ± 0.2	1.6 ± 0.2	0.94 ± 0.03	10.2 ± 0.6
cpxR	Class 2	4.4 ± 0.2	2.8 ± 0.1	1.38 ± 0.06	1.19 ± 0.07
cpxP	Class 2	4.1 ± 0.7	3.6 ± 0.6	1.37 ± 0.02	4.6 ± 0.5
yagI	Class 2	1.6 ± 0.3	1.4 ± 0.3	1.01 ± 0.03	11 ± 1
ompC	Class 2	2.1 ± 0.4	1.9 ± 0.5	1.10 ± 0.05	13.2 ± 0.5
cspA	Class 2	3.2 ± 0.6	2.9 ± 0.7	1.32 ± 0.07	9.3 ± 0.5
pspD	Class 2	3.9 ± 0.7	3.4 ± 0.6	1.08 ± 0.04	17 ± 3
pspB	Class 2	1.0 ± 0.4	2.1 ± 0.4	1.2 ± 0.2	13 ± 3
ymgB	Class 2	1.7 ± 0.6	2.0 ± 0.2	1.16 ± 0.02	9 ± 1
gadC	Class 2	3.6 ± 0.8	2.1 ± 0.5	1.1 ± 0.1	12 ± 2
pspC	Class 2	2.8 ± 0.5	2.1 ± 0.4	1.04 ± 0.04	4 ± 1
rseC	Class 2	3.0 ± 0.5	2.4 ± 0.4	1.23 ± 0.08	15 ± 2
ompF	Class 2	4.3 ± 0.8	3.6 ± 0.7	1.5 ± 0.3	19 ± 2
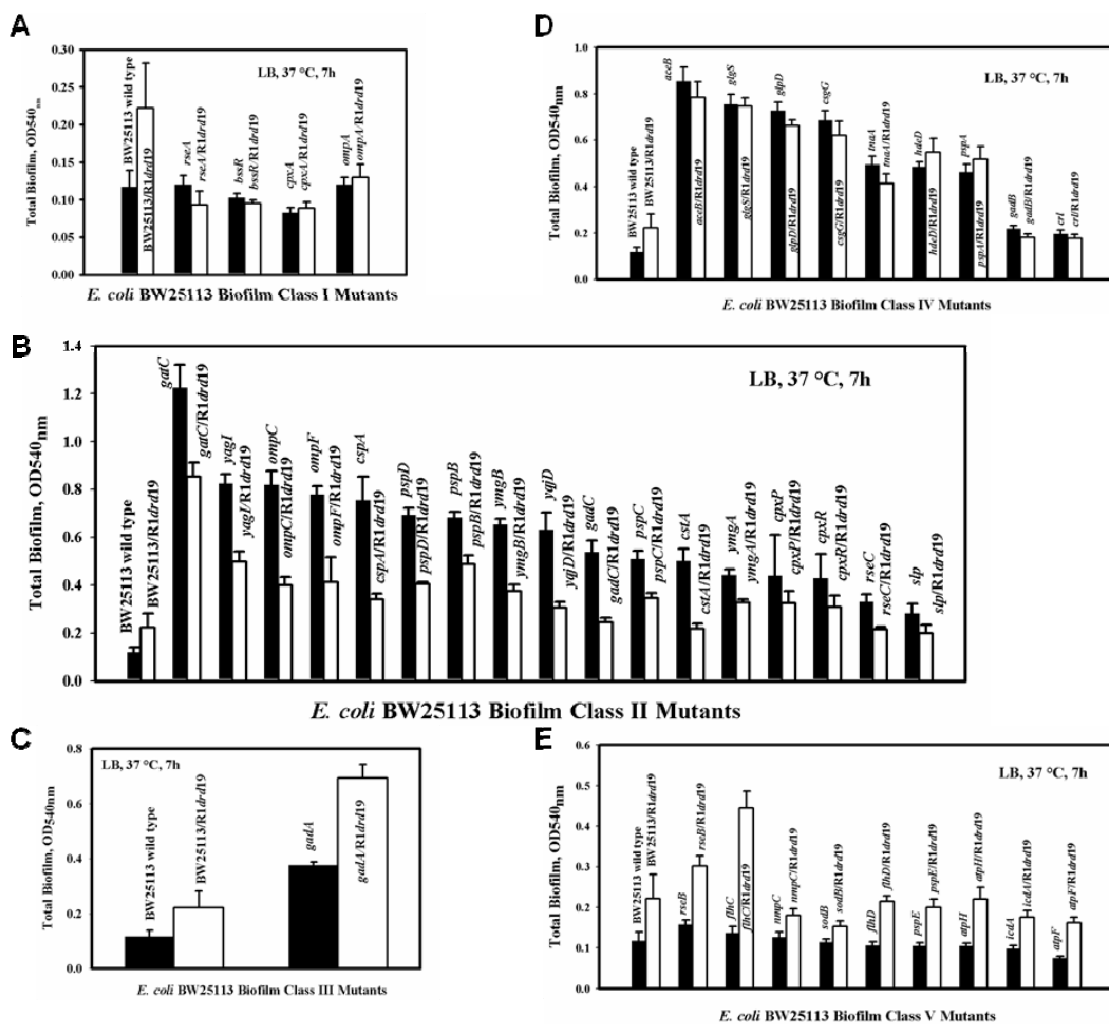
Figure 1 Biofilm formation of *E. coli* BW25113 biofilm Class I through V mutants in LB medium after 7 h at 37°C in 96-well. (A) Class I mutations have no difference in biofilm formation compared to the wild-type strain and do not increase biofilm formation upon adding R1*drd*19. (B) Class II mutations increase biofilm formation compared to the wild-type strain but decrease biofilm formation upon adding R1*drd*19. (C) Class III mutations increase biofilm formation compared to the wild-type strain and increase biofilm formation upon adding R1*drd*19. (D) Class IV mutations increase biofilm formation compared to the wild-type strain but have no difference in biofilm formation upon adding R1*drd*19. (E) Class V mutations have no difference in biofilm formation compared to the wild-type strain but increase biofilm formation upon adding R1*drd*19.
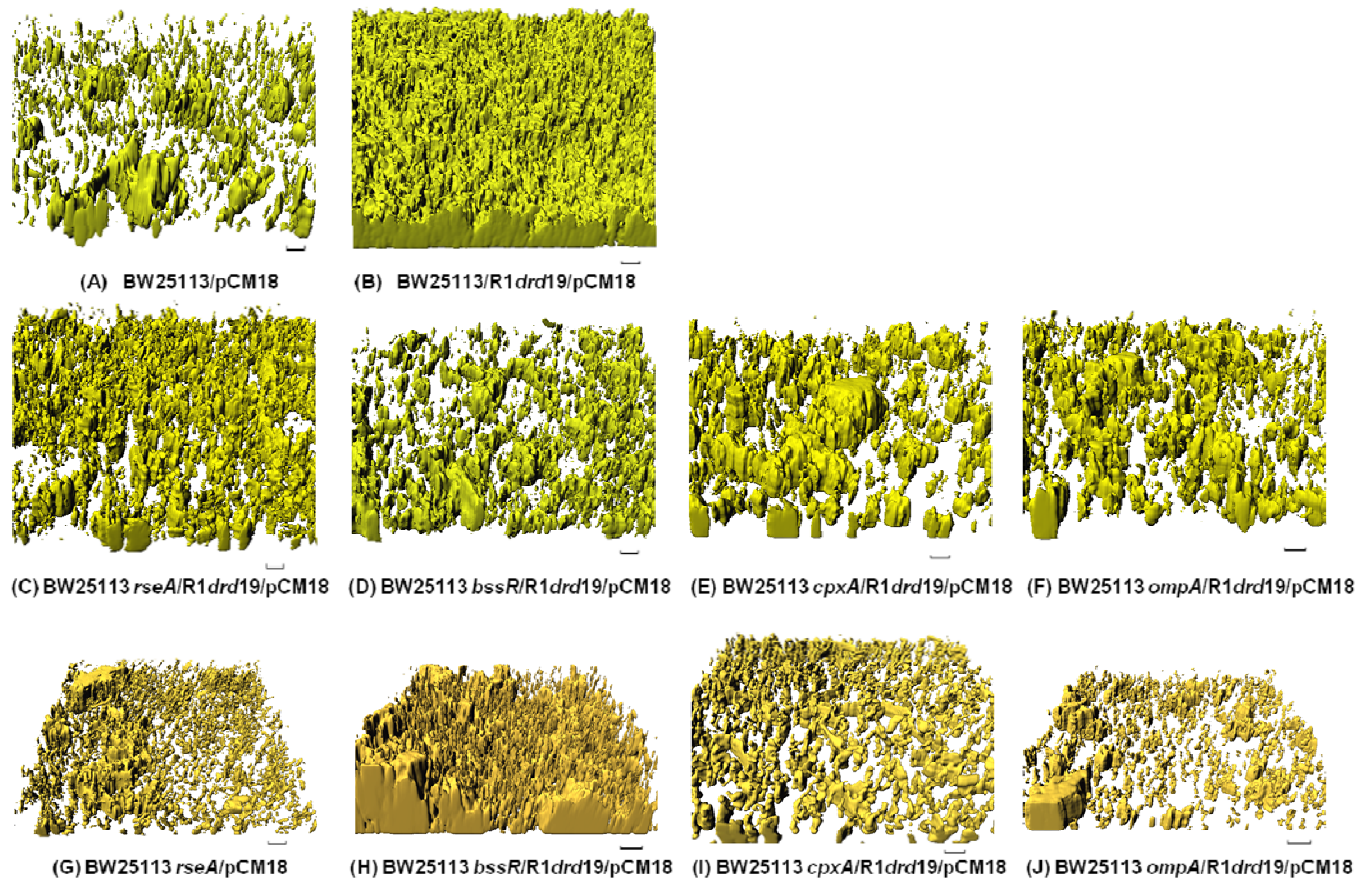
Figure 2   **IMARIS images of flow cells *E. coli* biofilms in LB medium after 24 h at 37°C.** (A) *E. coli* BW25113/pCM18, (B) *E. coli* BW25113/R1*drd*19/pCM18, (C) *E. coli* BW25113 *rseA*/R1*drd*19/pCM18, (D) *E. coli* BW25113 *bssR*/R1*drd*19/pCM18, (E) *E. coli* BW25113 *cpxA*/R1*drd*19/pCM18, and (F) *E. coli* BW25113 *ompA*/R1*drd*19/pCM18, (G) *E. coli* BW25113 *rseA*/pCM18, (H) *E. coli* BW25113 *bssR*/pCM18, (I) *E. coli* BW25113 *cpxA*/pCM18, (J) *E. coli* BW25113 *ompA*/pCM18. Scale bar is 10 µm.
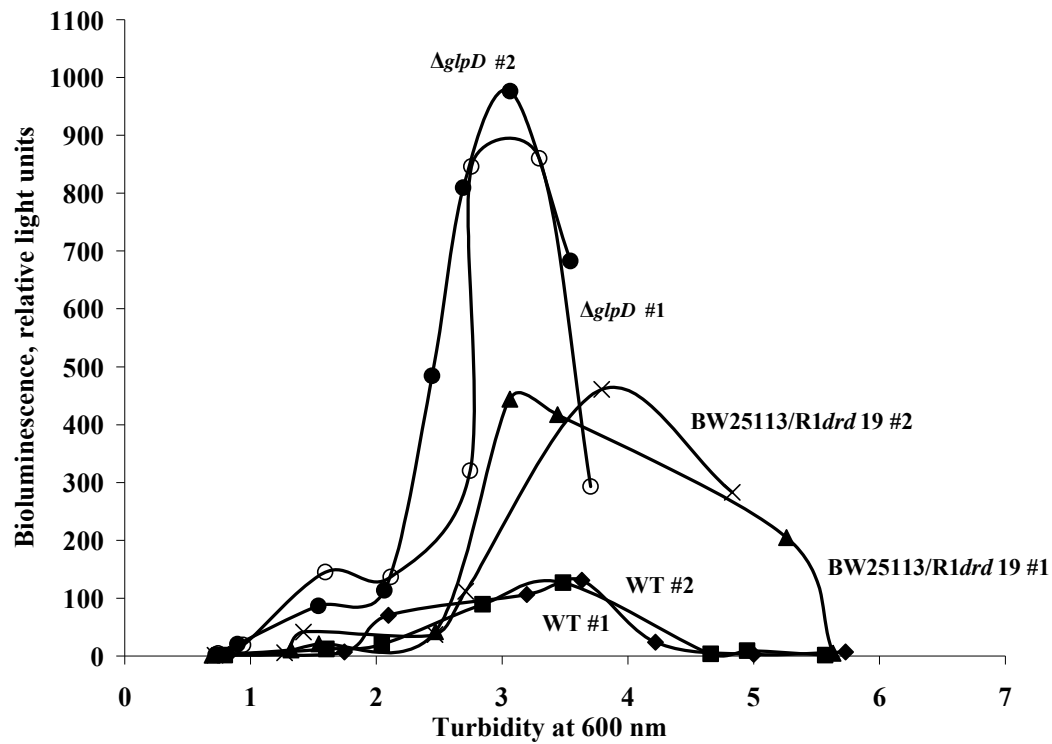
Figure 3 **Extracellular AI-2 concentrations reported by *V. harveyi* bioluminescence for *E. coli* BW25113, BW25113/R1*drd*19, and BW25113 *glpD*.** Two replicates are shown.
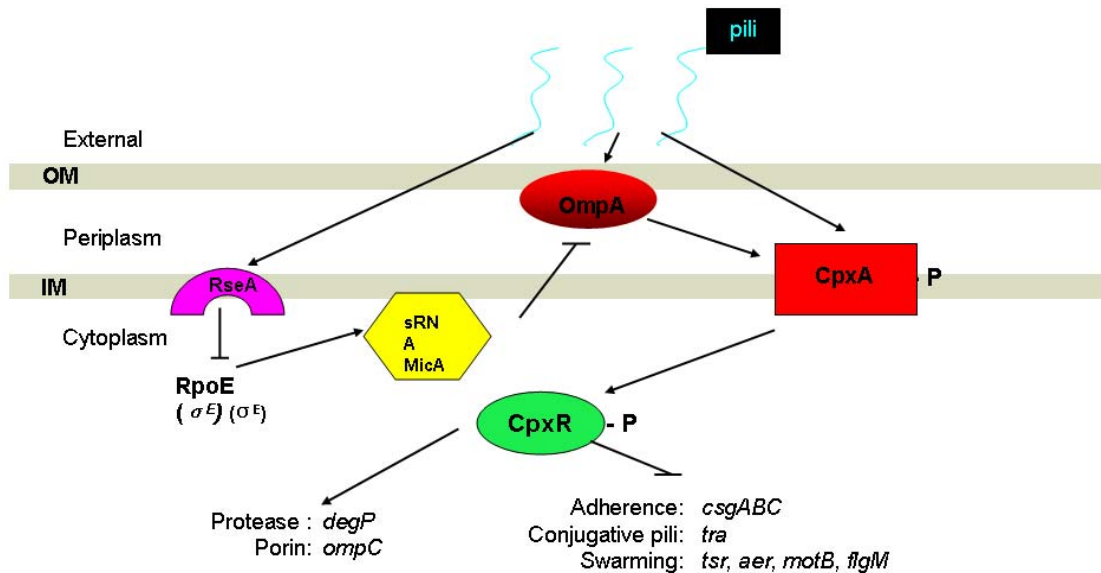
Figure 4 **The hypothesized mechanism of *E. coli* biofilm formation with R1*drd*19.** Envelope stress caused from conjugative pili initiates the network. OmpA is the potential outer-membrane protein that receives the signal from conjugative pili which then translates the signal to the sensor, CpxA, of the two-component system in which CpxR is the response regulator. Phosphorylated CpxR (CpxR-P) then regulates biofilm-related genes expression. RseA-σ^E is another system involved in the envelope-stress response system, and to some extent, overlaps with CpxAR system. In this pathway, RseA is the sensor to detect the envelope stress caused by conjugative pili. MicA is a negative antisense regulator of OmpA synthesis, and this sRNA is induced by overexpression of σ^E. OM is outer membrane and IM is inner membrane.

VITA

Name: Qun Ma

Address: Texas A&M University, Department of Chemical Engineering, 3122

                   TAMU, College Station, TX 77843-3122

Email: qunmazd@neo.tamu.edu

Education: B.S., Pharmaceutical Engineering, Zhejiang University, 2006

                   Ph.D., Chemical Engineering, Texas A&M University, 2011